

This is to certify that the

dissertation entitled

Synthesis and Analysis of Crystalline Alkalides

presented by

Bradley Van Eck

has been accepted towards fulfillment of the requirements for

Ph.D. degree in Chemistry

Date __29 August 1983

MSU is an Affirmative Action/Equal Opportunity Institution



RETURNING MATERIALS:
Place in book drop to remove this checkout from your record. FINES will be charged if book is returned after the date stamped below.

TOOM USE CHAY

SYNTHESIS AND ANALYSIS OF CRYSTALLINE ALKALIDES

Ву

Bradley Van Eck

A DISSERTATION

Submitted to

Michigan State University
in partial fulfillment of the requirements

for the degree of

DOCTOR OF PHILOSOPHY

Department of Chemistry

ABSTRACT

SYNTHESIS AND ANALYSIS OF CRYSTALLINE ALKALIDES

Ву

Bradley Van Eck

The synthesis and analysis of crystalline salts which contain alkali-metal anions and alkali-metal cations, the latter complexed by various macrobicyclic diamines (C_{MNO}, cryptand) or a crown ether (18C6), are described. These salts were obtained by precipitation from amine and/or ether solvents containing dissolved metal and complexing agent. Syntheses were performed by using very high purity metals, ligands, and solvents at reduced temperature, in vacuo. Analysis included measurement of evolved hydrogen after decomposition with water, pH titration of OH and the cryptand, flame emission determination of metal, and lh NMR spectra of the complexant.

Analyses were in good agreement with the expected stoichiometry for $Cs^+C322 \cdot Na^-$, $Cs^+18C6 \cdot Na^-$, and $K^+C222 \cdot Na^-$.

Analyses of $Rb^+C222 \cdot Na^-$, $Li^+C211 \cdot Na^-$, $Na^+C221 \cdot Na^-$, $Rb^+C222 \cdot Rb^-$, and $K^+18C6 \cdot Na^-$ are in general accord with the proposed stoichiometry. However, in these cases some of the results are in poor agreement with the presumed stoichiometry.

probably because of either partial decomposition of the complexant during the hydrogen evolution step or contamination of the crystals with excess metal. Crystals were also precipitated from solutions whose solution stoichiometry corresponded to Cs⁺C222·Na⁻, K⁺C222·K⁻, and Cs⁺C222·Cs⁻. Analyses of the crystals were very poor and suggested extensive decomposition and/or contamination. Attempts to synthesize Ba²⁺C222·(Na⁻)₂ failed to yield satisfactory results.

Solid state ²³Na NMR spectra of crystalline samples of Na⁺C222·Na⁻ yielded a broad line at -64.1 ppm probably due to Na⁻ and a poorly resolved shoulder at ~-25 to +25 ppm believed to be due to Na⁺C222. A crystalline Na⁺C222·I⁻ sample produced a single line at -12.7 ppm. Solution ²³Na NMR spectra of Na⁺C221·Na⁻ showed peaks at -61.6 ppm and -3.5 ppm due to Na⁻ and Na⁺C221 respectively.

Low temperature x-ray powder patterns of Cs18C6 produced diffraction lines which are not attributable to either cesium metal or 18C6 and these patterns thus imply that Cs18C6 powders produced by solvent evaporation are crystalline.

Thermodynamic estimates of $\Delta G_{\mathbf{f}}^{\circ}$ for alkalides and electrides were obtained by using a modified Born-Haber cycle. These estimates show that many alkalides and electrides should be stable, although only marginally so, near room temperature. Lithide salts, although estimated to be stable, have not been observed.

To Mary, Emily, and My Parents.

ACKNOWLEDGMENTS

The author wishes to express his sincere gratitude to Professor James L. Dye for his guidance and encouragement throughout this study. I would like to thank the members of Dr. Dye's research group for their many suggestions. In particular, I would like to thank those with whom I worked most closely, Long Dinh Le, Steve Landers, Harlen Lewis, Mike DaGue, Mike Yemen, Dheeb Issa, Mary Tinkham, Margie Faber, Ahmed Ellaboudy, Steve Dawes, and especially Pat Smith who originally recruited me into Dr. Dye's research group.

Thanks also go to glassblowers Keki Mistry, Andy Seer, Jerry DeGroot and Manfred Langer for their excellent and timely service; for without their help, this work would have been impossible. Machinists Russell Geyer, Ben Stutsman, Richard Menke, and Leonard Eisle are gratefully acknowledged for their valuable assistance. I also wish to thank electronics specialists Martin Rabb, Ronald Haas and Scott Sanderson for their much needed aid.

I wish to thank Naomi Hack for her help as secretary but more importantly for our many friendly conversations.

Above all, I wish to thank my wife, Mary, whose understanding and extremely long patiences was vital to

the completion of this degree.

Research support from NSF grant No. DMR-79-21479 is also gratefully acknowledged.

TABLE OF CONTENTS

Cha	pter	Pag	e
LIS	T OF	TABLES	X
LIS	T OF	FIGURES	i
I.	INT	RODUCTION	1
	Α.	Metal-Ammonia Solutions	2
	В.	Metals in Amines and Ethers	7
	С.	Crowns and Cryptands	L
	D.	Alkalides	L
	Ε.	Electrides	3
	F.	Thermochemistry 25	5
	G.	Dissertation Objectives and	
		Difficulties)
II.	EXI	PERIMENTAL	,
	Α.	Glassware Cleaning	,
	В.	Reagents)
		1. Solvents	ļ
		2. Complexing Agents	
		3. Metals	
		4. Miscellaneous Reagents	
	С.	Greaseless High Vacuum Equipment and Techniques	
	D.	Analysis	
	υ·	MIIdivsis 42	

Chapter																				P	age
	1.	Samp Hydr			_		· ıti	· on	•	•	•	•	•	•	•	•	•	•	•		42 44
	3.	Titr	_									•	•	•						•	46
	4.	Flan							ct	· ·		· enn	v	•	•	•	•	•	•	•	47
	5.	1 _H N										_	-		•	•	•	•	•	•	47
	6.	Solv												•		•					49
Ε.	NMR	Spec	tr	ome	ter	's		•	•	•	•	•		•	•	•					50
F.	X-ra	ay Po	wd	er	Pat	te	ern	ıs				•	•	•	•	•					53
G.	Opt	ical	Sp	ect	ra	•		•	•		•			•	•	•		•	•	•	55
Н.	Inei	ct At	mo	sph	ere	e S	Sys	te	m	•	•	•	•	•		•		•	•	•	55
	1.	Circ	ul	ati	on	Sy	st	em	١.		•	•		•							57
	2.	Scri										•							•		59
		a.	Wa	ter gen	Re	emc	va	1	•	•	å	N/ -	•	•	•	•			•	•	59
		b.	ке Si	gen eve	era	olu	ımn	1 0 1.	•	4	A •	• MC	• •	•	• •	•					60
		с.	Sm	all lec	Or ule	ga F	ni Rem	c ov	ar al	nd	Ir	or •	ga	ini •	lc						61
		d.	Re	gen	era	ıti	on	0	\mathbf{f}	13	X	Μc			ıla	ır					61
		0		eve yge											•	•	•	•	•	•	61
		e. f.		gen											•	•		·	•	•	
			Co	lum	ns						•	•	•	•	•	•	•	•	•	•	62 64
		g.	Ni	tro gen	ger	1 1 1 1	em	OV	a] f	ጥብ	• + =	· ni	•	•	:01	• 11m	· ın	•	•	•	67
		h.	ne	Rem	61.0		.01		, 1		. 00	4114			, 0 -	- an	•••	Ĭ	•	•	•
	3.	Glov	re	Вох	•	•	•	•	•	•	•	•	•	•	•	•	•	•	•	•	70
		a.	En	try	Po	rt			•	•	•	•	•	•	•	•	•	•	•	•	70
		b.		ov e									•	•	•	٠	•	•	•	•	71 71
				ld									•	•	•	•	•	•	•	•	73
		d.		11i									•	•	•	•	•	•	•	•	1)
		е.		ove						•							•	•			73
III. SY	ואיימי	ESIS										•		•							76
-11. D																					78
Α.	Synt	thesi													•	•	•	•	•	•	10
	1.	Puri	lfi	cat	ior	n a	and	Н	Iar	nd l	.ir	ng	of						_	_	78
		Meta	als		•	•	•	•	•	•	•	•	•	•	•	•	•	•	•	•	, ,

Ch	apte:	r Pag	zе
			30
		3. Purification of Complexing Agents	2 -
		// (3000000 03000)	31 31
		E Columbia Milana a Granda	31
		a. Glassware Design	32
			34
		The state of the s	37
		and a second rice or youars	90
	В.	Observation and the second sec	0
	C.	· · · · · · · · · · · · · · · · · · ·	10
	0.	Compounds Studied	
			4
		2. cs [†] c222·cs ⁻	8
		3. Rb ⁺ C222·Rb ⁻ 9	9
		4. Na ⁺ C221·Na ⁻	1
		5. Cs ⁺ C322·Cs ⁻	6
		6. Ba ²⁺ C222·(Na ⁻) ₂	8
		7. Cs ⁺ C322·Na ⁻	
IV.	Ana	alysis	
	Α.	Analysis Methods	
		1. Hydrogen Evolution	
		2. Titration	
		3. Flame Emission	
	В.	Results	7
	С.	Estimation of Errors	}
	D.	Discussion	ı

Cha	apte:	? Pa	ıgε
٧.	Mi	scellaneous Experiments	25
	Α.	Solution ²³ Na NMR of Na ⁺ C221·Na ⁻	25
		1. Introduction	
		2. Results and Discussion	رے 26
	В.	22	
		1. Introduction	
		2. Results and Discussion	
	С.	Low Temperature X-Ray Powder Patterns of Electrides	34
		1. Introduction	34
		2. Results and Discussion	37
VI.		namics of Formation of Alkalides d Electrides	45
	Α.	Introduction	45
	В.	Experimental Determinations	47
		1. Thermodynamic vs. Kinetic Stability of Na+C222·Na	47
		2. Calorimetric Determination of ΔH° for Na+C222·Na	1 9
		3. Electrochemical Determination of ΔH_f^o , ΔG_f^o , and ΔS_f^o for Na+C222·Na 15	52
		4. Free Energy of Solution of C222 15	54
	С.	Theoretical Calculations	54
		1. Modified Born-Haber Cycle 15	54
		a. Atomization (M)	7 8 2 2 3

Pa Pa	ge.
i. Lattice Energy	69
j. Final Results; ΔH° and formation	71
 Theoretical and Experimental Enthalpies for Alkali Cryptate 	
Halides	82
D. Discussion	95
II. Summary and Suggestions for Future	
Studies	01
A. Summary	01
B. Suggestions for Future Study 2	02
EFERENCES	^ ^

LIST OF TABLES

Table		Page
1	Peak Positions of Alkali Metal	
	Optical Spectra	. 10
2	Alkali Metal Solubilities with and	
	Without Complexing Agents	. 14
3	Thermodynamic and Kinetic Data for the	
	Complexation of Alkali Metals in Water	. 86
4	Conditions Used for Alkalide	
	Crystallization	100
5	Analysis of Crystalline Alkalides	. 118
6	²³ Na Chemical Shifts for Na ⁺ C221·Na ⁻	
	in Ethylamine	127
7	²³ Na Solid State NMR Chemical Shifts	
	and Linewidths	133
8	X-ray Powder Diffraction Lines for	
	1806	141
9	Powder Diffraction Lines for Cesium	
	and Copper Metals	142
10	Atomization Enthalpy and Free	
	Energy	156
11	Ionization Enthalpy and Free	
	Fnengu	150

Table	Page
12	Aquation Enthalpy and Free Energy 161
13	Electron Attachment Enthalpy and
	Free Energy
14	Complexation Enthalpy and Free
	Energy
15	Cryptate Solvation Enthalpy and
	Free Energy
16	Alkali Halide Entropies
17	Alkaline Earth Halide En-
	tropies
18	$\Delta H_{\mathrm{LAT}}^{\circ}$ and $\Delta G_{\mathrm{LAT}}^{\circ}$ for Lithide Salts 174
19	$\Delta H_{\rm LAT}^{\circ}$ and $\Delta G_{ m LAT}^{\circ}$ for Sodide Salts 175
20	$\Delta H_{\rm LAT}^{\circ}$ and $\Delta G_{ m LAT}^{\circ}$ for Potasside Salts 176
21	$\Delta H_{\rm LAT}^{\circ}$ and $\Delta G_{\rm LAT}^{\circ}$ for Rubidide Salts 177
22	$\Delta H_{\rm LAT}^{\circ}$ and $\Delta G_{\rm LAT}^{\circ}$ for Ceside Salts 178
23	$\Delta H_{\rm LAT}^{\rm o}$ and $\Delta G_{\rm LAT}^{\rm o}$ for Cupride Salts 179
24	$\Delta ext{H}^{\circ}_{ ext{LAT}}$ and $\Delta ext{G}^{\circ}_{ ext{LAT}}$ for Argentide and Auride
	Salts
25	$\Delta ext{H}^{\circ}_{ ext{LAT}}$ and $\Delta ext{G}^{\circ}_{ ext{LAT}}$ for Electrides 181
26	$\Delta H_{\text{formation}}^{\circ}$ and $\Delta G_{\text{formation}}^{\circ}$ for
	Lithide Salts
27	$\Delta H_{\text{formation}}^{\text{o}}$ and $\Delta G_{\text{formation}}^{\text{o}}$ for
	Sodide Salts
28	$\Delta H_{ ext{formation}}^{\circ}$ and $\Delta G_{ ext{formation}}^{\circ}$ for
	Potasside Salts

Table				Page	
29	$^{\Delta H^o}$ formation and				
	Rubidide Salts.	• • • • • •		186	
30	$\Delta H_{ ext{formation}}^{ ext{o}}$ and	ΔG° formation	for		
	Ceside Salts			187	
31	$^{\Delta H^{o}}_{\text{formation}}$ and	$\Delta G_{ ext{formation}}^{\circ}$	for		
	Cupride Salts .			188	
32	$\Delta H_{ ext{formation}}^{ ext{o}}$ and				
	Argentide Salts			189	
33	$\Delta H_{ ext{formation}}^{ ext{o}}$ and				
	Auride Salts			190	
34	$\Delta H_{ ext{formation}}^{ ext{o}}$ and				
	Electride Salts			191	
35	Enthalpy of Form	nation for A	lkali		
	Cryptate Halides			192	

LIST OF FIGURES

Figure		Page
1	Optical Spectra of Alkali Metals	
	in Ethylenediamine	9
2	Cryptand and Crown Molecular	
	Structures	12
3	Stability Constants of Various	
	Cryptates of Alkali Metals in	
	95% Methanol	19
4	The Dependence of the Formation	
	Constant on the Ratio of the Size	
	of the Ion to the Ligand Cavity	
	Size	20
5	Solvent Purification System	30
6	Molecular Distillation Apparatus	
	for the Purification of Cryptands	33
7	Alkali Metal Distribution Apparatus	36
8	Alkalide Analysis Scheme	43
9	Hydrogen Evolution Apparatus	45
10	pH Titration Curve of H2 Evolution	
	Residue	48
11	23 Na Solid State NMR Probe	52

Figure		Page
12	Cold X-ray Powder Pattern	
	Camera	54
13	Glove Box Circulation System	58
14	Nitrogen Scrubber	65
15	Na ⁺ C222·Na ⁻ Synthesis Apparatus	95
16	Synthesis Apparatus for Na ⁺ C221·Na ⁻	
	and Cs ⁺ C322·Na ⁻	103
17	Ba ²⁺ C222·(Na ⁻) ₂ Synthesis Ap-	
	paratus	109
18	NMR Sample Preparation Apparatus	128
19	²³ Na Solid State NMR Spectra of	
	Na + C222 · Na and Na + C222 · I	135
20	Cold X-ray Powder Pattern Sample	
	Holders	139
21	Thermodynamic Cycle Used to	
	Estimate the Stability of Alkalide	
	Salts	7 J. O

I. INTRODUCTION

Alkali metals dissolve in liquid ammonia. These blue (and gold) solutions have been the focus of a tremendous amount of research for well over 100 years. The beginnings of this work were originally thought to date to 1863 when Weyl (1) observed that a blue solution resulted when either sodium or potassium was dissolved in liquid ammonia. However, Edwards (2) has reported the unpublished observations of potassium-ammonia solutions in 1808 by Sir Humphrey Davy. Research with metal-ammonia solutions is very active Five international conferences, "Collegue Weyl I-V", named for the original researcher, have been held throughout the world (3-7). The literature in this field is immense and includes several review articles (8-14). Metal-ammonia research has primarily been the search for a solution model which would describe the solution properties on the basis of the proposed chemical species present in solution. When this work was extended to amine and ether solvents, solubilities were frequently too low to be of real utility. The introduction of alkali cation complexing agents to these solutions caused a dramatic solubility increase in most cases. It was the addition of these complexing agents which made possible the synthesis of two new

classes of compounds, and it is these compounds which form the subject of this dissertation. These two classes are the alkalides and the electrides. The alkalides examined here are salts which contain complexed alkali metal cations and alkali metal anions, M⁺C·N⁻, where M⁺C denotes a complexed alkali metal cation and N⁻ denotes an alkali metal anion. The electrides presented here are also salts containing complexed alkali metal cations, but in this case the positive charge of the cation is balanced by a solvent-free trapped electron, M⁺C·e⁻. Because these two new classes of compounds are direct descendents of metal-ammonia research, a brief review of this research area will serve as a proper introduction to this dissertation.

I.A. Metal-Ammonia Solutions

Liquid ammonia is a very good solvent. It has a relatively large dielectric constant (D = 23 at the boiling point). Its small size and large dipole moment account for the high solubility of the alkali metals. Saturated solutions of sodium and potassium contain about 15 mole percent metal (MPM). At -33°C saturated solutions of lithium contain 20 MPM, while cesium solutions contain 65 MPM cesium. In fact, at its melting point cesium is completely miscible with liquid ammonia (15).

Metal-ammonia solutions can be arbitrarily divided

-			

into three concentration regions: dilute solutions, lower than 10^{-3} M; intermediate, 10^{-3} to 1 M; and concentrated, 1 M to saturation. This division is arbitrary because the solution properties do not change abruptly with increasing concentration but vary smoothly. In the dilute region most investigators agree that the primary species present in solution are alkali metal cations and solvated electrons. This occurs by Reaction (1).

$$M_{(S)} \xrightarrow{NH_3} M^+ + e_{(SOLV)}^-$$
 (1)

However, in more concentrated solutions the interactions between these ions becomes important and a more complex solution model is required to explain the observed solution properties.

At low concentrations the optical spectra show a strong absorption in the near infrared which tails into the visible region. The absorption maximum occurs at 6800 cm⁻¹ (1450 nm) and the blue color is due to the tail in the visible region. This absorption is independent of metal and leaves little doubt that the species responsible for the optical absorption is the solvated electron. Pulse radiolysis studies (16,17) have shown that electrons injected into liquid ammonia produce optical spectra essentially the same as those of dilute metal-ammonia solutions. Electron spin resonance spectra of dilute metal-ammonia

solutions display a single, very narrow absorption (.05 G) with a g-value equal to 2.0012 (18). This single narrow line near the free electron value implies there is little interaction between the electron and either cation or solvent. The results of electrical conductivity studies of dilute metal-ammonia solutions (19-21) are also consistent with a simple electrolytic solution model.

Solutions of intermediate concentration show marked deviations from this simple electrolytic model. Alkali metal NMR, magnetic susceptibilities, and ESR spectra all change as the metal concentration is increased. Paramagnetic shifts in alkali metal NMR spectra (22,23) imply increased interaction between the cation and the solvated electron which may form some type of ion pair. Both ESR spin susceptibilities (24,25) and static magnetic susceptibilities (18,26-28) show that the electron spins interact to form diamagnetic states. These interactions appear to increase gradually as the metal concentration is increased and the formation of other ion pairs, triples, and even higher aggregates is possible.

At even higher metal concentrations (~8 MPM and above) these solutions have electrical conductivities higher than that of liquid mercury. Optical spectra (29) show the solvated electron absorption being replaced by an absorption edge (plasma edge) as the solution concentrations are increased and the solution becomes metallic. In this same

٥. د concentration range the color of these solutions also changes from blue to a metallic gold-bronze.

A variety of solution models have been proposed to describe these solution properties (15). Much controversy still exists in the field, especially in the area of the metal-to-nonmetal transition. Several good reviews of these models have been published (8-15).

Several solid compounds of the general formula $M(NH_3)_4$ or 6 can be formed by cooling concentrated metal-ammonia solutions. These compounds are gold in color and are highly conducting. For example, $Li(NH_3)_4$ has an electrical conductivity about the same as that of platinum metal. Metal-ammine compounds can be thought of as ammoniated alkali metal cations with their valence electrons contributing to a conduction band. Because the large size of these cations decreases the concentration of electrons when compared to typical metals, these compounds are called "expanded metals". These expanded metals frequently have properties intermediate between metals and non-metals. They are of great theoretical interest for the study of the metal-to-nonmetal transition.

Lithium tetramine appears to have a face centered cubic structure between 82°K and 88°K which changes to a hexagonal form below 82°K (15). Recently, Stacy and Sienko (30) proposed that the structure for Li(NH₃)₄ is actually cubic below 82°K. In lithium metal the Li-Li distance is

 ~ 3.5 Å but in lithium tetramine it is ~ 7 Å. This "lattice expansion" with the resulting decrease in electron concentration undoubtedly influences the electrical properties.

Recently Sienko has examined the lithium-methylamine, $\text{Li}(\text{MA})_{4}$, system (31-33). Although the existence of $\text{Li}(\text{MA})_{4}$ can be inferred from the data, it is not proven at this time.

Neither Na nor K form compounds with ammonia. When concentrated solutions of these metals are frozen, the metals precipitate to form suspensions of finely divided metal. When Cs/NH₃ solutions are frozen, they retain their golden appearance but all other evidence suggests the formation of a frozen mixture and not a compound (15).

In addition to $\mathrm{Li}(\mathrm{NH}_3)_4$ and possibly $\mathrm{Li}(\mathrm{MA})_4$, other compounds have been synthesized that contain ammonia and Ca, Sr, Ba, Eu, or Yb. In general, these compounds are prepared by cooling metal solutions that contain excess ammonia or by adding stoichiometric amounts of ammonia to the powdered metal. The structures (15) of the hexammines, $\mathrm{M}(\mathrm{NH}_3)_6$, appear to be very similar to one another. The metals assume a body-centered cubic arrangement with the ammonia molecules octahedrally oriented about each metal. However, the detailed structure of $\mathrm{Ca}(\mathrm{NH}_3)_6$ appearently involves considerable distortion of the ammonia molecules. Powder neutron diffraction studies of $\mathrm{Ca}(\mathrm{ND}_3)_6$ (34) show that not all N-D bonds are equal, the D-N-D angles are not all equal, and the ND3 pseudotrigonal axis

is not coincident with the Ca-N bond. This distortion of the ND_3 molecule appears to be common to the other hexamines (Sr, Ba, Yb) as well (35) but until single crystal structures are available, little more can be said about these observed distortions or about other electrical and magnetic data obtained from the compounds.

I.B. Metals in Amines and Ethers

Alkali metals also dissolve in amine and ether solvents but to a much smaller extent. Lithium/methylamine is one exception. In fact, at the eutectic temperature (155.4 K) lithium dissolves to a greater extent in methylamine (\sim 22 MPM) than it does in liquid ammonia (\sim 20 MPM), (36,37). The solubilities of the alkali metals in ethylamine, tetrahydrofuran, and diethylether are very low, ranging from millimolar to undetectable.

The optical spectra of these solutions are particularly useful for the identification of the species present. These spectra usually show two absorption bands, one in the near infrared and the other in the visible. The position of the absorption in the near infrared is solvent-dependent and metal-independent. The position of the visible absorption is nearly solvent-independent and strongly metal-dependent. The species responsible for the metal-independent band has been identified as the solvated electron. Pulse

radiolysis studies (38-43) have verified this by injecting electrons into these pure solvents and mapping the optical spectra. It is now generally agreed that the metal-dependent band is due to alkali metal anions; however, this assignment was disputed for several years. This will be discussed in more detail in Section D of this chapter. Figure 1 and Table 1 show the solution spectra and peak positions for the alkali metals in ethylenediamine. Note that in Figure 1 the band labeled Li is due to esolv and there is no evidence for the presence of Li (44).

In addition to M⁺, M⁻, and e⁻ there is also evidence for another species in metal solutions. This fourth species is called the "monomer", has stoichiometry M, and appears to be present in very low concentrations. Optical spectra (41,45-50) and ESR data (51-53) support a model in which the monomer is some type of ion-pair between M⁺ and e⁻.

The following equilibrium scheme was proposed by Dye (54) for alkali metals dissolved in amine and ether solvents.

$$2M_{(S)} \rightarrow M^{+} + M^{-} \tag{2}$$

$$M^- \rightarrow M + e^-_{(SOLV)}$$
 (3)

$$M \rightarrow M^{+} + e^{-}_{(SOLV)} \tag{1}$$

In methylamine for example M^- , M^+ , M and $e^-_{(SOLV)}$

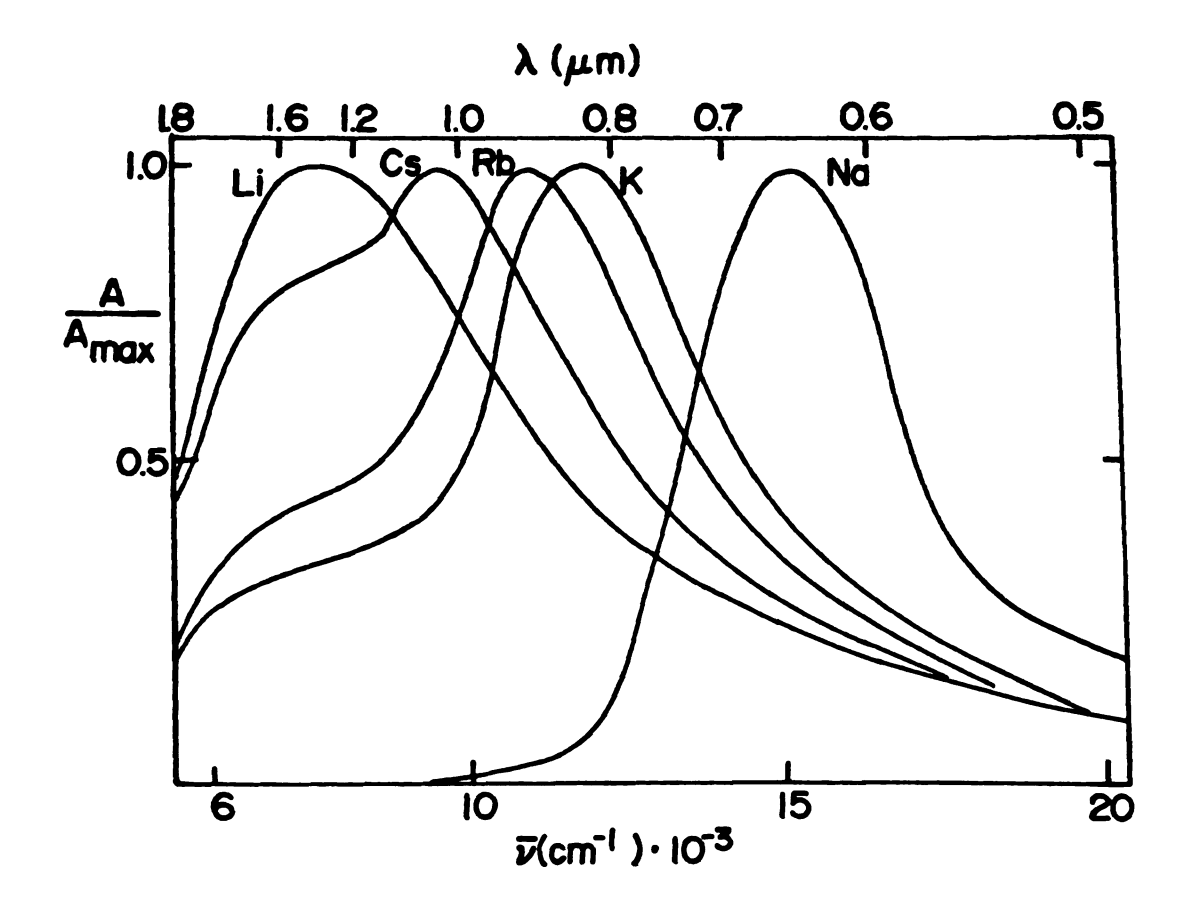


Figure 1. Optical Spectra of Alkali Metals in Ethylene-diamine.

Table 1. Peak Positions of Alkali Metal Optical Spectra.

Species	Peak Pos	ition	
Na -	15,400 cm ⁻¹	650 nm	
K ⁻	12,000	833	
Rb ⁻	11,200	893	
Cs ⁻	9,800	1020	
e_solv	7,810	1280	

can be detected but in less polar solvents such as ethylamine and tetrahydrofuran, the concentrations of M and $e^-_{(SOLV)}$ are very low, and these solutions consist primarily of M⁺ and M⁻.

I.C. Crowns and Cryptands

In 1970 (55) and in 1971 (56) Dye et al. reported the use of two classes of organic complexing agents to increase the solubility of alkali metals in amine and ether sol-These chemicals form remarkably strong complexes with alkali metal cations. Members of the first of these two classes are the crown-ethers which were first synthesized by Pedersen (57,58). Crown-ethers are cyclic polyethers whose trivial names denote both the number of atoms in the ring and the number of oxygens in the ring. For example, 18-crown-6 or 18C6 (Figure 2) contains a ring of 18 atoms, 6 of which are oxygens. A second class of complexing agents is the cryptand class. These were first synthesized by Lehn and co-workers (59) and are bicyclic diamines which have a 3-dimensional cavity for complexation of metal cations. The trivial or common name for these chemicals denotes the number of oxygens in each of the 3 polyether strands which bridge the two nitrogens. Cryptand 222, or C222 shown in Figure 2, contains 2 oxygens in each strand. Other cryptands used in this work include C322,

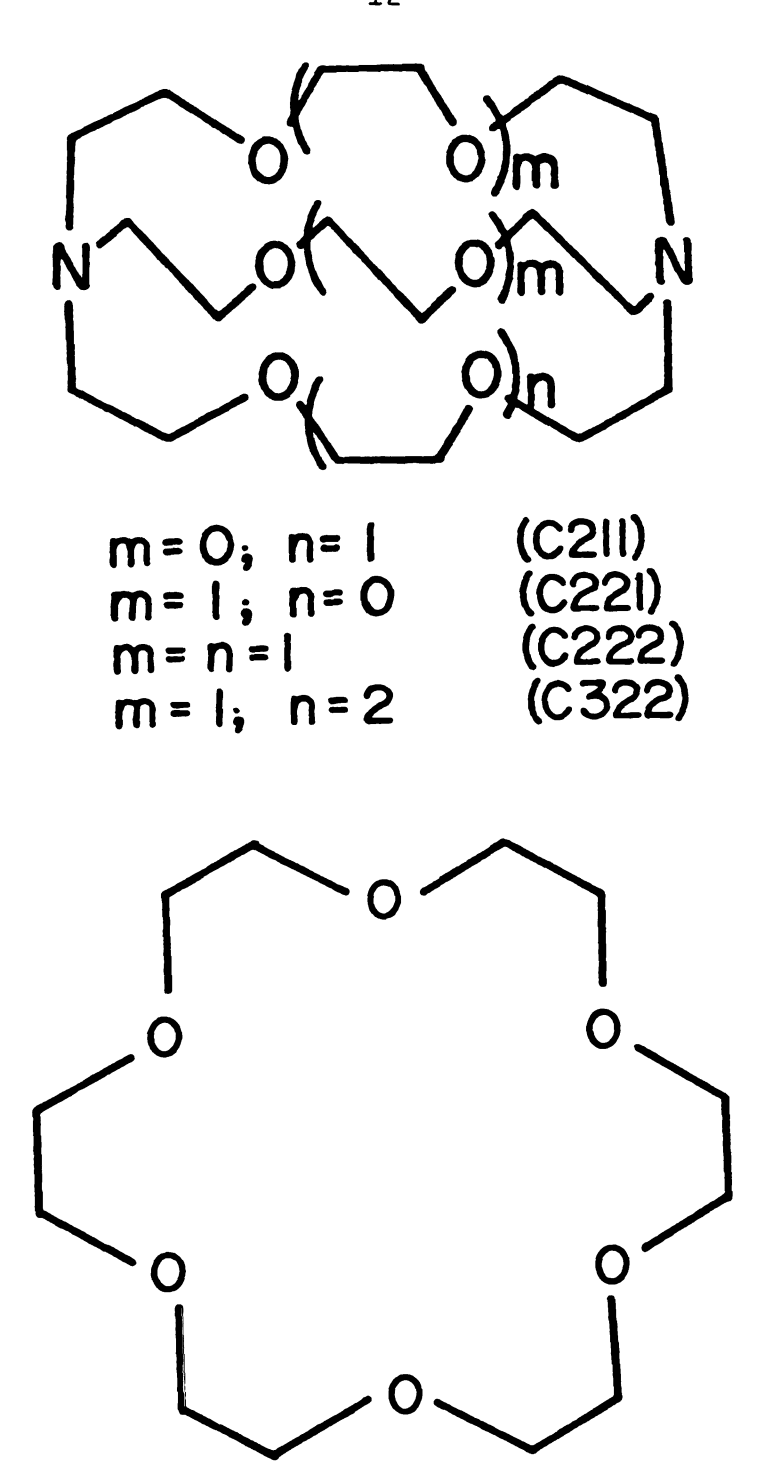


Figure 2. Cryptand and Crown Molecular Structures.

•		

C221, and C211. Cryptands form very strong complexes with alkali metal cations, with complexation constants at least as high as 10^8 . These macrocyclic complexing agents have received a considerable amount of attention and are currently being used by a large number of researchers to study solution properties, biological cation transport through membranes, phase transfer catalysis, isotropic separations, and many other phenomena. Several review articles are available (60-65).

The solubilities of alkali metals in amine and ether solvents are increased dramatically by the introduction of these cation complexation agents. Table 2 gives the solubilities for various combinations. For example, the solubility of Na in ethylamine is increased from $<10^{-6}$ M to 0.08 M by the addition of C222, an increase of nearly 5 orders of magnitude. The solubility of K in THF is increased by a comparable amount when C222 is added. This increased solubility makes it possible to study metalamine solutions in solvents that had previously been too dilute to be of real utility.

As described earlier, Equations 1-3 can be used to represent the metal-solution equilibria.

$$2M_{(S)} \rightarrow M^{+} + M^{-} \tag{2}$$

$$M^- \rightarrow M + e^-_{(SOLV)}$$
 (3)

Table 2. Alkali Metal Solubilities With and Without Complexing Agents.

Metal	Solvent	Complexing Agent	Solubility (M)	Temp
Li	EDA		0.29	25
	MA		$\chi_{Li} = 0.15$	
Na	EDA		2.4x10 ⁻³	25
	MA		>2x10 ⁻⁴	- 50
	MA	1806	0.37	0
	MA	C222	>0.06	- 78
	EA,THF, Et ₂ O,RNH ₂		<10-6	
	EA	C222	0.08	0
	EA	C222	∿0.2	25
	THF	C222	>0.09	25
	Et ₂ 0	C222	<10-4	0
K	EDA		1.04x10 ⁻²	25
	THF		5x10 ⁻⁶	24
	MA	C222	>0.14	
	MA	1806	>0.06	
	THF	C222	>0.12	
Rb	EDA		1.31x10 ⁻²	25
	MA	C222	>0.06	
	EA	C222	>0.02	
		C222	>0.04	
	Et ₂ 0 MA	1806	>0.03	

Table 2. Continued.

Metal	Solvent	Complexing Agent	Solubility (M)	Temp.
Cs	EDA		0.054	25
	MA		>2x10 ⁻³	- 50
	MA	18c6	>0.07	
	EA	C222	>0.1	-
	MA	C222	>0.05	- 70
	THF	C222	>0.1	

$$M \rightarrow M^{+} + e_{(SOLV)}^{-}$$
 (1)

The addition of a crown or cryptand, C, introduces another equilibrium,

$$M^+ + C \rightarrow M^+C \tag{4}$$

This new equilibrium in most cases lies far to the right and decreases the concentration of M^+ , which will in turn shift (1) to the right and increase the amount of dissolved metal. If equal amounts of the appropriate metal and complexing agent are dissolved in methylamine, a solvent that can support a high concentration of solvated electrons, the resulting solution will contain essentially M^+ C and $e^-_{(SOLV)}$ and very little M or M^- . However, the addition of complexing agent and excess metal to ethylamine, a solvent that normally supports only a very low concentration of $e^-_{(SOLV)}$ in the presence of metal, produces a solution that contains predominantly M^+ C and M^- . The judicious choice of solvent and the relative amounts of metal and complexing agent make it possible in many cases to control the anionic species present.

The above arguments are based on a solution model that includes equilibria 1-4. This model is strongly supported by evidence obtained by using alkali metal NMR (66,67). Solutions of Na and C222 in several solvents show two 23 Na

NMR signals. In the absence of complexing agents the solubility of Na in these solvents is too low to observe 23 Na NMR signals. Furthermore, in at least one case a significant concentration of e_(SOLV) results when no cryptand is used. High concentrations of e_(SOLV) can result in such extensive broadening of NMR signals that they are undetectable. For these reasons the use of a complexing agent was critical for the observation of the NMR signals. Recently, however, Edwards et al. (68) observed an NMR signal for Na in HMPA at 1°C. He did not observe a signal for Na⁺. This was probably due to the presence of $e_{(SOLV)}^{-}$ causing line broadening. The use of excess metal with C222 in these solvents should produce solutions that contain primarily Na + C222 and Na - according to the solution model presented above. The peak positions and linewidths observed are consistent with this assignment. The Na chemical shift shows no solvent dependence in methylamine, ethylamine, and THF and is equal to that calculated for Na (gas). In addition, the Na signal is very narrow, indicating symmetry and little interaction between the sodium's 2p orbitals and the solvent. This is expected of a true centrosymmetric Na ion with 2 electrons in its 3s orbital. The chemical shift and linewidth of the Na⁺C222 species also correlate well with those observed in other systems that contain sodium salts and C222 (66,67).

The cryptands not only exhibit very large complexation constants and thereby promote increased solubility of the alkali metals, they also show a dramatic selectivity among the alkali cations. Figure 3 shows a graph of the log of the formation constant versus the alkali metal cation radius for C322, C222, C221, and C211 in 95% methanol (69). Because the cryptands possess a well-defined 3-dimensional cavity, their selectivity is based upon the ratio of the cavity to the ion size (63). Figure 4 demonstrates this graphically as plots of the log of the formation constant versus this ratio for C222, C221, and C211. This selectivity will be used in synthesis for determining which cryptand should be used in order to synthesize a particular alkalide or electride. For example, the synthesis of K⁺C·Na⁻ requires that K⁺ be inside the cryptand cavity and Na outside. When choosing the proper cryptand it can be seen from Figure 3 that both C222 and C221 form strong complexes with both Na and K[†]. However, the proper choice is C222 because its formation constant with K⁺ is nearly 3 orders of magnitude greater than with Nat.

The optical spectra of solutions that contain alkali metals is very useful for solution species identification as shown earlier in Figure 1. The same is true for metal solutions that contain crowns and cryptands. However, there is an important difference between these two

F.

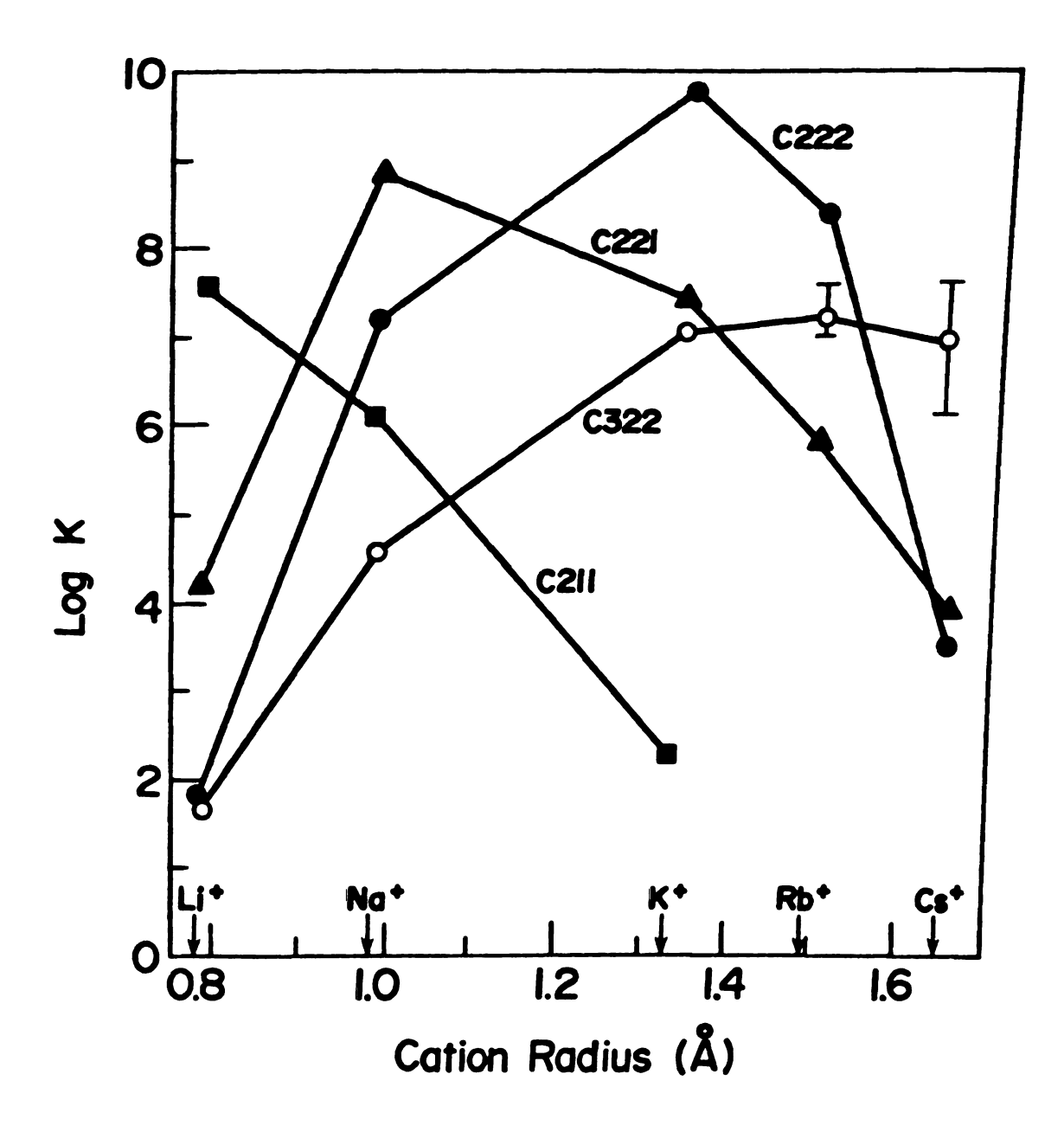


Figure 3. Stability Constants of Various Cryptates of Alkali Metals in 95% Methanol.

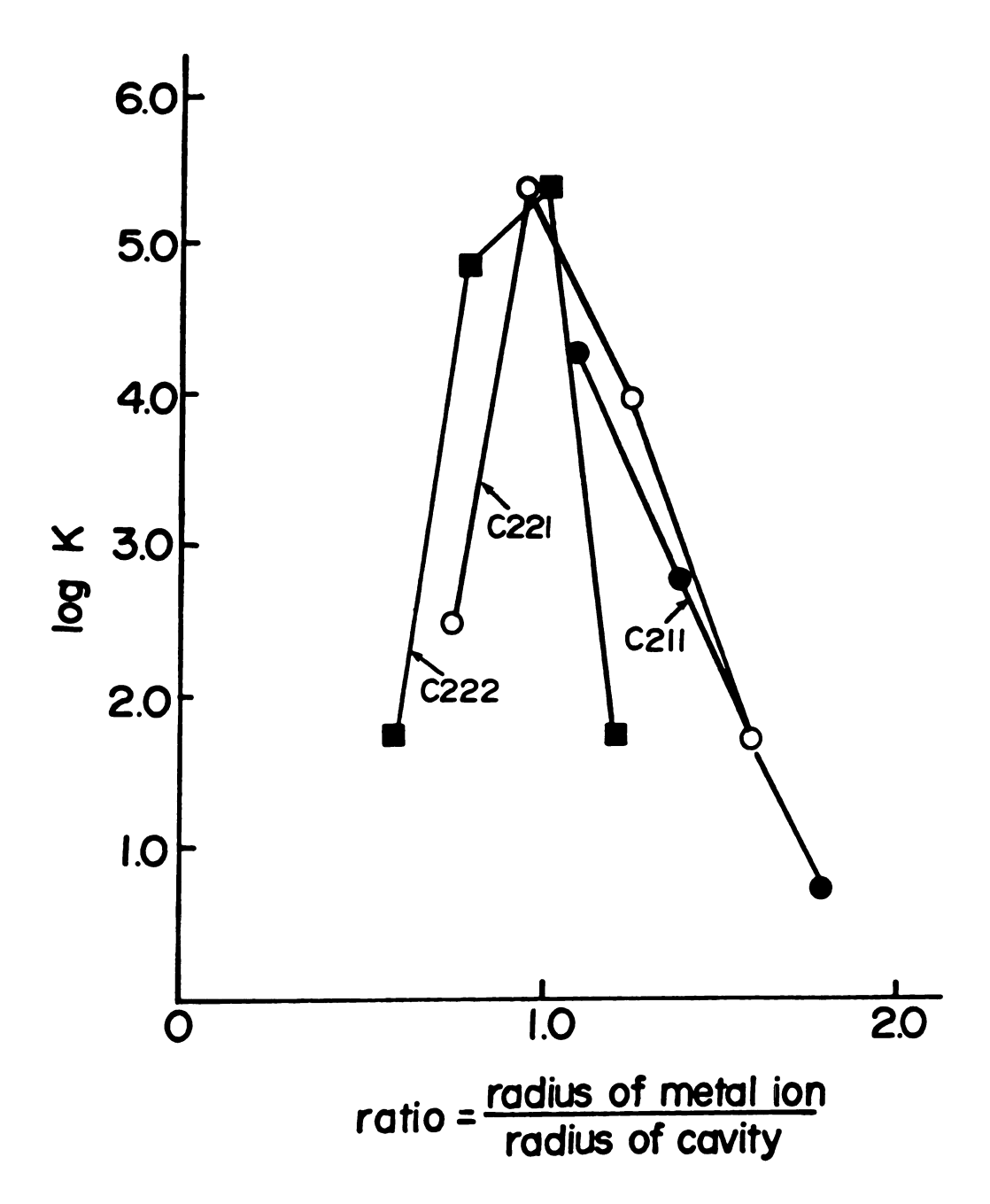


Figure 4. The Dependence of the Formation Constant on the Ratio of the Size of the Ion to the Ligand Cavity Size.

solutions. When the solvent is removed from metal solutions, the M^+ , M^- , and $e^-_{(SOLV)}$ recombine to form free metal, but when the solvent is removed from metal solutions that contain a complexing agent, recombination to form free metal is prevented. Optical spectra of thin solvent-free films show in many cases the same general features as the optical spectra of the original solution (56,64,70-73). The information from these thin films is extremely useful in synthesis for determining the proper choice of metals, complexing agents and solutions.

I.D. Alkalides

Alkalides as defined earlier are salts that contain alkali metals in the unusual -1 oxidation state. However, it should not be too surprising that these compounds can be formed because the evidence for this -1 oxidation state has been accumulating for many years. The existence of alkali metal anions in the gas phase was established in 1948 (74). Electron affinities for all the alkali metals have been measured and tabulated (75). In every case the electron affinities are positive. In addition, alkali metal anions were proposed in metal-ammonia solutions in 1965 (76,77) and also in metal-amine solutions in 1969 (78). Optical spectra of metal-amine solutions (56,64,70-73) and especially alkali metal NMR results (66,67)

have left little doubt that these anions exist in solution. In 1974 the isolation and characterization of the first crystalline salt containing an alkali metal anion was reported (79,80).

This salt is composed of cryptated sodium cations and sodium anions. The crystals were prepared by cooling a solution of C222 which had been allowed to contact excess sodium metal. (See the experimental section and the synthesis section for details.) The crystals produced were shinny gold-colored hexagonal plates. These crystals are air, water, and light-sensitive and must be handled in vacuo or in an inert atmosphere. They are stable indefinitely at room temperature under vacuum in the dark. Samples of Na⁺C222·Na⁻ melt with decomposition at 83°C to form molten C222 and precipitated sodium metal (80). The structure (80) was shown to contain closest packed cryptated sodium cations in ABCA. . . layers with the sodium anions occupying octahedral holes in the cation lattice. This structure is very similar to that of Na+- $C222 \cdot I^{-}$ (81) and $K^{+}C222 \cdot I^{-}$ (82); however, the Na ion appears to be somewhat larger than the iodide ion. The Na - Na intraplane distance is 8.8 Å and the Na - Na interplane distance is 11.0 Å. This difference may produce anisotropy of those properties which depend on the anion-anion distance. Single crystal conductivity studies may quantify this anisotropy. Packed powder conductivity

studies (83) show $Na^+C222 \cdot Na^-$ to be a semiconductor with a band gap of 2.4 eV.

The observation of Na, Rb, and Cs in solution with alkali metal NMR spectroscopy (66,67) and the observation of Na, K, Rb, and Cs from solvent-free film spectra (71-73) as well as the observation of crystalline precipitates from solutions that contain these anions strongly suggest the possibility of synthesizing an entire series of alkalides. A major portion of this dissertation is devoted to the systematic synthesis and analysis of new compounds that belong to this class.

I.E. Electrides

If equal amounts of metal and complexing agent are dissolved in an appropriate solvent (NH₃ or CH₃NH₂) solutions that contain essentially M⁺C and e_(SOLV) can be prepared. Complexation of the cation prevents the recombination of M⁺ and e⁻ to form metal when the solvent is removed; instead, removal of the solvent causes the precipitation of dark blue powders of stoichiometry M⁺C·e⁻. Several of these blue powders have been prepared (71-73). These electrides are believed to consist of a lattice of complexed cations with the electrons trapped interstitially. At the time that this research was completed no single crystals of these compounds had been observed, although

some precipitates appeared to be microcrystalline. Landers (84) and DaGue (85) have examined Li⁺C2ll·e⁻ and K⁺C222·e⁻, respectively. The ESR spectra of Li⁺C211·e⁻ samples show a single narrow line with a g-value near the free electron value. These same spectra showed no evidence for the presence of free lithium metal. Both EPR and static magnetic susceptibility data show a temperature-dependent spin-spin pairing, and some samples displayed metallic character as evidenced by optical spectra, microwave conductivity, and ESR spectra. The K+C222·esystem displays metallic characteristics also. Narrow ESR signals near the free electron value, plasma-type optical spectra, and high microwave conductivity show that this compound may be metallic or nearly metallic. This evidence indicates that these electrides may be examples of expanded metals similar to the metal amine compounds. The electrides, however, contain no solvent.

A number of attempts have been made over the years to grow single crystals of electrides. All these attempts ended in failure. After completion of this thesis research, Ellaboudy (86) has finally succeeded in synthesizing a crystalline electride. A portion of the work presented here is the effort to establish whether electrides produced by solvent evaporation are truly crystalline or amorphous. Because single crystals were not yet available, powder x-ray methods were used.

I.F. Thermochemistry

Estimates of the thermodynamic stability of alkalides and electrides have been made by using a Born-Haber cycle (83). These thermodynamic predictions serve as useful guides in synthesis when selecting appropriate solvents, metals, and complexing agents. Some of these estimates are reasonably accurate; however, others are much less certain either because important thermodynamic data are unavailable or the theoretical estimates for certain steps in the cycle are of questionable accuracy. However, even in the worst cases, the <u>relative</u> values should be reasonably accurate and this should permit comparisons among various alkalides and electrides. The presentation and discussion of these calculations are found in Chapter 6.

In an effort to test whether alkalides are thermodynamically stable to dissociation, DaGue (85) grew crystals of Na $^+$ C222·Na $^-$ isothermally from a solution that contained Na and C222. This result proves that ΔG for this reaction is negative. The calculations indicate that ΔG is nearly zero in this case. In a further attempt to verify the calculations, a sample of Na $^+$ C222·Na $^-$ was synthesized and a calorimetric determination was made for the following reaction.

$$Na^{+}C222 \cdot Na^{-} + 2H_{2}O + 2Na^{+} + C222 + H_{2} + 2OH^{-}$$
 (5)

The results of this determination as well as the experimental details are presented in Chapter 6.

I.G. Dissertation Objectives and Difficulties

The primary objective of this dissertation is the development of systematic methods for the synthesis of alkalides. Research with metal-amine solutions poses a variety of very difficult experimental problems. The metal solutions, final products, and some of the starting materials are extremely reactive. Alkali metals react rapidly with oxygen and water. Metal solutions are thermodynamically unstable with respect to reduction of the solvent by either M or e to form amide and hydrogen gas. The complexing agent used, even though resistant to reduction, is also somewhat susceptible to reduction by either M or e both in solution and in solvent-free precipitates of alkalides and electrides. Certain solvent-free compounds decompose spontaneously at -40°C or above; and most compounds appear to be light-sensitive. However, kinetically stable metal solutions can be prepared if solvents, metals, and complexing agents are appropriately treated to remove all easily reducible impurities. use of rigorously clean glassware, high vacuum techniques, and syntheses at reduced temperatures is equally important for the preparation of stable solutions.

The air, water, light, and thermal sensitivity of alkalides makes commercial analysis unreliable because of decomposition during shipping and handling. Therefore, an in-house analytical scheme was designed and used. Its design and use are described as well as the analytical results obtained on alkalide samples. Because of the thermal sensitivity of these compounds, a commercial inert atmosphere glove box was extensively upgraded to include cold wells for handling samples that must be kept cold. In addition to synthesis, analysis, and handling techniques of the alkalides, this dissertation also describes solution and solid-state NMR experiments as well as attempts to obtain powder x-ray patterns of electrides.

II. EXPERIMENTAL

II.A. Glassware Cleaning

The reactivity of alkalides and electrides makes it essential to use rigorously clean glassware. In order to minimize decomposition problems, the following procedure was applied to all glassware used in the synthesis and handling of these compounds and their solutions.

First the apparatus was rinsed with a hydrofluoric acid cleaning solution (see Miscellaneous Reagents). It was then rinsed at least five times with distilled water and filled with aqua regia (3:1, hydrochloric acid 12 M/nitric acid 16 M) and left to stand overnight. When a shorter cleaning time was required, the apparatus was heated to promote the liberation of Cl₂ and allowed to stand for several hours. At the end of the aqua regia cleaning procedure, the solution was poured out and the apparatus was rinsed seven times with distilled water and seven more times with conductance water (see Miscellaneous Reagents). The apparatus was then oven-dried at 125°C. To avoid contamination by dust during storage, the orifices of the apparatus were covered with Parafilm-M (American Can Co.).

Note: Chromic acid baths are not recommended because of possible contamination by paramagnetic species.

II.B. Reagents

II.B.1. Solvents

The solvents used for this work were all stored in vacuum storage bottles (Figure 5) and were degassed by freeze-pump-thaw cycles before use.

Ammonia (NH3) and Dimethylamine (DMA)

Ammonia (Matheson, anhydrous, 99.99%) and dimethylamine (Matheson, anhydrous, 99%) were individually distilled onto Na/K alloy (see Metals) and freeze-pump-thaw cycles were repeated until gas evolution ceased. The solvent was then distilled onto fresh Na/K alloy. If there was no evidence of gas evolution and the solution remained blue (NH₃ only) for 24 hours, the solvent was distilled into a heavy-walled storage bottle.

Methylamine (MA) and Ethylamine (EA)

Methylamine (Matheson, anhydrous, 98%) and ethylamine (Matheson, 98.5%) were individually stirred over calcium hydride for 24-28 hours with accompanying freeze-pumpthaw cycles followed by two Na/K alloy treatments before

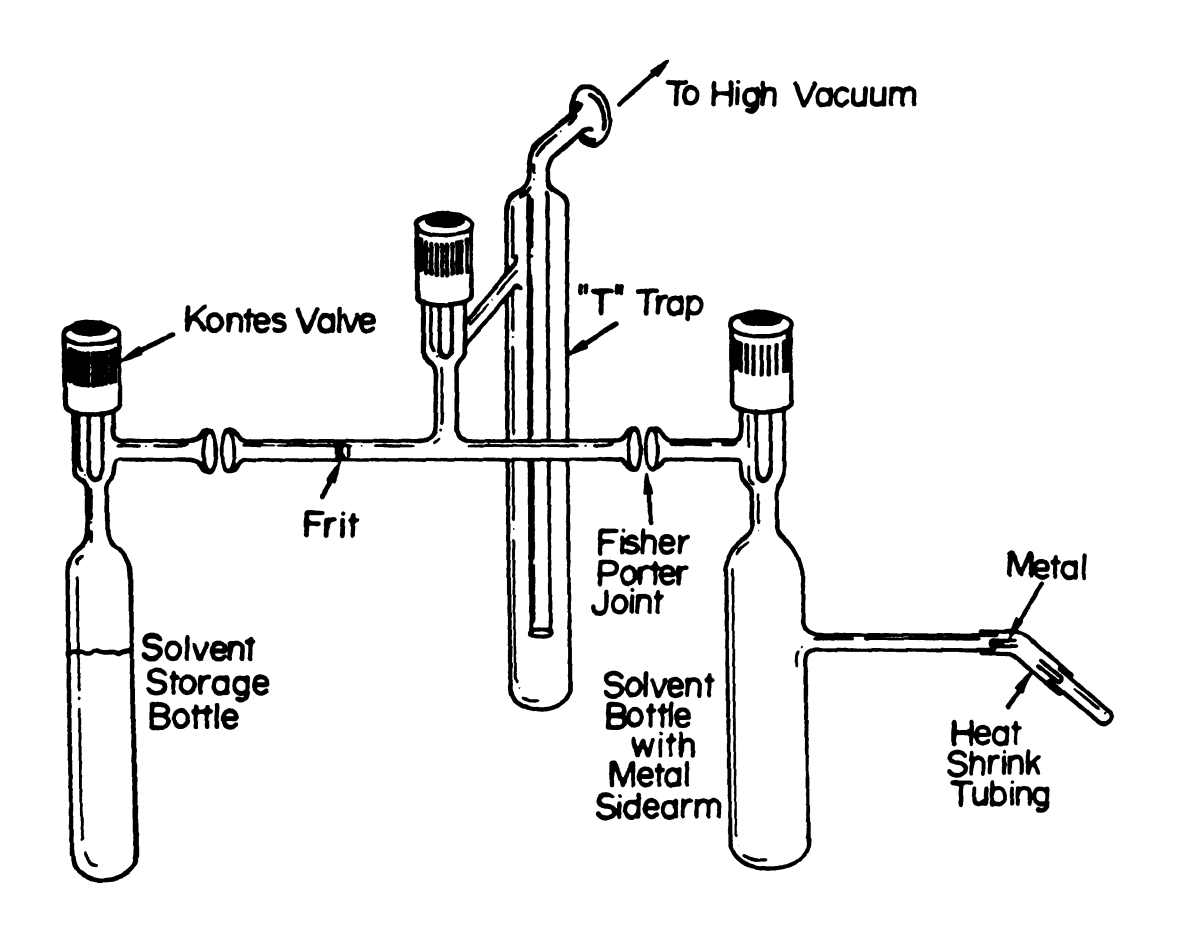


Figure 5. Solvent Purification System.

distillation into storage bottles. Methylamine was stored in a heavy-walled bottle.

Isopropylamine (iPA) and t-Butylamine (tBA)

Isopropylamine (Eastman Kodak) and t-butylamine (Eastman Kodak) were treated similarly to MA and EA except that benzophenone was added to the second Na/K treatment which contained excess metal. The purple color of the benzophenone ketyl radical-diamion mixture served as an indicator of dryness.

Dimethylether (DME), Diethylether (DEE), and n-Pentane (nP)

Dimethylether (Matheson, anhydrous, 99.87%) was treated with Na/K alloy twice, with a small amount of benzophenone also present in the second treatment. Diethylether (Mallinckrodt, anhydrous, ACS) and n-pentane (Matheson, Coleman & Bell, 98%) were treated with calcium hydride and then with Na/K and/or with a mixture of Na/K and benzophenone. When dryness was indicated for these three solvents, they were distilled into storage bottles that contained fresh Na/K alloy (with no benzophenone) for storage. These three solvents need not be stored over Na/K provided they are treated with Na/K just prior to use. It should be noted that final storage over Na/K with benzophenone or over a blue solution of Na/K requires careful

distillation into the measurement system in order to prevent carry-over of solids along with the solvent vapor.

Deuterium Oxide (D20)

Deuterium oxide (Norell Chemical Co., 99.85% D), used for $^{1}\mathrm{H}$ NMR analysis, was used without further purification.

II.B.2. Complexing Agents

The complexing agents were stored in the dark at -20°C prior to purification. After purification they were stored in the dark with Drierite (W. A. Hammond) at room temperature.

2,1,1-Cryptand (C_{211} or IUPAC: 4, 7, 13, 18-tetraoxa-1,10-diazabicyclo-[8.5.5] eicosane). C2ll (PCR, Inc.) was purified by high vacuum distillation (Figure 6). The impure cryptand was heated to 65-68°C in an oil bath at 1 x 10^{-5} torr in semidarkness. The cold finger was cooled to -50°C with cold N_2 gas. When distillation was complete, the cold finger was warmed to 35°C, the cryptand liquified and dropped into the cup. The cup was then broken off and stored.

Alternatively, small amounts of impure cryptand were distilled directly into a synthesis apparatus for immediate use. This distillation was effected by weighing

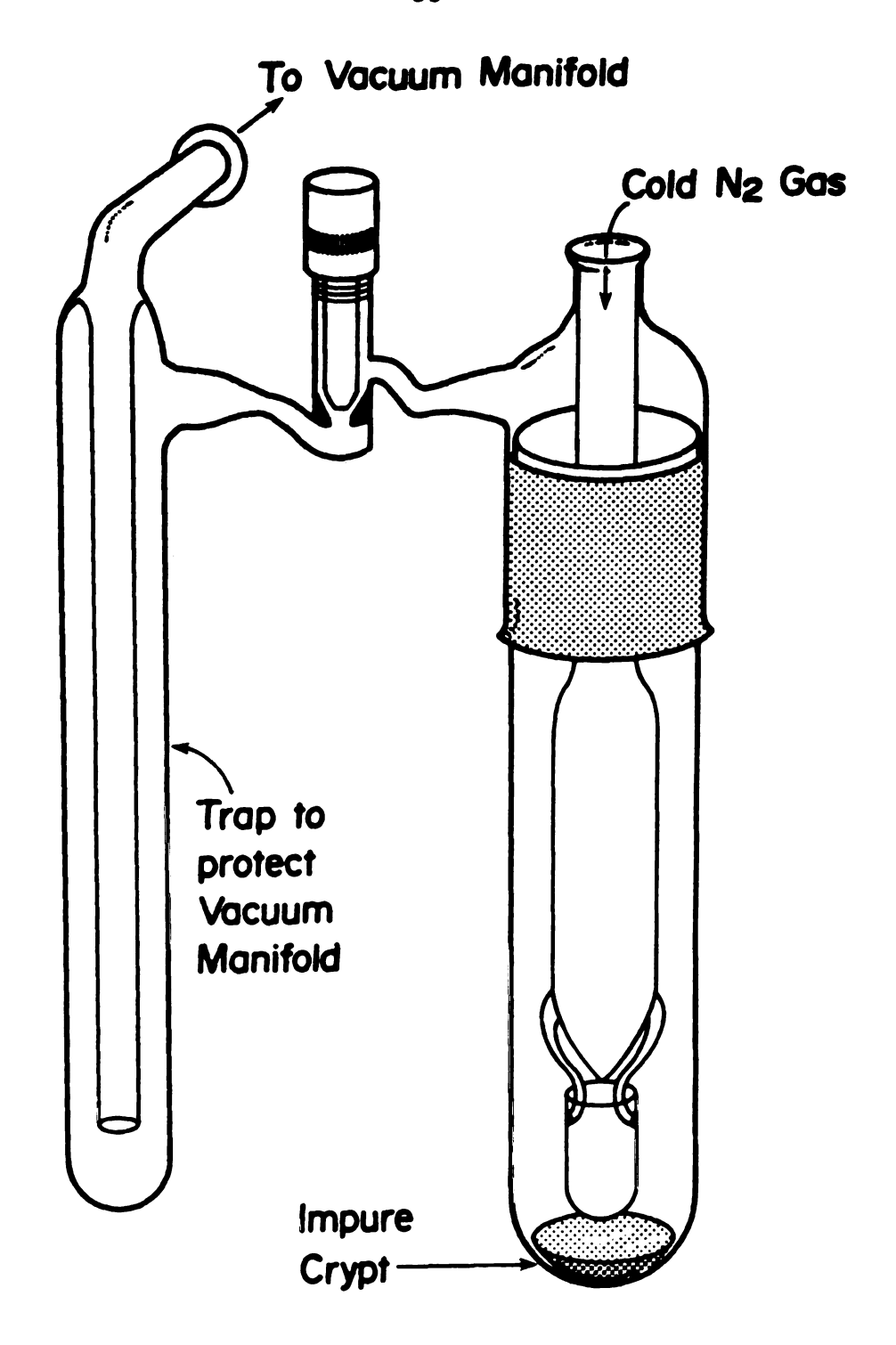


Figure 6. Molecular Distillation Apparatus for the Purification of Cryptands.

the cryptand into a short length (vl cm) of 5 mm glass tubing, which had been sealed at one end, and inserting this into a larger piece of glass tubing also sealed at one end. This was then butt sealed to an arm of the synthesis apparatus (Figure 16). The system was then evacuated and the cryptand distilled by using an oil bath. When the distillation was complete, a vacuum seal-off was made to remove the sidearm along with any undistilled residue.

- 2,2,1-Cryptand (C₂₂₁ or IUPAC: 4,7,13,16,21-pentaoxa-1, 10-diazacyclo[8.8.5]tricosane). C221 (PCR, Inc.) was purified only by direct distillation (100°C) into the synthesis apparatus as described above for C211.
- 2,2,2-Cryptand (C₂₂₂ or IUPAC: 4,7,13,16,21,24-hexaoxa-1,10-diazabicyclo[8.8.8]hexacosane). C222 (PCR, Inc.) was purified by high vacuum sublimation at 110°C with the cold finger at -20°C. The white powder (M.P. 68-69°C; lit. (87): 68-69°C) was scraped from the cold finger and stored.
- 3,2,2-Cryptand (C₃₂₂ or IUPAC: 4,7,10,16,19,24,27-hepta-oxa-1,13-diazabicyclo[11.8.8]nonacosane). C322 prepared by Patrick B. Smith, Michael G. DaGue, and Michael R. Yemen following J.-M. Lehn's method (59) was purified in the same manner as C211 except it was distilled at 145-

150°C. Note: Even when C322 is stored under vacuum and in the dark, it slowly decomposes to give a light yellow liquid.

18-Crown-6 (18C6 or IUPAC: 1,4,7,10,13,16-hexaoxacyclo octadecane). 18C6 (PCR, Inc.) was recrystallized from warm acetonitrile to give the crown-acetonitrile complex (88). The crown, obtained by vacuum decomposition of the complex was high vacuum sublimed to yield a white powder (M.P. 39°C; lit. (89): 39-40°C).

II.B.3. Metals

Sodium, Potassium, and Rubidium

These metals (Alfa-Ventron; Na 99.95%, K 99.95%, Rb 99.93%) were supplied under argon in sealed glass ampoules with breakseals. Transfer of these metals from the 5 g ampoules to glass tubing with sealed ends was accomplished as follows. The apparatus shown in Figure 7 was constructed using tubing whose inside diameter had been measured. After evacuation to 1×10^{-5} torr, the break-seal was broken using the break bar; the metal was heated to melting and allowed to run down to fill the three reservoirs. Vacuum seal-offs were then made at the constrictions and the metal was poured into the straight portions of the tubing. Vacuum seal-offs were then made to isolate partially filled

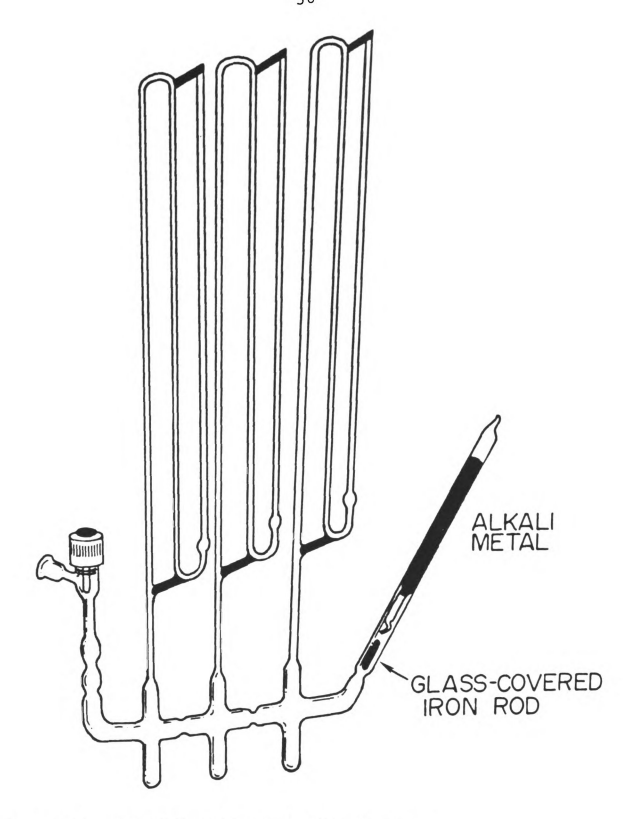


Figure 7. Alkali Metal Distribution Apparatus.

lengths of tubing for later use. Inside diameters used in this work ranged from 1 to 8 $\,\mathrm{mm}$.

Cesium

The metal (donated by the Dow Chemical Co.) was distributed in the same manner as sodium, potassium, and rubidium above.

Lithium

This metal (Alfa-Ventron, 99.9%, ribbon under argon) cannot be distributed in the same manner as above because it reacts with both hot pyrex and quartz. Several methods for obtaining known quantities were attempted and abandoned (84) before a Cahn Electrobalance (Model RTL, ±0.1 mg) was obtained for weighing lithium samples. The electrobalance was used in an argon glove box (see Inert Atmosphere System) to avoid reaction with water, oxygen, and nitrogen. A clean knife was used to cut small pieces of lithium; they were weighed and placed in 5 mm glass tubes sealed at one end. A glass cap to which polyolefin heatshrinkable tubing (Alfa Wire Corporation) had been previously attached was shrunk onto the tube with a woldering gun. This process makes a gas-tight seal and the sample can then be removed from the glove box, the end containing the metal cooled, and a flame seal-off made to produce

a sealed glass ampoule containing a known amount of metal.

Barium

This metal (Metals Mart, 99.92%, rod under argon) was loaded in the glove box as described above for lithium.

Sodium-Potassium Alloy (Na/K)

Sodium and potassium when mixed in a 1:3 mole ratio produce a low melting alloy (\sim -10°C) which is a very efficient drying agent. The alloy was prepared in situ for solvent purification by co-distilling the metals from the sidearm of a vacuum storage bottle (Figure 5).

II.B.4. <u>Miscellaneous Reagents</u>

Potassium Hydrogen Phthalate (KHP)

Potassium Hydrogen Phthalate (Matheson, Coleman & Bell, Reagent, ACS) was oven dried at 110°C for at least three hours and allowed to cool in a vacuum desiccator.

Benzophenone (\emptyset_2 CO), Calcium Hydride (CaH₂, and Magnesium Sulfate (MgSO₄)

Benzophenone (Matheson, Coleman & Bell), Calcium Hydride

(Fisher), and Magnesium Sulfate (Mallinkrodt, anhydrous) were all used without further purification.

t-Butanol

This compound (Fisher) was dried over anhydrous $MgSO_4$ and distilled. The fraction boiling at $80^{\circ}C$ was collected and stored in a desiccator.

Hydrofluoric Acid Cleaning Solution

The HF glass cleaning solution was prepared by mixing $33\% \ \text{HNO}_3$ (16 M), $5\% \ \text{HF}$ (28 M), $2\% \ \text{acid-soluble}$ detergent (Tide), and $60\% \ \text{water}$; all by volume. All acids were reagent grade.

Conductance Water

House-distilled water was deionized (Crystalab Deeminizer) and distilled in a 70 cm glass column packed with 7 cm lengths of glass tubing. The water was stored in a sealed polypropylene container. Conductance measurements typically gave specific conductances of 2 x 10^{-6} ohm⁻¹cm⁻¹.

Standard NaOH, KOH, and HCl Solutions

These were all prepared with reagent-grade chemicals and conductance water and were standardized with KHP.

Flame Emission Standards

All flame emission standards (Aldrich) were purchased as 1000 $\mu g/ml$, diluted with conductance water, and stored in sealed polyethylene bottles.

II.C. Greaseless High Vacuum Equipment and Techniques

Atmospheric gases (O_2, N_2, CO_2, H_2O) react readily with or are absorbed by both the starting materials and the products of this research. The use of greaseless high vacuum techniques not only excludes these gases but also facilitates the purification of complexing agents and metals, and provides a convenient method for transferring dry solvents.

The high vacuum system used for this work consisted of an all-glass manifold and a liquid nitrogen trap. The system was evacuated with an oil diffusion pump (Veeco, Model EP2A-1; Dow Corning 704 oil) which was backed by a two-stage mechanical pump (Cenco HV-7). The manifold was continuously heated to 70°C with heating tape. Grease-less Teflon-stem vacuum valves (Kontes, K-826610-0004) were used on the manifolds, solvent bottles, and on all synthesis and analysis glassware. Vacuum connections between the manifold and other vacuum glassware were made using "Solv-Seal" glass joints with Teflon inserts (Lab-Crest Division, Fischer & Porter Co.). Both the valves and the

connectors were routinely used at 1 to 5×10^{-6} torr. Vacuum measurements were made by using an ionization gauge tube (Veeco RG 75-P), which was connected directly to the manifold, and an ionization gauge controller (Veeco RG-830).

Solvents were distilled through a tee (Figure 5). The tee was evacuated and the valve to the manifold was closed prior to all distillations. The liquid nitrogen trap was provided to protect the manifold from contamination with solvents and complexing agents (some have relatively high vapor pressures). The frit was used to protect against spray and particulate matter (i.e., CaH₂ during distillation.

Pure alkali and alkaline earth metals were introduced into vacuum glassware by using heat-shrinkable (H/S) tubing (Flo-Tite Tubing, Pope Scientific Co.). This tubing consists of two concentric parts, the outer tube (Teflon TFE) shrinks when heated, and the inner tube (Teflon FEP) softens and forms a vacuum-tight seal to glass or metal tubing. The glass tubing which contained the metal (see Metals), was scribed with a glass knife, put into the sidearm (Figure 5), and a glass cap was sealed on with heat-shrinkable tubing. The system was then evacuated and the metal ampoule was broken by bending the H/S tubing. After the ampoule had been moved, a vacuum seal-off was made behind it to remove the H/S tubing. At this point

the metal was either distilled through the sidearm (Na, K, Rb, Cs) or dissolved directly (Ba, Li) with solvent.

II.D. Analysis

The sensitivity of alkalides and electrides to air, water, light, and heat make commercial analyses unreliable because of decomposition during shipping and handling. Because of these problems which led to inconsistent analytical results, an in-house analytical scheme was designed and the necessary apparatus was constructed. This scheme was predicated on the reaction of these highly reducing compounds with water to form H_2 and OH^- . The amount of H_2 produced gives the total reducing power of the sample. Titration of the residue gives the amount of OH^- present as well as the amount of cryptand present (cryptands have two basic amine groups). The flow diagram for this analysis scheme (Figure 8) outlines the method used for a general alkalide salt, $M^+C \cdot N^-$.

II.D.1. Sample Weight

Most alkalide and electride salts are not stable at room temperatures and therefore cannot be easily weighed. However, because of built-in redundancy, the analysis does not require knowledge of the mass of the sample. Several of the salts studied were stable at room temperatures and

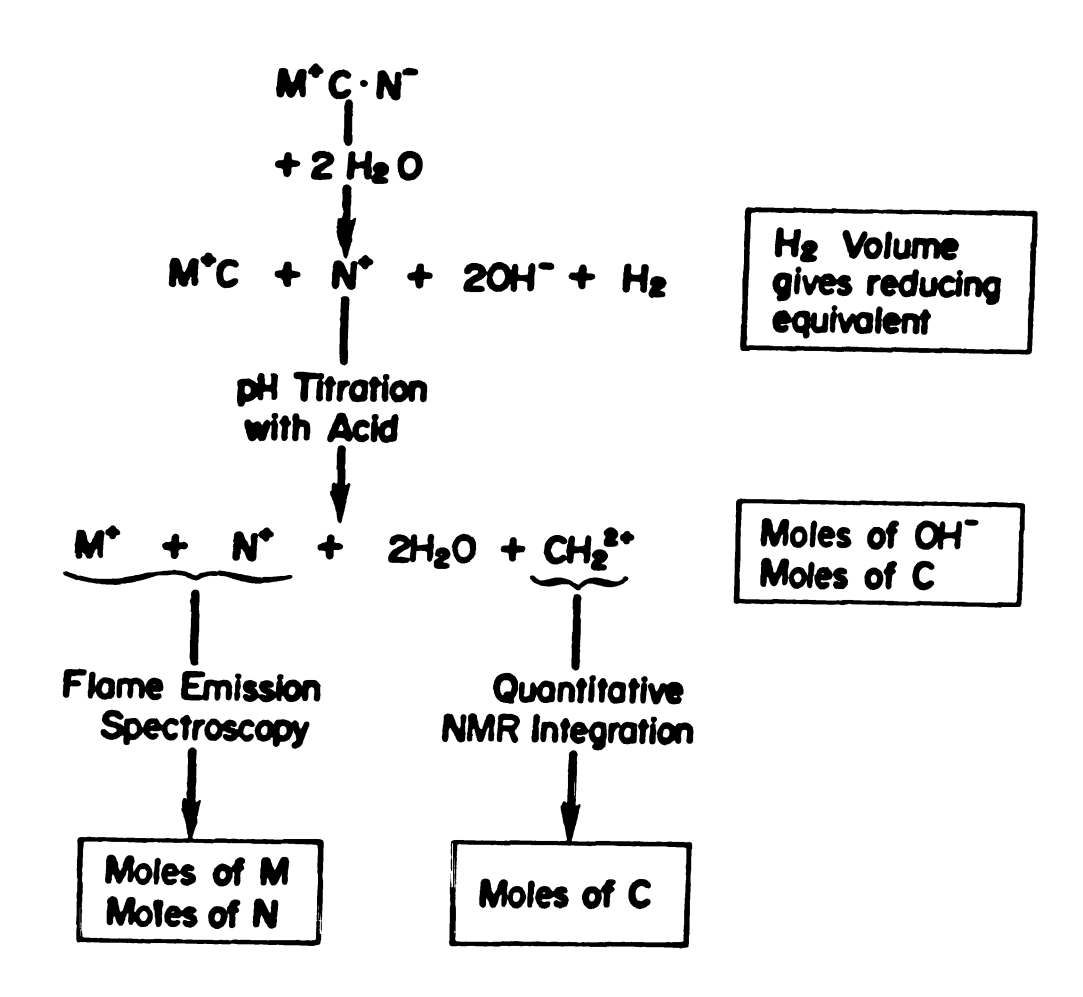


Figure 8. Alkalide Analysis Scheme.

could be weighed in their sealed glass ampoules with an analytical balance (Mettler, Type B6, ±.00005 g). These samples were scribed with a glass knife previous to weighing, and after completing the analysis, the empty glass ampoules were reweighed to obtain the sample mass by difference.

II.D.2. Hydrogen Evolution

The hydrogen evolution apparatus (Figure 9) used in this study was patterned after a similar device used by Mei-Tak Lok (90) and was built with the help of Dr. Harlen F. Lewis. The apparatus had several components; the sample compartment, the water bulb, the double liquid nitrogen trap, a mercury Toepler pump with leveling bulb, and a calibrated pipet. Temperature-sensitive compounds were kept cold until they had completely reacted with water. Failure to keep these samples cold not only permits decomposition prior to analysis, but also allows too rapid a reaction with water. Both of these effects cause errors in the hydrogen evolution analysis. These errors are caused by decomposition of the complexing agent instead of the desired oxidation-reduction reaction between water and the alkali metal anion. A temperature-sensitive compound was treated in the following manner.

The cold sample tube was scribed with a glass knife and rapidly transferred to the pre-chilled sample compartment

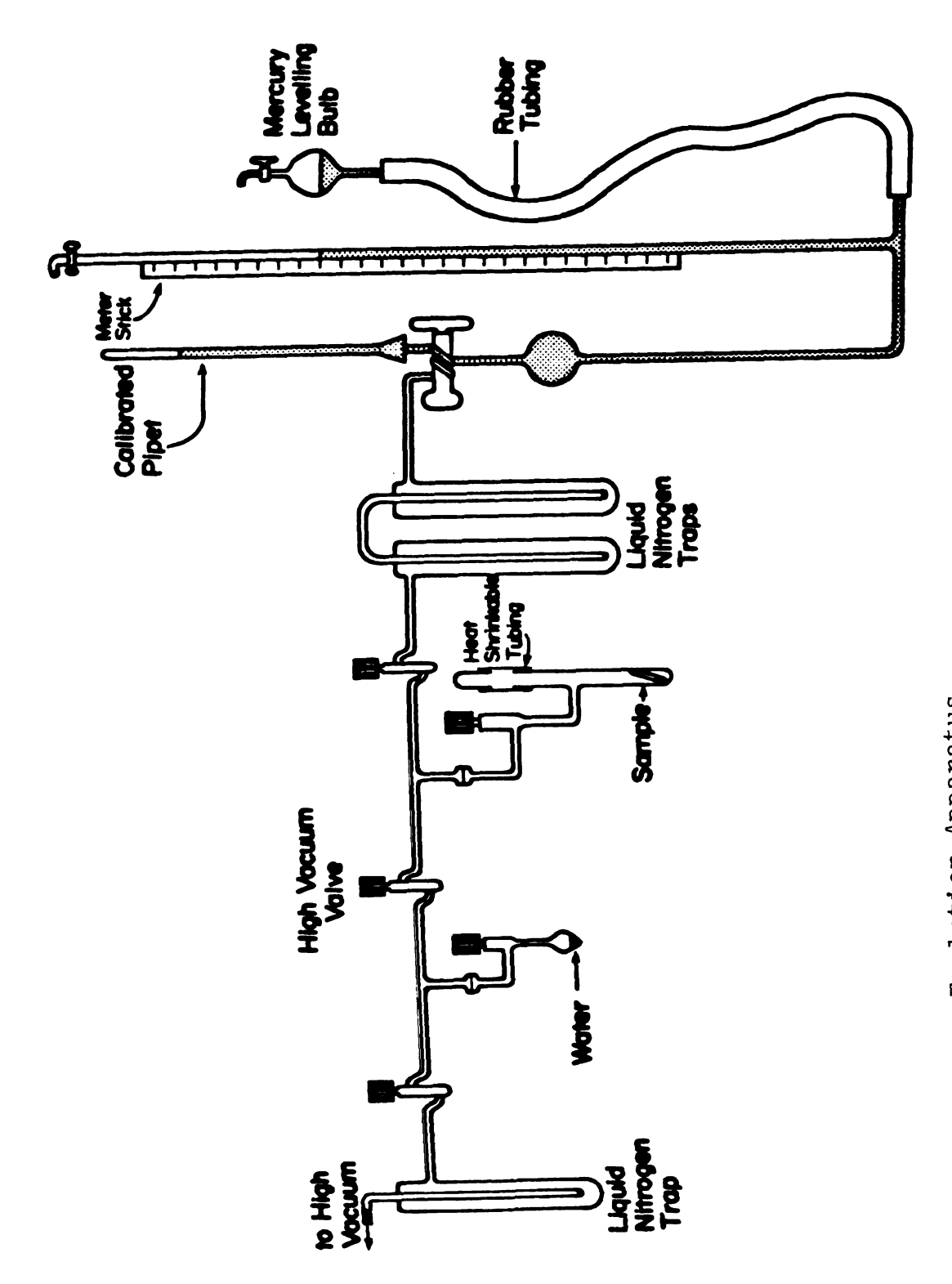


Figure 9. Hydrogen Evolution Apparatus.

(Figure 9). The sample compartment was then capped by using heat-shrink tubing (see High Vacuum Techniques and The entire system was then evacuated to 1×10^{-5} torr, thus removing any moisture that might have condensed. The sample was then moved to the heat-shrink tubing, broken at the scribe mark, and quickly moved back to the lower chilled area. After final pumping of the entire apparatus, the sample and water (degassed) compartments were isolated from the liquid nitrogen traps. water was slowly distilled onto the chilled sample. reaction was complete the Ho gas was Toepler pumped into the calibrated pipet by using the mercury-leveling bulb and the 3-way valve. Pumping was continued until no change in H_2 pressure was observed (usually 30-50 cycles). The double liquid nitrogen trap was used to prevent water from reaching the calibrated pipet. The volume, temperature, and pressure were then noted and the number of moles of H_2 was calculated by assuming ideal behavior.

II.D.3. <u>Titration</u>

After the $\rm H_2$ evolution step, a residue remains which contains alkali metal cations, complexing agent, and hydroxide ion. This residue was dissolved in water and titrated under $\rm N_2$ gas (to avoid $\rm CO_2$ absorption) with a standardized HCl solution. This pH titration was done by using a pH electrode (Corning, No. 476050) and a

digital pH meter (Orion Research, Model 701A). Graphical analysis (Figure 10) of the resultant pH curve gives the number of moles of cryptand and OH present. Care must be taken during the titration of slowly decryptated cations (see Analysis, Chapter 4). The titration of alkalide residues containing crown ethers gives only the total OH present.

II.D.4. Flame Emission Spectroscopy

The residue was also analyzed for metal content with a Jarrell-Ash Atomic Absorption/Flame Emission Spectrometer. The samples were diluted to usable concentrations with conductance water and adjusted to pH 2-3. The instrument analog signal was averaged for 10, 20, or 30 seconds to produce a digital value by using an integrator designed by Martin Rabb. A plot of the relative emission vs. concentration for standard metal samples yielded a curve from which the unknown metal concentrations were determined.

II.D.5. ¹H NMR Analysis

The residue after H_2 evolution was also analyzed for cryptand by using quantitative NMR integration (see NMR Spectrometers). This analysis technique provides another method for determining the amount of cryptand present. This method also indicates whether or not the cryptand

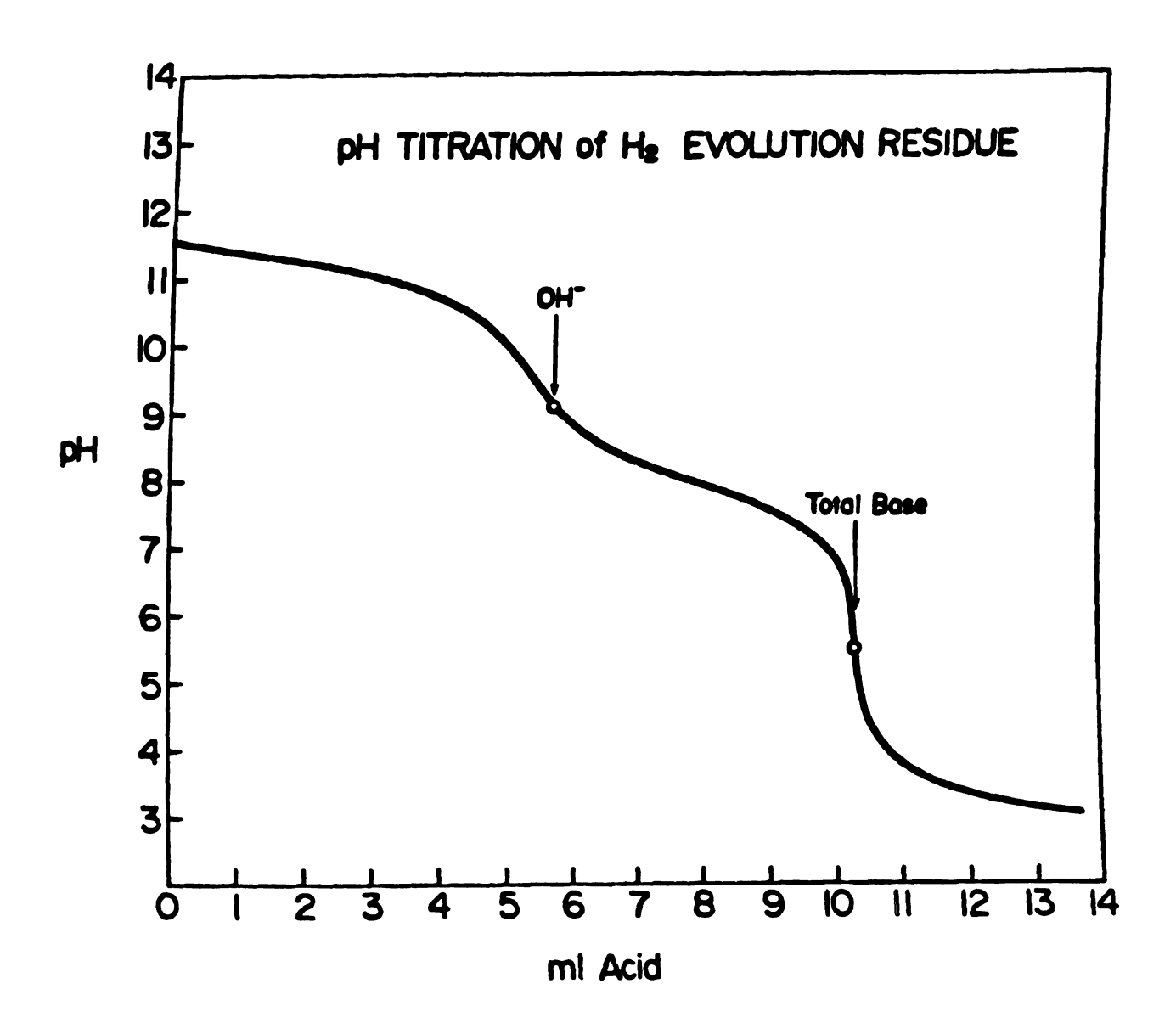


Figure 10. pH Titration Curve of H_2 Evolution Residue.

(or crown ether) had decomposed prior to or during analysis.

The internal integration standard first used was t-butanol. A weighed quantity of t-butanol was dissolved in 100 ml of D₂O to produce a solution of known concentration. An aliquot of solution from the pH titration was evaporated to dryness and dissolved in 2 ml of the standard t-butanol solution. The relative ¹H NMR integrations of the t-butanol and the complexing agent were used to calculate the amount of complexing agent present. Problems with evaporation of t-butanol from presumably tightly sealed glass containers forced a change to potassium hydrogen phthalate (KHP) as the ¹H NMR integration standard.

II.D.6. Solvent Content

Several of the compounds that precipitated from solution were suspected of containing solvent of crystallization. Any solvent present (NH3, MA, EA, iPA, tBA) would be released during H2 evolution and would distill into the double liquid nitrogen trap. To check for solvent after the H2 measurement had been completed, the contents of the trap were distilled into a vacuum bottle and a measured amount of conductance water was added. The pH of this solution was then measured. From the pH, the volume of

water, and the base hydrolysis constant of the amine solvent it was possible to calculate the amount of solvent originally present in the precipitate.

II.E. NMR Spectrometers

Three NMR spectrometers were used for this work.

Proton NMR studies were done with a Bruker WH-180 (4.228 tesla) and a Bruker WM-250 (5.872 tesla). Both are superconducting pulse and Fourier transform instruments and are completely computer controlled; the 180 by a Nicolet 1180 computer and the 250 by an Aspect 2000 computer.

Both spectrometers have multinuclear capabilities and employ internal deuterium locks.

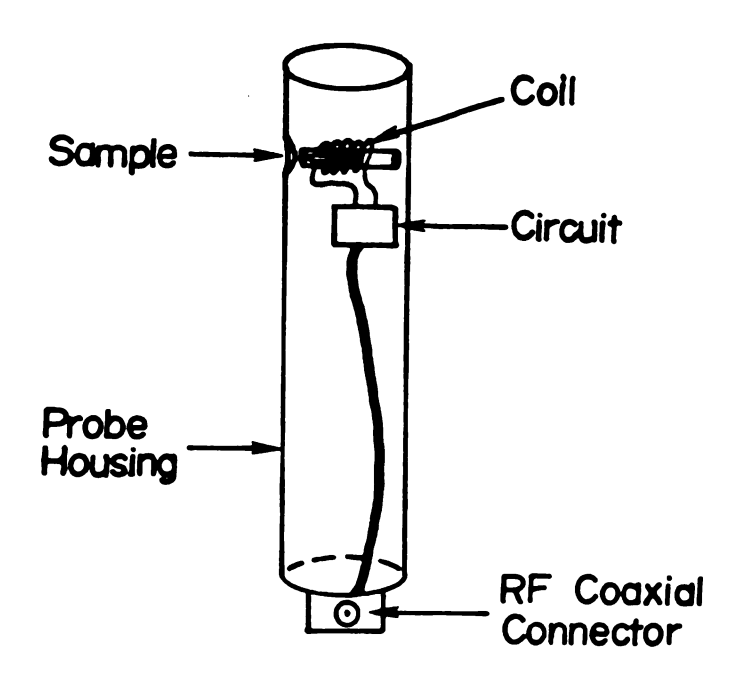
The ¹H NMR integrations were done by using the program supplied with the computer. In order to obtain reliable integrations, several precautions were taken. A small pulse width (1-3 µsec) was used to assure a uniform power distribution across the entire spectrum. The largest data block available was used (16K/180; 32K/250) to provide a long acquisition time. The smallest sweep-width, which still retained the signals of interest, was used to provide a long acquisition time. This assures completion of the free induction decay (FID) and avoids baseline distortion due to truncation of the FID. The delay between the pulse and the data acquisition was minimized to prevent artificial

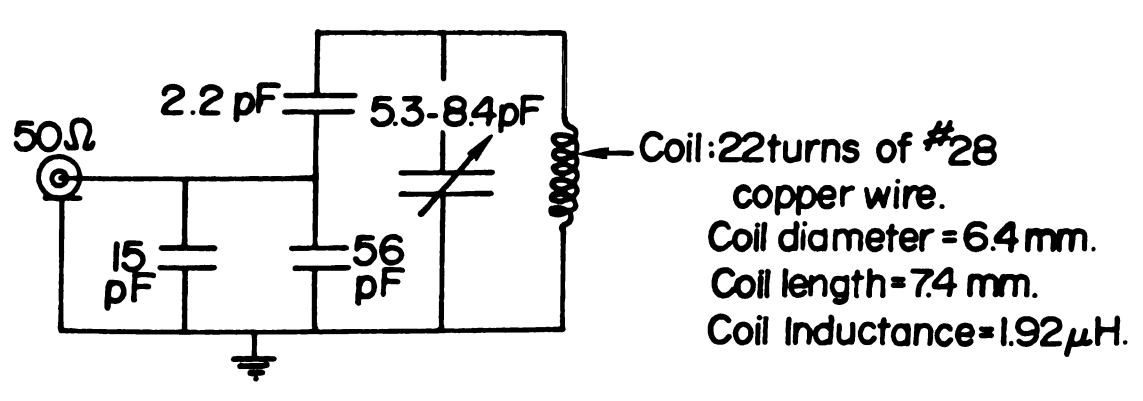
intensity decreases in the case of rapidly relaxing nuclei. The signal was time-averaged to obtain signal-to-noise ratios of 100:1 or better, and the resultant FID was transformed without exponential multiplication. Experiments using known concentrations of potassium hydrogen phthalate and C222 produced ¹H NMR integrations which were in error by less than 2%.

Metal solution NMR studies (²³Na) were done by using a greatly modified Varian DA-60 spectrometer (1.409 tesla). This instrument operates in the pulse and Fourier transform mode and uses a Nicolet 1080 computer. The system was equipped with an external lock, and a variable temperature probe. This spectrometer is described in greater detail in the Ph.D. dissertation of Dr. Joseph M. Ceraso (91).

Solid-State NMR

The solid-state NMR experiments employed the WH-180 spectrometer and a probe designed and built at Michigan State University by Wayne Burkhardt. This probe (Figure 11) contained a single coil circuit that could be tuned to resonate at 47.62 MHz (the resonance frequency of ²³Na at a magnetic field strength of 4.228 tesla). The single coil circuit design required that the coil be mounted at a right angle to the magnetic field. In order to accommodate this geometry, the sample was loaded into the coil





Impedance Matched Parellel Resonance Circuit

Figure 11. ²³Na Solid State NMR Probe.

through a hole cut into the probe housing. Once the sample was in place, the probe was carefully positioned in the bore of the superconducting solenoid. During construction of the probe, the coil was wound around a length of thin-wall glass tubing which had an inside diameter just large enough to accept a 5 mm NMR sample tube. No provisions were made for temperature control and therefore all samples were run at ambient temperatures. Saturated aqueous NaCl was used as a chemical shift reference.

II.F. X-ray Powder Patterns

X-ray powder patterns were obtained by using a Philips Electronics Instruments Model XRG-3000 x-ray generator with CuK $_{\alpha}$ radiation (λ = 1.542 Å) and MoK $_{\alpha}$ radiation (λ = 0.709 Å). Nickel and zirconium filters were used; and the generator was set to 35 kV/20 mA and 48 kV/30 mA for Cu and Mo radiation, respectively. A Debye-Scherer powder camera (Philips Electronics, 114.6 mm diameter, Model No. 170 102 00) was modified (Figure 12) to allow cold N $_{2}$ gas to chill the sample. Sample temperatures were measured with a copper-constantan thermocouple and a Doric digital readout (Model DS-350).

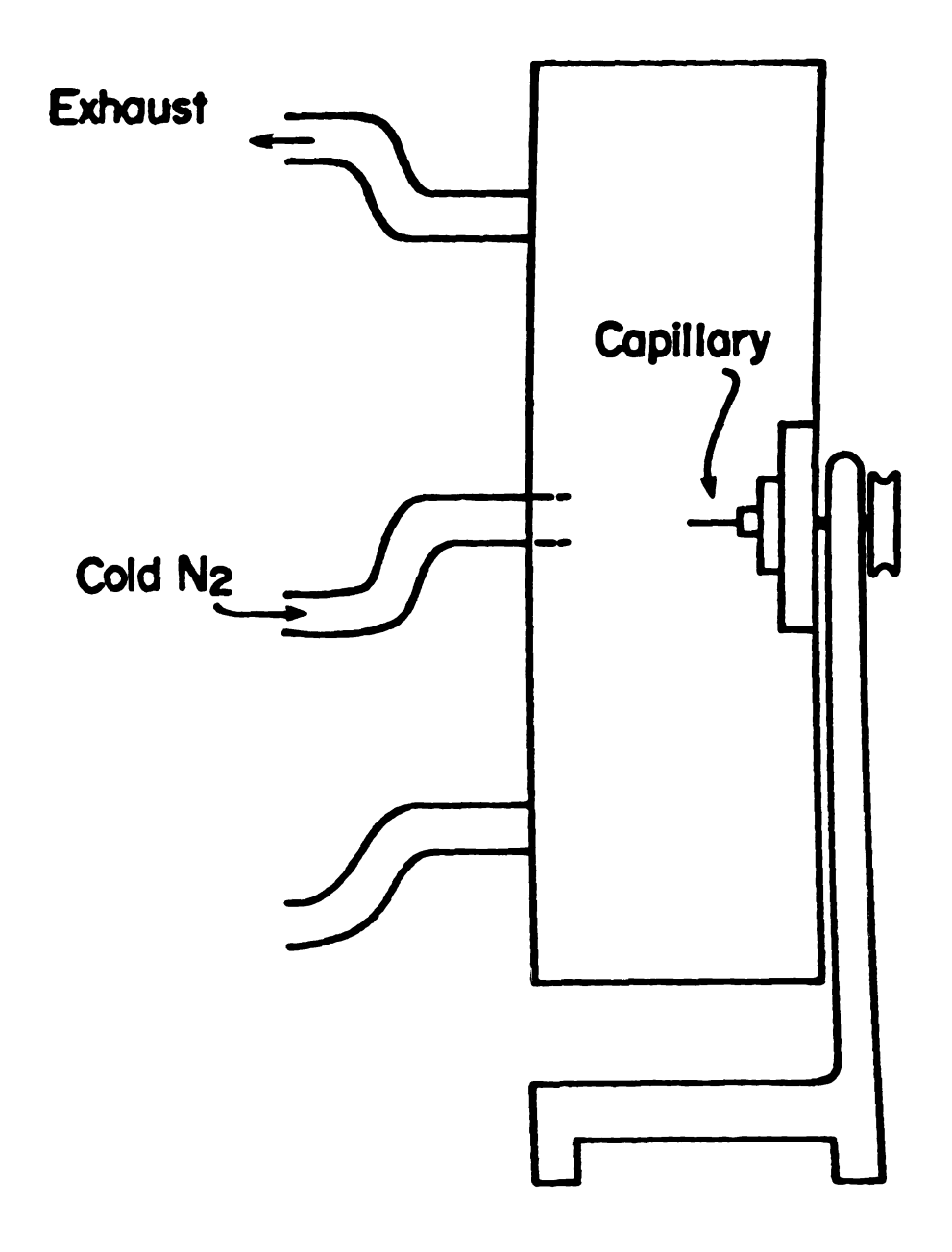


Figure 12. Cold X-ray Powder Pattern Camera.

II.G. Optical Spectra

Optical spectra of thin films prepared both from solution and by vapor deposition were recorded by using a double beam recording spectrophotometer (Beckman DK-2A). The instrument had been modified to allow temperature control of the sample compartment from -65°C to room temperature. A circulating ethanol cooler (Neslab Model LTE-9) and liquid nitrogen cooled No gas were used to chill the sample compartment. The temperature was monitored with a copper-constantan thermocouple placed near the sample. Optical spectra were obtained using fused silica, Infrasil, and Suprasil optical cells (Markson Science, Inc.). The reference beam passed through air. The spectra were baseline-corrected by subtracting the spectrum of an empty cell or the decomposed sample. Spectra were normalized by scaling the lowest absorbance to zero and the highest to 1.0.

II.H. Inert Atmosphere System

A highly modified glove box (Controlled Atmosphere Enclosures Manufacturing Co., Inc., Model 39) was used for all inert atmosphere manipulations.

The glove box was constructed of heavy gauge steel with a tempered glass viewing window, and it was equipped

with glove port doors. These features make it possible to evacuate the entire glove box. Initially the glove box atmosphere was purified by evacuation/fill cycles and use of tank argon. This method of purification was not sufficient and the system was later modified by Michael R. Yemen and Michael G. DaGue to include a circulating purification system. The system included a circulating pump to pump the argon through columns for scrubbing water (4 Å molecular sieves), oxygen (MnO/MnO₂), and small organic molecules (13X molecular sieves).

Subsequent work with alkalides, electrides, and the pure alkali and alkaline earth metals indicated that further improvements were required. First, the circulation plumbing, which had been constructed with glass, copper, and rubber tubing, had many small leaks. Second, the inability to scrub N_2 caused the formation of nitrides when Li and Ba were used in the box. Finally, thermally sensitive alkalides and electrides could not be kept cold in the glove box. In order to address these problems, a large number of modifications were made to improve the circulation system and the glove box itself. This work was made possible with the help of staff members in the Chemistry Department. They are: Russell Geyer, Ben Stutsman, Richard Menke, and Leonard Eisele (Machine Shop); Keki Mistry, Andrew Seer, and Manfred Langer (Glassblowing Shop); and Martin Rabb (Electronics Designer). A description of the glove box system, including the details

of the modifications, which form a portion of this dissertation, are presented below.

II.H.l. Circulation System

The circulation system (Figure 13) was vastly improved by using only metal and glass components. The connections between the copper tubing, stainless steel bellows, and brass bellows valves were made by using either silver solder welds or "Swagelok" connectors. The scrubbing columns were constructed of Pyrex and are connected to the circulation system with copper-to-glass seals. The circulation pump (Robbins & Meyers, Inc.) uses a hermetically sealed metal bellows (to prevent contamination) and pumps 60-75 cubic feet/hour. The entire circulation system, including the scrubbing columns and circulation pump can be isolated from the glove box and evacuated to 25 u or less. A Veeco DVIM thermocouple gauge readout and a Veeco Type TG-6 pressure gauge tube were used for all pressure measurements. After evacuation the system was refilled with argon from a compressed gas cylinder. During circulation the argon pressure in the system was regulated by using a Photohelic (Dwyer, Series 3000) switch/gauge. The photohelic is a pressure measuring device that is connected directly to the system. The gauge also has two adjustable set points; one is a high pressure limit and the other a low pressure limit. When the system pressure exceeds the

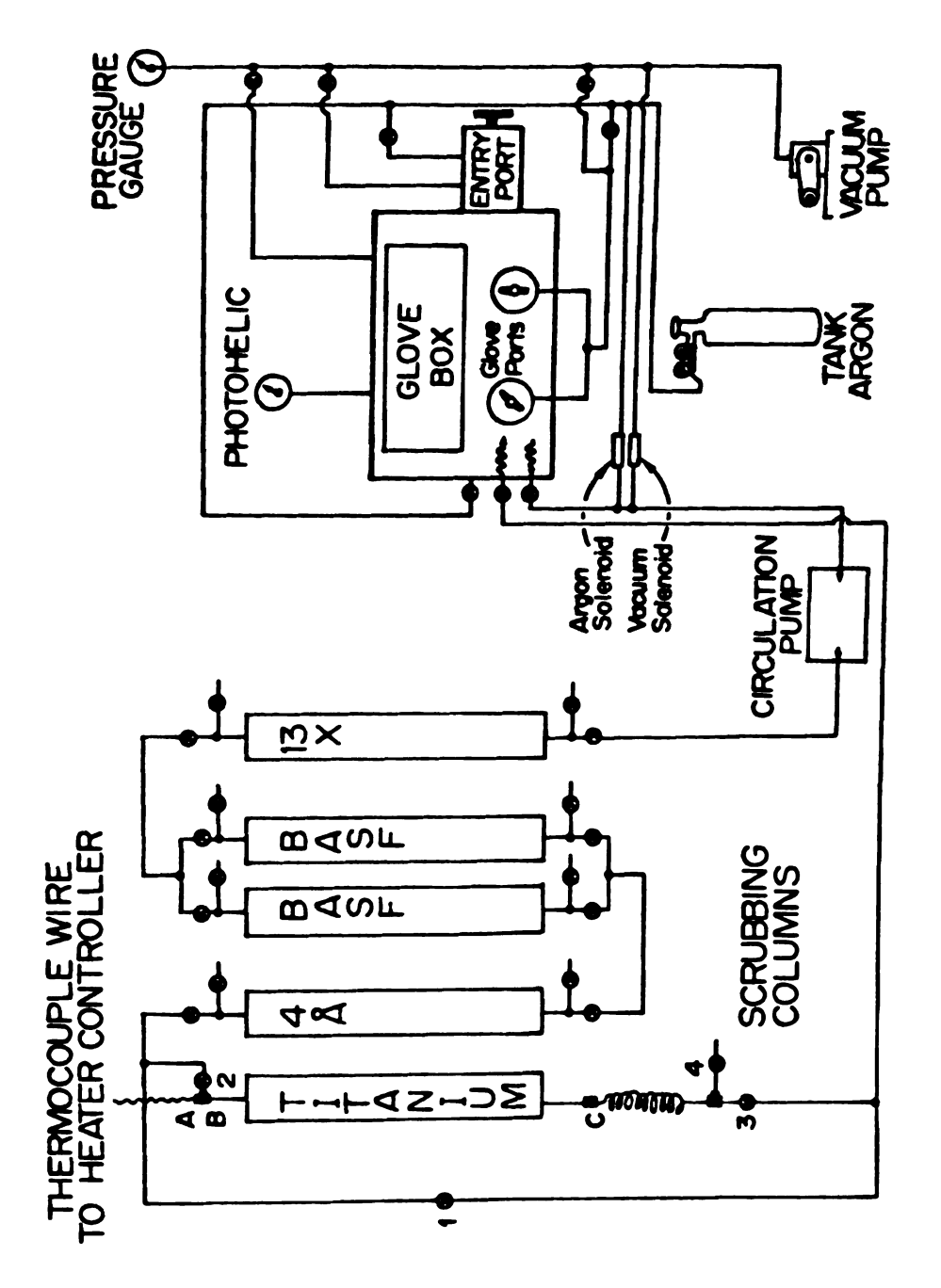


Figure 13. Glove Box Circulation System.

high pressure set point, a solenoid valve (Asco, 8262C90VM) is actuated and a mechanical vacuum pump (Cenco HV-7) removes argon from the system. Conversely, when the system pressure falls below the low pressure set point, another solenoid valve is actuated and argon is added to the system from a cylinder of compressed argon. The set points were normally set at 0 (1 atmosphere) and +3 inches of $\rm H_2O$ pressure. The system was designed for continuous circulation and only rarely requires the addition or removal of argon.

II.H.2. Scrubbing Columns

II.H.2.a. Water Removal

Water was scrubbed from the circulating argon with a Pyrex column containing 5 Kg of 4 Å molecular sieves (Union Carbide, Linde Div.). The beads were supported by a piece of metal screen at the bottom of the column. Loosely packed plugs of glass wool were used to prevent molecular sieve dust from contaminating the circulation system. The column had four ground-glass high vacuum valves. The top and bottom valves were used to isolate the column from the rest of the circulation system; and the two side valves allowed access to the sieves during regeneration. A copperconstantan thermocouple was attached to the side of the column with a high temperature furnace cement. The column

was wrapped with nichrome heating wire and had an outer coating of Fiberglass steampipe insulation. During normal operation (continuous circulation) the 4 Å column provided efficient water removal for several months.

II.H.2.b. Regeneration of 4 A Molecular Sieve Column

Even though the molecular sieves have a large water capacity, they must be regenerated from time to time. The regeneration steps are as follows:

- 1) STOP THE CIRCULATION PUMP!
- 2) Close the top and bottom valves of the 4 ${\mbox{\sc A}}$ column to isolate it from the rest of the circulation system.
- 3) Attach a thermocouple vacuum gauge to one of the side valves.
- 4) Evacuate the column through the other side valve using a liquid nitrogen trap and a mechanical pump. The pressure even after an hour may still be 1 torr or more due to argon outgassing of the sieves.
- 5) With a variable transformer apply 80 volts to the nichrome heating wires. At this voltage the column will slowly heat to 200°C over an 18-24 hour period. The pressure may rise as the sieves warm but it will begin to fall after 6-12 hours.

- 6) Allow the column to cool to room temperature (6-12 hours). The pressure will fall to 5-10 μ .
- 7) Close the two side valves.
- 8) Turn the Photohelix on.
- 9) Very slowly open the top and bottom valves to allow argon back into the column. This causes a partial vacuum in the circulation system and the Photohelix will activate the solenoid valve to admit more tank argon.

II.H.2.c. <u>Small Organic and Inorganic Gas Molecule</u> Removal

The 13X molecular sieve column (Union Carbide, Linde Div.) was used to scrub ${\rm CO_2}$, ${\rm NH_3}$, MA, etc. and any other molecule with an effective 10 Å diameter or less. This column is constructed identically to the 4 Å column.

II.H.2.d. Regeneration of 13X Molecular Sieve Column

The same method was used for the 13X column as was used for the 4 Å column except 70 volts was used to produce a temperature of 200°C .

II.H.2.e. Oxygen Removal

Molecular oxygen was removed from the circulating argon by using a Pyrex column filled with 3 Kg of BASF

catalyst R3-11 (Badische Anilin- and Soda Fibrik AG). The catalyst contains 30% highly dispersed copper metal. The removal of oxygen depends upon the reaction: Cu + $1/20_2$ + CuO; and the column regeneration depends on the reaction: CuO + H_2 + Cu + H_2 O. There are two BASF columns connected to the circulation system in parallel, so one column could be in use while the other was being regenerated. The BASF columns were constructed similarly to the 4 Å and 13X columns containing the same valve system, a thermocouple, nichrome wire, and insulation.

II.H.2.f. Regeneration of the BASF Columns

BASF catalyst has a very large oxygen scrubbing capacity. The columns used in this work required regeneration less than once a year. BASF catalyst is black when reduced and dark green when oxidized. The columns were regenerated by using the following steps:

CAUTION! REGENERATION REQUIRES THE USE OF HYDROGEN GAS. USE NO OPEN FIRES OR FLAMES AND HANG A SIGN ON THE DOOR TO THIS EFFECT.

1) Close the top and bottom valves of the column to be regenerated, isolating it from the circulation system. The top and bottom valves of the other BASF column are left open so circulation can continue uninterrupted.

- 2) Connect a piece of rubber tubing, which leads to a fume hood, to the bottom side valve of the column being regenerated.
- 3) Using a tee, connect both a compressed argon tank and a compressed hydrogen tank to the upper side valve of the column. The hydrogen tank must be equipped with a metering needle valve so the hydrogen flow can be carefully controlled.
- 4) Open the side valves and begin a slow argon flow (NO HYDROGEN) through the column and into the fume hood.
- 5) With a variable transformer, apply ∿35 volts to the Nichrome heating wires. The argon flow rate will determine the exact voltage required. Adjust the voltage until a constant temperature between 120° and 140°C is attained (usually 6-8 hours).
- 6) Without changing the argon flow rate, begin the addition of H₂. A very slow flow of H₂ will cause the column temperature to rise markedly. The flow of H₂ must be controlled at a rate such that the BASF catalyst does not exceed 230°C. Reduction of the catalyst is followed as the color changes from dark green to black. This process requires 2-5 hours. Note: If water condenses in the column, increase the argon flow rate in order to carry the water away without condensation.

- 7) When reduction is complete, as evidenced by a falling column temperature, the argon/hydrogen mixture is slowly changed to pure hydrogen. A 15-minute flow of pure hydrogen completes the reduction.
- 8) Turn the heater off.
- 9) Turn the $\rm H_2$ flow off and return to a rapid argon flow for 15 minutes to completely remove all traces of $\rm H_2$ from the system.
- 10) Turn the argon off and close both side valves, completely isolating the column. CAUTION: AT THIS POINT THE COMPLETELY REDUCED BASE CATALYST IS PYROPHORIC!
- 11) Open the top and bottom valves of the column.

II.H.2.g. Nitrogen Removal

Plans were made to remove molecular nitrogen from the circulating argon by using a stainless steel (330 alloy) column (Figure 14) filled with 2.3 Kg of titanium sponge (Vacuum Atmospheres). At the time of this writing the system had not been completed. Therefore, these instructions refer to future use when the system has been finished and tested. A titanium sponge is heated to 950°C with a ceramic-coated resistive heater (Thermcraft, Inc., No. RH 258). At this temperature the $\rm N_2$ reacts with the titanium

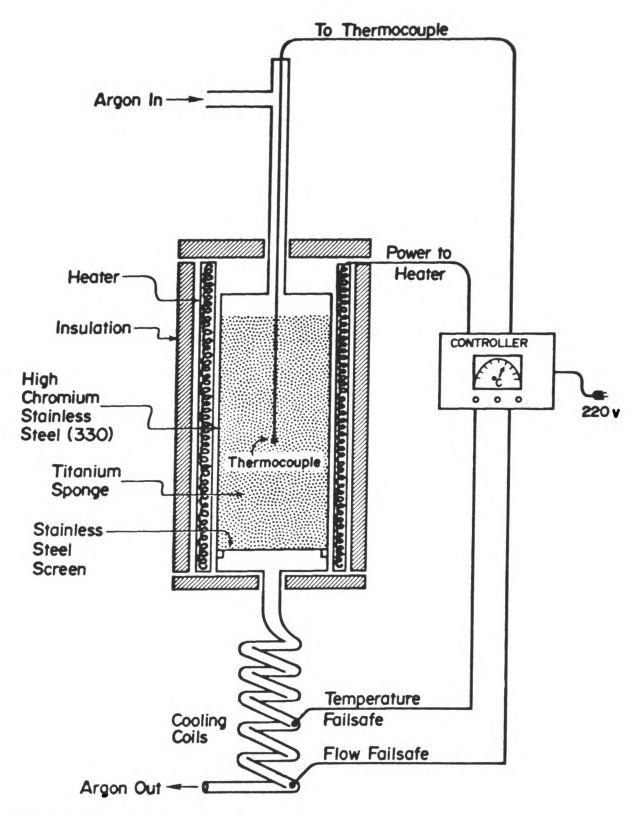


Figure 14. Nitrogen Scrubber.

to form titanium nitride and is thereby scrubbed from the flowing argon. The system was insulated with a fibrous alumina-silica material (Zircar Corp., Type ASH). Argon leaving the scrubber is cooled by flowing it through a coil of copper tubing immersed in a cold-water bath.

The heater is regulated with a home-built proportional control unit which monitors the column temperature by using a chromel-alumel thermocouple imbedded in the titanium sponge. The control unit has been designed with a "fail-safe" feature which would shut down the system by turning off the titanium heater and the circulation pump. The control unit will trigger a system shutdown if any one or more of the following conditions is detected:

- The column temperature exceeds 1000°C (which could be caused by improper operation of the control unit.
- 2) The argon circulation stops (which could be caused by a burnout of the circulation pump or a break in the circulation plumbing).
- 3) The cooling coil argon exhaust temperature exceeds 30°C (which could be caused by a loss of cooling water).

The shutdown of the system due to either a general power failure or the triggering of the "failsafe" requires an operator-initiated manual restart of the entire system.

The circulation system (Figure 13) was designed so that the $\rm N_2$ scrubber could be bypassed when $\rm N_2$ scrubbing was not required.

II.H.2.h. Regeneration of Titanium Column (Including Start-Up Procedures)

Actual regeneration of the titanium sponge is not practical. The column is regenerated by replacing spent titanium sponge with new material. The procedure for this replacement as well as instructions for system start-up are presented below.

Titanium Replacement

- 1) If the system is currently operating, turn the oven heater switch off and allow the system to continue to circulate until cool.
- When cool, open the bypass valve (Figure 13; valve #1) to allow the argon to continue to circulate without going through the N₂ scrubber.
- 3) Close the valves (Figure 13; valve #2 and #3) which will isolate the N_2 scrubber from the circulation system. The bypass valve (#1) <u>must be open</u> if the circulation pump is running.
- 4) Disconnect the thermocouple wires at the location marked "A" in Figure 13.

- 5) Disconnect the $\rm N_2$ scrubber from the circulation system at the Swagelok fittings marked "B" and "C" in Figure 13.
- 6) Pull the N_2 scrubbing column straight up and out of its holder.
- 7) Disconnect the Swagelok "T" from the top of the column and carefully pull the thermocouple straight out to avoid bending the ceramic thermocouple insulation.
- 8) Pour out the spent titanium sponge.
- 9) Replace the thermocouple and pour in fresh titanium sponge being careful to keep the thermocouple bead at the center of the titanium bed. A stainless-steel screen near the bottom of the column serves as a support for the titanium.
- 10) Reconnect the Swagelok "T" using <u>new</u> Swagelok inserts.
- 11) Return the column to its holder and reconnect it to the circulation system, using new Swagelok inserts.
- 12) Connect a mechanical pump at valve #5 (Figure 13).
- 13) Close valves #2, 3, and 4 and evacuate through valve #5, using a liquid nitrogen trap. Pump to 20 μ or less.
- 14) Close valve #5.
- 15) Turn on Photohelix.

- 16) Very slowly open valves #2 and #3 admitting argon from the circulation system into the column. This causes a partial vacuum in the circulation system, but the photohelix will admit tank argon to offset it.
- 17) When valves #2 and #3 are completely open, close valve #1 (the bypass valve).

Start-up of N2 Scrubber Oven

- 1) Turn photohelix on.
- 2) Assure that the system is ready for circulation.
- 3) Open valves #2 and #3 (Figure 13).
- 4) <u>Close</u> valves #1, 4, and 5.
- 5) Plug the circulation pump into a 110-volt outlet on the HEATER CONTROL UNIT. If the circulation pump is not plugged into the heater control unit, a "failsafe" feature is lost!
- 6) Turn the MASTER POWER switch on.
- 7) Turn the 110-VOLT POWER switch on.
- 8) Push the 110-VOLT RESET button to energize the 110-volt circuit (the circulation pump should start).
- 9) Turn the OVEN HEATER switch on.
- 10) Push the OVEN RESET button to begin oven heating. Follow the temperature on the pyrometer.
 The system should now be self-regulating with all
 "failsafe" features in operation.

Shutdown

Turn the OVEN HEATER switch off and allow it to cool with the circulating pump running. When the system is cool, the MASTER POWER switch can be turned off; however, this will also turn off power to the circulating pump.

II.H.3. Glove Box

The circulation system and scrubbing columns were designed and built to maintain a pure argon atmosphere in the glove box itself. The key features of the glove box, including standard procedures for its use, follow.

II.H.3.a. Entry Port

The entry port was of standard design. It consisted of a metal cylinder with two vacuum-tight doors, the inner opening to the glove box and the outer door opening to the room. To minimize drag-in, the following procedure was used.

The sample was placed in the entry port and the door was closed. The port was then evacuated to 20 μ or less and then refilled with argon. At least three evacuate/fill cycles were repeated with the final evacuation to 5 μ or less. After a final argon fill, the sample was brought into the glove box.

II.H.3.b. Glove Ports

Another potential source of contamination was diffusion through the rubber gloves (Buta-Sol; Norton Co.).
To prevent this diffusion (when the gloves were not in
use), the gloves were pushed into the box and the glove
port doors were closed. The gloves were then flushed
several times with argon which greatly reduces air diffusion into the glove box.

The glove port doors also make it possible to evacuate the entire glove box without damage to the gloves (see Glove Box Evacuation Procedure for details).

II.H.3.c. Cold Wells

Most alkalides and electrides are not stable at room temperature. Handling these compounds in the glove box was made possible by the construction of cold wells in both the entry port and the glove box itself. The cold wells were constructed from 4"-diameter brass cylinders. A flat brass bottom was silver soldered in place. Viton O-rings were used to make a vacuum-tight seal between the well and the glove box. The wells were filled with loosely packed copper wool and cooled from the outside with dry ice/isopropanol baths (-78°C). Samples were pushed down into the copper wool, making good thermal contact. The temperature of the cold well was monitored with a copperconstantan thermocouple. The thermocouple wire was

brought out of the glove box via a high-vacuum thermo-couple feedthrough. The temperature of the copper wool 1" below the top surface was -60°C when a dry ice-cooling bath was used.

A potential problem was the condensation of water into the cold well of the entry port during sample loading.

Two methods were used to minimize water condensation. Because the samples must be kept cold at all times, both methods require the cold wells to be pre-chilled with dry ice/isopropanol baths.

Method 1. The sealed-glass ampoule containing the sample was stored in an acetone bath at -80°C just prior to loading. The entry port door was opened to the room simultaneously with a very high flow rate argon flush of the port. The rapid flow of argon out of the port minimizes the amount of room moisture that can condense in the cold well. The sample was immediately removed from the cold acetone and pushed into the cold copper wool in the cold well. The port door was closed as the flow of argon was stopped. The port was then evacuated until the pressure reached $\sim 3 \mu$ ($\sim 45 \text{ minutes}$). Five more fill/evacuate cycles followed, the final one to 1 µ. The port was then filled with argon, the inner door was opened, and the sample was rapidly transferred to the cold well inside the glove box (no frost was observed).

Method 2. A plastic glove bag containing the sample (in a $1-N_2$ dewar) was attached directly to the entry port so the port door would open into the glove bag. The bag was flushed with dry argon (or N_2) several times. The port door was then opened, and the sample was then transferred rapidly from the $1-N_2$ to the copper wool. Evacuation of the entry port followed as described for Method 1.

II.H.3.d. Millibalance

In order to weigh small samples (see Metals) in the glove box, an electrobalance was installed (Cahn, Model DTL). The balance had three ranges: 0-1000 mg ± 1 mg, 0-100 mg ± .1 mg, and 0-10 mg ± .01 mg. The power input to the balance was brought into the glove box via a high-vacuum electrical feedthrough. The analog output signal of the balance exited the box through another high-vacuum electrical feedthrough and was then converted to digital form by using a digital voltmeter (Datel, DM-4100N). The balance was permanently installed in the glove box and can be evacuated without damage.

II.H.3.e. Glove Box Evacuation Procedure

The following method was used to evacuate the glove box and to check for leaks after all the modifications were made to the glove box. This method can also be used to clean the glove box in the event of massive air contamination (i.e., a large hole in a glove).

- 1) Close the valve to the Photohelic. The metal bellows in the Photohelic is permanently damaged if evacuated.
- 2) Close the outer entry port door.
- 3) Stop the circulation pump.
- 4) Close the argon entry and exit valves, thereby isolating the glove box from the circulation system.
- 5) Cover the glove box viewing window with the plastic safety shield.
- 6) Close both glove port doors.
- 7) Partially open the main box evacuation valve, the entry port evacuation valve, and the glove port evacuation valve. During evacuation it is important to keep the pressure inside the box and inside the gloves nearly equal to avoid damage to the gloves. Careful control of the evacuation rates on both sides of the gloves is possible by partial opening or closing of the evacuation valves. This must be mointored continuously until the pressure is down to 20 torr. The glove box can be evacuated to 10 μ or less.

Refilling the glove box with argon requires the same care to avoid damage to the gloves. Argon must be admitted

simultaneously to the glove box and the gloves. Equal pressure can be maintained by control of the flow rate through the argon inlet valves. When the glove box is back to a pressure of 1 atmosphere of argon, the 2 valves leading to the circulation system can be reopened. The valve leading to the Photohelic can then be opened and circulation begun.

III. SYNTHESIS

INTRODUCTION

The first crystalline compound containing an alkali metal anion, Na[†]C222·Na⁻, was observed in 1973 by Ceraso (79). Investigation of this compound by Tehan (92) and Ceraso resulted in an elemental analysis and a crystal structure (80). Since then other researchers have observed several crystalline precipitates. Both H. L. Lewis and P. B. Smith (93) observed gold-colored precipitates believed to be Rb C222·Na and K C222·Na. In 1975 J. L. Dye observed a metallic gold precipitate of K+C222·K- while working in the laboratories of J.-M. Lehn in Strasbourg, France. This was the first evidence that crystalline compounds could be formed which contained alkali metal anions other than Na. Since that time observations have indicated that it might be possible to synthesize an entire family of alkalides. M. T. Lok (90) observed gold crystals precipitated from a solution containing rubidium metal and C222 only; presumably Rb + C222 · Rb -. P. B. Smith also observed a crystalline precipitate believed to be Cs⁺C222·Cs⁻. However, at this point the only compound that had been analyzed was Na⁺C222·Na⁻.

In addition to the work on alkalides, the synthesis and characterization of electrides was also progressing.

M. G. DaGue (85) used optical spectra, magnetic susceptibilities, and ESR to characterize K⁺C222·e⁻; and J. S. Landers (84) used similar techniques to characterize Li⁺-C211·e⁻. D. S. Issa used these same techniques to study Cs⁺18C6·e⁻ (94).

The desire to synthesize and characterize an entire series of alkalides and electrides made it important to devise a systematic synthetic approach. However, the extreme reactivity of these compounds and their solutions created a variety of very difficult experimental problems which had to be dealt with when devising a synthetic scheme. The techniques and equipment described here were used in a joint effort with L. D. Le and D. S. Issa to overcome these problems (135).

Two synthetic approaches were used. The first method was the precipitation of either alkalide or electride from an amine solvent in which the appropriate metal(s) and complexing agent had been dissolved. This was the primary method used and is representative of the vast majority of the work presented here. The second synthetic method used was the vapor phase co-deposition of metal and complexing agent on an inert substrate to form the appropriate alkalide or electride. This method was not used for bulk synthesis but instead was designed primarily to test the feasibility of completely solvent free vapor synthesis (95).

III.A. Synthetic Problems

The most difficult problem in the synthesis of alkalides and electrides is decomposition. Solutions of alkalides and electrides in amine solvents are thermodynamically unstable with respect to reduction of the solvent to form hydrogen and an amide. The complexation agents, even though very resistant to reduction, are also susceptible to irreversible decomposition by solvated electrons and alkali metal anions. However, kinetically stable solutions can be prepared if solvent, metal, complexing agent, and reaction vessels are rigorously free of easily reducible impurities and other decomposition catalysts. In order to meet these requirements and attain acceptable solution stabilities, the following techniques and equipment were used in the synthesis of alkalides and electrides. (See Experimental for a more detailed description of the techniques used.)

III.A.l. Purification and Handling of Metals

The metals, purchased in break-seal ampoules, were distributed into small diameter glass tubing by using the "Trombone" apparatus (Figure 7). The distribution of the metals was done under high vacuum to avoid oxidation and reaction with water vapor. This technique also makes it possible to obtain known amounts of metal which are contained in short lengths of glass tubing sealed at both ends.

These sealed ampoules can be introduced into the synthesis apparatus by using heat-shrinkable Teflon tubing. This tubing remains flexible when evacuated and allows the metal ampoule to be broken under vacuum and admitted to the synthesis apparatus, thus preventing reaction with atmospheric gases. The metals used were then distilled under vacuum directly into the synthesis vessel as a final purification step.

Both sodium and potassium can be purified by vacuum distillation but rubidium and cesium cannot be freed of oxides during distillation. The oxides of rubidium and cesium do not remain behind during distillation but instead decompose to the metal and oxygen which can then recombine during condensation. This makes it imperative that these metals be free of oxides prior to distillation into the synthesis vessel, and that they be distilled under dynamic vacuum.

Both lithium and barium metals react with Pyrex and quartz when heated and therefore cannot be transferred or purified by distillation. Small samples of these metals were distributed into glass ampoules in an argon glove box (nitrogen must be avoided due to nitride formation). The metals were cut, weighed, and placed into glass ampoules. The ampoules were then capped by using polyolefin heat-shrinkable tubing and removed from the glove box. Following a flame seal-off to remove the heat-shrinkable

tubing, the ampoules were introduced into the synthesis apparatus as with other metals. However, these metals are not distillable and must be dissolved directly.

These techniques make it possible to introduce reactive metals free of impurities due to reaction with atmospheric gases. Metals of the required purity (99.9% or more) are commercially available. When transfers are made by using the above techniques, solution decomposition due to impurities in the metal is largely eliminated.

III.A.2. Purification of Solvents

The solvents used for synthesis are susceptible to reduction by M⁻ and e⁻. This reduction is slow in favorable cases only if the solvent is free of easily reductible impurities and other impurities which catalyze the reduction. These impurities were removed by treatment with CaH₂ and Na/K alloy. These two reducing agents are effective in the prior reduction of all reducible impurities and allow the pure solvent to be distilled away from the reduced impurities. After these treatments, the solvents were stored in vacuum storage bottles equipped with high vacuum valves. Solvents such as pentane and ethers were stored over Na/K alloy but amine solvents, even if rigorously pure, cannot be stored over Na/K alloy due to the slow decomposition of the solvent.

III.A.3. Purification of Complexing Agents

The complexing agents used in synthesis are themselves susceptible to reduction. However, these organic compounds are quite resistant to reduction if free of impurities. The solid complexing agents, 18C6 and C222, were purified by sublimation (18C6 was recrystallized from acetonitrile prior to sublimation). The liquid complexing agents, C211, C221, and C322, were purified by high vacuum molecular distillation. Because these complexing agents absorb water and carbon dioxide and are light-sensitive, they were stored under vacuum in the dark.

III.A.4. Glassware Cleaning

Both Pyrex and fused silica vessels were cleaned with a hydrofluoric acid cleaner followed by treatment with aqua regia and were thoroughly rinsed with distilled water. This cleaning method has been very effective in minimizing metal solution decomposition. All glassware, which was used for metals, complexing agents, solvents, and metal solutions was cleaned in this way.

III.A.5. Solution Thermal Stability

As mentioned earlier, metal solution decomposition is thermodynamically favored. This process can be partially eliminated by the meticulous use of high vacuum techniques Decomposition can be further reduced by cooling the metal solutions. Many solutions of alkali metals in amine solvents are stable almost indefinitely (months) at dry ice temperatures. However, the advantages of increased thermal stability at low temperatures is partially offset by the experimental difficulties of working at these temperatures. The two major difficulties encountered are the design of glassware compatible with these temperatures and the kinetics of dissolution and complexation of the metals.

III.A.5.a. Glassware Design

The glassware used for synthesis was constructed of either Pyrex or fused silica. Each reaction vessel was equipped with a high vacuum valve. Evacuation of the synthesis apparatus not only permits the distillation of metal(s) and solvent but also provides a convenient method for removing atmospheric gases. The admission of trace amounts of water or oxygen can catalyze complete metal solution decomposition.

The extraction of sodium from borosilicate glass by metal solutions (96) frequently causes problems during spectroscopic work. In these cases the use of fused silica vessels is recommended. However, during bulk synthesis the small amount of sodium contamination from borosilicate glass is usually negligible.

The specific design of glassware for low temperature synthesis is severely limited. Glassware must be constructed to allow all areas in contact with metal solutions to be immersed in a cold bath. Care must be taken to assure that the high vacuum valve need not also be immersed. Cooling the Teflon valve stem causes it to shrink and open to the atmosphere. These design restrictions are more severe than they might appear. The entire synthesis from starting materials to the final isolation of solvent-free crystals or powder must take place in one single piece of vacuum-tight glassware. Thus, each synthesis vessel must contain chambers for all stages of synthesis. For example, the synthesis of an alkalide requires chambers for the metal and complexing agent, as well as areas for their distillation if required. In addition, a compartment is required for the solvent and the dissolution of starting materials. A compartment for precipitation of the alkalide is required as well as a chamber for the removal of the mother liquor after precipitation. The alkalide must also be rinsed and dried before it is distributed into small tubes which can be flame sealed and removed from the apparatus under vacuum. Compartments for all these manipulations must be present in one piece of glassware which is both evacuable to 1×10^{-5} torr and completely immersible in a cold bath (except for the vacuum valve).

III.A.5.b. Solution Kinetics

The synthesis of alkalides and electrides by precipitation from solution requires that both the metal(s) and the complexing agent be dissolved. This frequently poses serious kinetics problems if the synthesis is carried out at low temperatures. The rate at which alkali metals dissolve in amine solvents can be prohibitively slow at reduced temperatures. For example, during the synthesis of Na⁺C221·Na⁻ the dissolution of sodium in ethylamine at -10°C required √20 hours. Because solution decomposition competes with metal dissolution, syntheses that require large amounts of time can result in partial if not complete decomposition.

Frequently the kinetics of metal cation complexation can be an equally serious problem. Even in cases where the metals dissolve rapidly, the rate at which the cations are complexed could be slow. Care must be taken to assure that equilibrium has been established before further synthetic steps are taken. Observations made in this laboratory (84) indicate the rate of complexation of Li⁺ by C211 in methylamine may be very slow at -40° C. The half-life (t_{1/2}) for this reaction has been estimated to be 2 hours or more. Lithium dissolves rapidly in methylamine to form a dark blue solution which shows no visible changes as the slow complexation reaction proceeds.

Formation constants for the complexes of alkali metals

with cryptands are usually very large and at equilibrium essentially all the cations will be complexed. Table 3 contains data on the thermodynamics and kinetics of several complexation reactions in water. The rate constants were extrapolated to -40, -80, and -100°C by using Equation (6).

$$k_{T_2} = k_{T_1} \left(\frac{T_2}{T_1} \right) e^{-\Delta H^{\neq}} \left(\frac{1}{T_2} - \frac{1}{T_1} \right)$$
 (6)

Unfortunately few rate data are available for the solvents used in alkalide and electride synthesis (NH $_3$, CH $_3$ -NH $_2$, CH $_3$ -CH $_2$ -NH $_2$, and (CH $_3$) $_2$ -CH-NH $_2$). The rates in water can serve as a guide for choosing potentially slow reactions in these other solvents. In hypothetical liquid water at -80°C the half-life (t $_{1/2}$) for the formation of Li $^+$ C211 is $^+$ 3 minutes. It is likely that the complexation rates in the amine solvents are slower than in water (Li $^+$ -C211 in CH $_3$ -NH $_2$, t $_{1/2}$ $^+$ 2 hours). The Gutmann donor numbers (97) for these amine solvents are much higher than that of water. Higher Gutmann donor numbers may increase the $^+$ 4 of the complex formation reaction and thereby decrease the rate of complexation.

Another kinetics problem can arise that depends upon the order in which the metals are dissolved. For example,

Thermodynamic and Kinetic Data for the Complexation of Alkali Metals in Water. Table 3.

				+	
Complex	Уо	kf	k	1/2 (formation) seconds	(dissoc.) seconds
Li [†] C2ll;K _{eq} =3.2xl0 ⁵ AH [≠] =15600 cal AH [≠] =20700 cal	298 233 193	1.0x10 ⁺³ 5.0x10 ⁻¹ 3.7x10 ⁻⁴	4.9x10 ⁻³ 2.2x10 ⁻⁷ 1.7x10 ⁻¹¹	6.9x10 ⁻⁴ 1.4x10 ⁰ 1.9x10 ⁺³	1.4x10 ⁺² 3.1x10 ⁺⁶ 4.2x10 ⁺¹⁰
Na ⁺ C222;K _{eq} =7.9x10 ³ AH [≠] =8700 cal AH [≠] =16100 cal	298 233 193	1.2x10 ⁺⁶ 1.5x10 ⁺⁴ 2.5x10 ⁺²	1.5x10 ² 5.9x10 ⁻² 3.5x10 ⁻⁵	5.9x10 ⁻⁷ 4.6x10 ⁻⁵ 2.8x10 ⁻³	4.7x10 ⁻³ 1.2x10 ⁺¹ 2.0x10 ⁺⁴
K ⁺ C222;K _{eq} =3.8x10 ⁵ ∆H≠=9300 cal ∆H≠=14000 cal	298 233 193	3.0x10 ⁺⁶ 2.9x10 ⁺⁴ 3.7x10 ⁺²	7.8x10 ⁰ 8.3x10 ⁻³ 1.3x10 ⁻⁵	2.3x10 ⁻⁷ 2.4x10 ⁻⁵ 1.9x10 ⁻³	8.9x10 ⁻² 8.3x10 ⁺¹ 5.5x10 ⁺⁴
Ba ²⁺ C222; K _{eq} =3.2x10 ⁹ ΔH ⁷ =6800 cal ΔH ⁴ =20900 cal	298 233 193	7.0x10 ⁺⁴ 2.2x10 ⁺³ 8.7x10 ⁺¹	2.2x10-5 9.1x10-10 6.2x10-14	9.9x10 ⁻⁶ 3.1x10 ⁻⁴ 8.0x10 ⁻³	3.2x10 ⁺⁴ 7.6x10 ⁺⁸ 1.1x10 ⁺¹³

during the synthesis of K⁺C222·Na⁻ ethylamine can be used to dissolve Na, K, and C222. This solvent will support only a very low concentration of solvated electrons so the predominant solution species will be Na⁺C222, K⁺C222, Na⁻ and K-. The formation constant for K+C222 in an amine solvent is much larger than that of Na⁺C222 so at equilibrium the solution should consist primarily of K+C222 and Na-. However, if during synthesis the sodium were dissolved first or if the sodium dissolved more rapidly than the potassium metal, the initial solution could contain large amounts of Na⁺C222 and very little K⁺C222. In order for the thermodynamically favored species, K+C222, to form, Na+C222 must first dissociate. At low temperatures the rate of decomplexation of Na⁺C222 would be expected to be very slow and large amounts of time would be required to reach equilibrium. For example, extrapolation of the data for the rate of dissociation of Na⁺C222 in water to -80°C yields $t_{1/2}$ \sim 6 hours. If, during synthesis such a solution were further cooled or a co-solvent were added to cause precipitation before equilibrium had been reached, a mixture of Na + C222 · K - and K⁺C222·Na would probably be formed.

III.A.6. Crystallization Problems

When possible, one should dissolve the metal and complexing agent directly in a solvent from which crystals can easily be precipitated. For example, appropriate amounts

of Na and C222 dissolve directly in ethylamine at 0°C to form a saturated solution that will precipitate Na⁺C222. Na when cooled to -78° C. The preparation of other solutions is experimentally more difficult. Most solutions are less stable than Na⁺C222·Na⁻ solutions and during synthesis dissolution of metal and complexing agent must be carried out at lower temperatures to avoid irreversible decomposition. The use of ammonia, which readily dissolves the metals, is acceptable for electride synthesis, but may cause problems for alkalide synthesis. Because ammonia is a "good" solvent, it favors dissociation of M to form M to and e_(SOLV). Solution optical spectra indicate that appreciable concentrations of alkali metal anions are not present in liquid ammonia. During the synthesis of electrides, ammonia is frequently the solvent of choice because its use eliminates problems due to alkali metal anion contamination. In alkalide synthesis the use of ammonia to hasten metal dissolution is useful. However, the ammonia must be replaced by a "poorer" solvent which will not support high concentrations of $e_{(SOLV)}^{-}$ before crystallization of the alkalide salt.

The irreversible reduction (decomposition) of complexing agents by solvated electrons appears to be more rapid than the similar reduction by alkali metal anions. For this reason, the synthesis of electrides must be carried out at lower temperatures than is the case with alkalides.

For alkalide synthesis, the total removal of ammonia or methylamine (used to hasten metal dissolution) can lead to extensive decomposition. Gradual replacement by successive condensation of the less volatile solvent and removal of the more volatile by partial distillation is better but can be very time-consuming with consequent increases in decomposition. Finally, the use of solvent replacement techniques can lead to precipitation of free metal with the result that alkalide crystals are contaminated with free metal and/or electride. For example, early attempts to synthesize Li + C211 · Na used ammonia to hasten the dissolution of Li and Na metals. Isopropylamine was then added to promote formation of Na and cause precipitation. Li C211 Na crystals formed by this method were consistently contaminated with Na metal. In order to solve the problem, methylamine was used in place of ammonia to dissolve the metals and cryptand. Since the dominant negative species in such solutions is Na, gradual replacement of methylamine by isopropylamine simply decreased the solubility of Li + C211 · Na without significant complications from e and Na and without appreciable precipitation of sodium metal. In order to avoid contamination, it is advisable to select a crystallization solvent in which all species are completely dissolved before the temperature is reduced to cause crystallization.

III.A.7. Handling of Solvent-Free Crystals and Powders

The alkalides and electrides, once formed, are in most cases not stable at room temperature and must be stored cold and under vacuum. The handling of these compounds for analysis and other measurements must then be done under these same conditions. When synthesized for analysis only, the entire synthesis occurs in one piece of glassware and the resulting sealed glass ampoules are introduced into the H₂ evolution apparatus while still cold and under vacuum. All other manipulations were carried out in an argon glove box equipped with cold wells (see Experimental section).

III.B. Strategies for Synthesis

An experimental strategy for the synthesis of an entire family of alkalide salts must take into account the problems of stability, kinetics, and solution equilibria mentioned above. In order to develop such a strategy, it is helpful to have a solution model which describes the chemical species present in solution. Several techniques are particularly useful for the identification of solution and solid-state species. Solution spectra, solvent-free thin film spectra, and alkali metal NMR (all discussed in Chapter 1) are particularly useful for determining which chemical species are present in amine solvent systems

which contain alkali metals and complexing agents. Because the primary synthetic method is precipitation from solution, a knowledge of the solution species enables one to predict which compounds are likely to precipitate.

The synthesis of alkalide salts has been greatly aided by the ability to measure transmission spectra of thin solvent-free films produced by rapid solvent evaporation (64,71-73,83,98). These spectra permit ready identification of particular alkalides and also indicate when trapped electrons are likely to be present. An example of the utility of film spectra is provided by the salt K⁺C222·Na⁻. Equimolar solutions of sodium, potassium and C222 in methylamine probably contain primarily K[†]C222 and Na⁻, which is favored over Na[†]C222 and K⁻ both because of the greater stability of the K⁺C222 complex (99) compared with the Na C222 complex and because Na is much more stable than K (83). When such a solution is rapidly evaporated, the transmission spectrum of the resulting solvent-free film clearly shows the presence of Na with little or no K (73) and indicates that the crystals described here are probably K+C222·Na rather than Na C222·K. Thin film spectra also permit predictions to be made about stabilities in the presence of various complexing agents. Films of K⁺C222·Na⁻ were unstable above -10°C, suggesting that the corresponding crystals might also be thermally unstable. as is indeed the case, and because of instability, a

number of attempts were required to obtain reasonably pure crystals of this salt. By contrast, Li⁺C2ll·Na⁻, Cs⁺18C6·Na⁻, and Cs⁺C322·Na⁻ formed films that were stable up to room temperature. Crystals of these three alkalides proved to be much more stable than many of the others described here. However, crystals of Na⁺C222·Na⁻, the first alkalide prepared, remain the most stable alkalide crystals to date. Recent studies (Issa and Ellaboudy) show that this record may be challenged by Cs⁺18C6·Na⁻ and Rb⁺18C6·Na⁻. Very recently, M. Tinkham has synthesized Rb⁺(15C5)₂·Na⁻ which is actually more stable than Na⁺C222·Na⁻.

The choice of the most appropriate cryptand for a particular alkali cation can be made by reference to a table of the formation constants for various cation/cryptand pairs as represented graphically in Figure 3. Typically, the cryptand with the largest formation constant would be chosen for a particular cation. However, in several cases different choices were made. These other choices were usually made for reasons of cost or ease of handling.

Once metal(s), solvent(s), and complexing agent are chosen, the glassware must be designed in order to accommodate the entire synthesis. The appropriate temperatures were chosen on the basis of film spectra results as well as on a trial and error basis which indicated which temperature produced the most rapid dissolution of metal and complexing

agent consistent with minimal solution decomposition.

The typical sequence for synthesis involves the dissolution of the complexing agent, followed by the dissolution of the alkali metal (or metals). Then either by cooling, removing some solvent, or adding a co-solvent the desired crystals are precipitated from solution. Then the mother liquor is poured away and the crystals are rinsed in a different solvent (usually diethylether). The crystals are then dried and distributed into a tube or tubes built directly into the apparatus.

Thermochemical calculations indicate that suitable alkalide salts (Li through Cs) should be stable with respect to the free cryptand and metal. However, in some cases the reaction

$$M^{+}C \cdot N_{(S)}^{-} \rightarrow M^{+}C \cdot e_{(S)}^{-} + N_{(S)}$$
 (7)

in which M⁺C·e⁻ is an electride appears to be thermodyn-amically favorable. None of these calculations takes into account the ubiquitous irreversible decomposition of the complexing agent by M⁻ and/or e⁻, which is always thermodynamically possible, but may be slow under favorable circumstances. Laboratory experience indicates that lithium always forms electrides rather than lithide salts and that potassides, rubidides, and cesides have a much greater tendency to decompose irreversibly than do sodides.

III.C. Compounds Studied

III.C.1. Na⁺C222·Na⁻

This compound, although previously prepared by a number of workers in this laboratory, was synthesized here for the thermochemistry measurements described in Chapter 6. The synthesis of Na⁺C222·Na⁻ is described in detail below to illustrate the synthetic method used for a well-behaved alkalide salt.

First, 3.34 mmol of cryptand [2,2,2] was added through the sidearm of the apparatus shown in Figure 15. The sidearm was then removed with a flame seal-off. A sealed glass ampoule containing excess sodium metal, 7.0 mmol was scribed with a glass knife and put into the metal sidearm. The sidearm was then capped with heat-shrinkable tubing. The apparatus was connected to a vacuum manifold through a T-trap (Figure 5; Chapter 2) and evacuated to 1×10^{-5} torr. The metal ampoule was broken at the scribe by bending the heat-shrinkable tubing and then moved into the sidearm. A flame seal-off was then made behind the ampoule to remove the heat-shrinkable tubing. The sodium was then distilled under dynamic vacuum through the sidearm into the metal chamber and the sidearm was removed by a flame seal-off. Ethylamine (70 ml) was then distilled into the cryptand chamber by cooling this chamber to -10°C with an isopropanol bath. The cryptand was dissolved and the

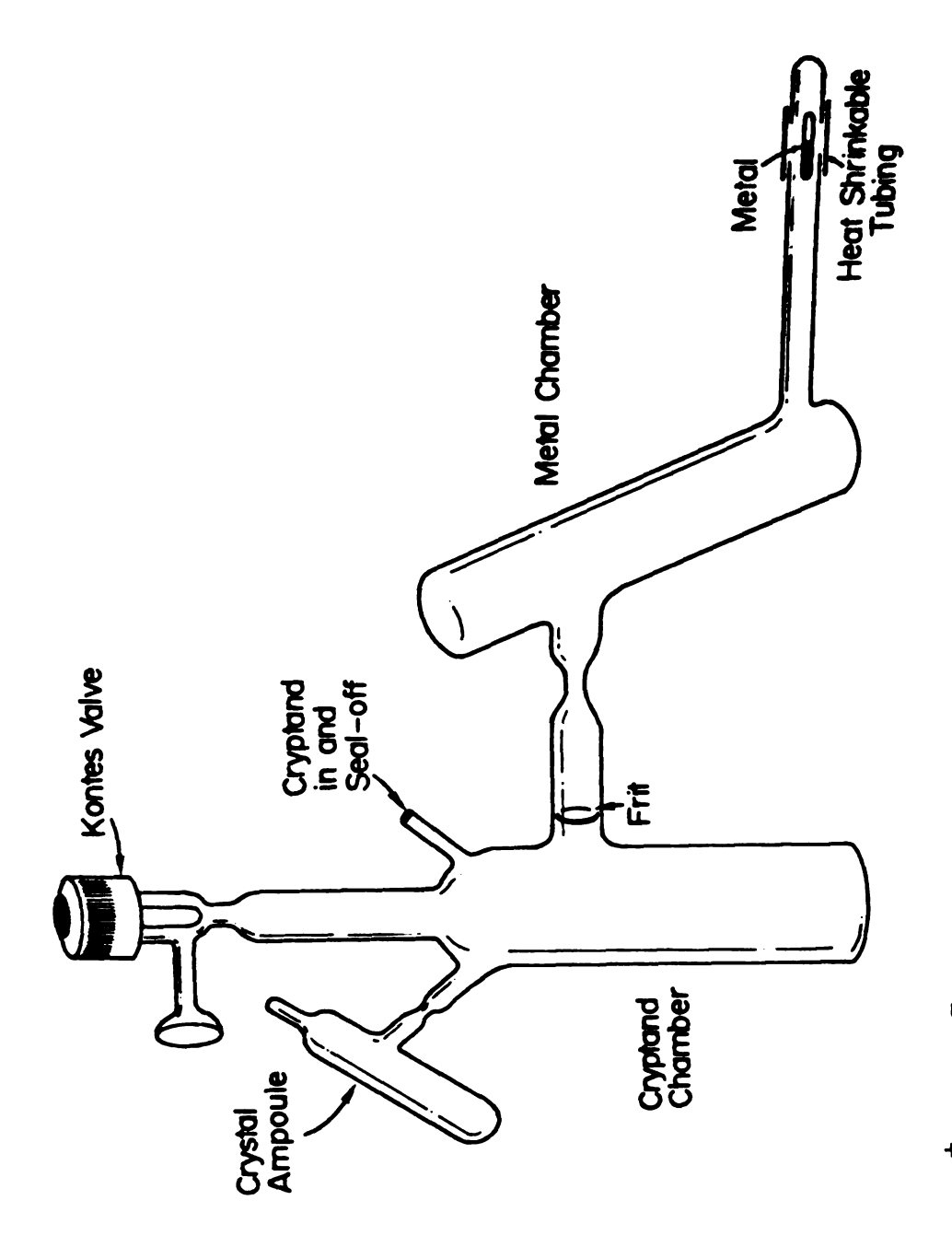


Figure 15. Na C222.Na Synthesis Apparatus.

solution was poured through the frit onto the sodium metal. The sodium began to dissolve immediately, forming a dark blue solution. The solution was kept at -10°C and stirred occasionally for 10 hours. At this point much of the sodium was still undissolved and the system was cooled to -78°C with a dry ice bath and stored overnight. The second day the apparatus was warmed to -10°C and stirred occasionally for 10 hours before recooling to -78°C for overnight storage. Much of the sodium still remained undissolved so the system was again warmed to -10°C and stirred occasionally for 8 hours. At this point it appeared that the dissolution of sodium had stopped and very little of the sodium mirror remained. The solution was poured out of the metal chamber through the frit and into the cryptand chamber. The frit was placed here to prevent the transfer of any undissolved sodium metal into the cryptand chamber. Then by using a -20°C isopropanol bath, the metal chamber was cooled from -10°C to -20°C and several mililiters of ethylamine were distilled from the cryptand chamber into the metal chamber. The distillate was then poured back into the cryptand chamber. This procedure was repeated several times until all traces of the blue alkalide solution had been rinsed into the cryptand chamber. The solution was then cooled to -78°C overnight. The next day a very large amount of gold-colored crystals had formed. The mother liquor was then poured through the frit while

the entire system was kept at -78°C. The apparatus was warmed to -50°C and a -78°C "basting swab" was used to condense ethylamine on the frit and constriction areas to rinse them completely free of any residual blue solution. The mother liquor was then frozen by using liquid nitrogen while the crystals were kept at -78°C. A flame sealoff was then made at the constriction to remove the mother liquor from the apparatus. Diethylether (10 ml) was distilled onto the crystals and they were rinsed into the crystal ampoule. The entire apparatus (except the Kontes valve) was kept at -30°C by using an isopropanol bath during the diethylether rinse. The rinse solvent was then poured back into the cryptand chamber. The crystals were left in the ampoule. Several mililiters of ether were distilled up onto the crystals and stirred before pouring the liquid back down to the cryptand chamber. This rinsing process was repeated three times, after which the ether was frozen in the cryptand chamber by using liquid nitrogen. After one hour, to assure the complete removal of all traces of diethylether from the crystal ampoule, a flame seal-off was made and the crystal ampoule was removed from the synthesis apparatus. The crystal ampoule, cooled to -78°C during the seal-off, was then stored in the dark at -78°C.

III.C.2. $Cs^+C222 \cdot Cs^-$

Eight different attempts were made to isolate pure crystals of Cs⁺C222·Cs⁻. Of these four produced dark copper-colored crystals but in each case the crystals were extremely small and could not be isolated free of solvent and/or decomposition products for analysis.

Typically 0.2 mmol of C222 and a slight excess of cesium metal were sealed into an apparatus similar to the one shown in Figure 15. Following evacuation, the cesium ampoule was broken and the metal distilled. Extreme care was taken during this step to assure complete evacuation prior to the distillation of the cesium. metal cannot be distilled away from any oxide impurities that can form during distillation. Not only was the system evacuated to 1×10^{-5} torr or lower, the entire apparatus (except for the cryptand, Kontes valve, and heat-shrinkable tubing) was heated with a torch in order to drive off any residual adsorbed gases before the cesium ampoule was broken. In addition, because cesium is a liquid near room temperature (29°C), the entire metal sidearm was chilled to prevent molten cesium from flowing out of the broken ampoule and reacting with the heat-shrinkable tubing. Following a successful distillation of the metal, 5-8 ml of ethylamine was distilled into the apparatus and the cryptand and metal were dissolved at a reduced temperature (\sim -20 to -30°C). This solution was then poured through the frit and back into the cryptand chamber. Cooling this solution to -78°C produced small amounts of extremely small copper-colored crystals. Many of these crystals remained suspended in the solvent, some even floating on the surface. When attempts were made to pour away the mother liquor, most of the crystals stayed with the solvent and clogged the frit. Attempts to unclog the frit were very time-consuming and in more than one case caused partial decomposition of the solution. In order to isolate these crystals for analysis, they must be free of solvent and all traces of blue solution must be removed from the seal-off areas before a flame seal-off can be made.

Two glassware design changes as well as different crystallization conditions failed to produce crystals that were sufficiently free of solvent and/or decomposition impurities. However, further work by L. D. Le produced crystals that could be separated from the mother liquor without appreciable decomposition. See Table 4 for crystallization conditions, and see Chapter 4 for analytical results.

III.C.3. Rb⁺C222·Rb⁻

Three attempts were made to synthesize crystals of Rb⁺C222·Rb⁻. These syntheses employed the same procedures and apparatus design as was used for the synthesis of Cs⁺C222·Cs⁻. The solvent used for all three syntheses of

Conditions Used for Alkalide Crystallization. Table 4.

	dendritic crystals, stable up to ~+20 °C	dec violently at 20 °C	12 attempts under various conditions gave only dull bronze films mixed with white deen product	cools changed crystals, whose up to ~0 °C; color changed reversibly from dark broams at ~78 °C to bright metallic green at ~13 °C; solvent content ~0,9 mote 5.	120' angles evident, stable up to 35 °C	dec at ~~25 °C compact agglomerated crystals, 120° augles	forg flat crystals, 120° angles evident, det at -20°C angles evident,	dec at ~~20 °C dendritie crystals dec at ~~24 °C	flat, mixture of square and rectangular crystals, very reflective, stable at room temperature for	at least 30 min, solvent content <0.1 mole % reflective crystals, stable at room temperature for days, solvent content <0.1 mole % dendritte rods, stable up to ~+10 °C, solvent content ~16 mole %
crysta conditions	3 mL of EA + 7 mL of DEE + 2 mL of n 78 °C/24 h.	Superaturates easily 2 mL of EA + 3 mL of DEE + 2 mL of a.P 78 °C/24 h.	3 mL of NH, + 9 mL of MA, -78 °C/24 h 2 mL of EA + 3 mL of DEE 4	n-P (trace), -78 °C/24 h, supersaturates easily	6 mL of t-PA/-92 "C/2 h, -78 "C/24 h 6 mL of t-PA/-90"C/1 h,	- 78°C/24 h 7 mL of +PA/-92°C/3 h,	15 mL of tPA, -90 °C/4 h	4 mL of tPA/-90 °C/4 h 4 mL of tPA/-90 °C/2 h	-78 °C/24 h 9 mL of i-PA + MA (trace), -78 °C/24 h	10 mL of tPA, -78°C/24 h 4 mL of tPA + 2 mL of DEE, -78°C/24 h
dissoln conditions	0.37 mmol/9 mL of EA, -20 °C/6 h	0.13 mmol/4 mL of EA, -30 °C/2 h	0.3 mmol/12 mL of NH, -40 °C/6 h 0.51 mmol/7 mL of EA,	-10 C/20 h	0.4 mmol/5 mL of NH.,	-35 °C/1 h Q6 mmol/5 mL of NH; -40 °C/1 h	1.0 mmo/15 mL of NH, -35 °C/1 h	0.25 mmol/3 mL of NH ₃ , -33 °C/1 h 0.36 mmol/4 mL of NH ₃ ,	-33 C/1 n 1.3 mmol/8 mL of MA, -35 °C/3 h	Q 81 mmol/10 mL of MA, -30 °C/2 h Q 31 mmol/8 mL of MA, -20 °C/30 min
pdwoo	Ca*C322·Na-	G-C322-C5-	Ba-"C222-(Na-), ? Na-"C221-Na-	K*C222.Na-	Ca*C222Na*	Rb-C222-Na-	Rb-C223-Rb-	K*C222-K*	LI*C211:Na*	Ca1806-Na- K+1806-Na-

Rb + C222 · Rb - was t-butylamine.

One attempt resulted in solution decomposition without the formation of any precipitate; the second, which used higher alkalide concentrations, produced copper-bronze films but no crystals and the third resulted in the formation of a small quantity of copper-bronze crystals. Further work by L. D. Le produced 3 samples of Rb⁺C222·Rb⁻ crystals which were analyzed (see Chapter 4 for the analytical results).

III.C.4. Na + C221 · Na -

This compound, initially assumed to be very similar to $Na^{\dagger}C222 \cdot Na^{\dagger}$, proved to have entirely different solubility properties and was very difficult to precipitate from solution. At 0°C, a saturated solution of $Na^{\dagger}C222 \cdot Na^{\dagger}$ in ethylamine is ~ 0.04 M. However, a 0.5 M solution of $Na^{\dagger}C221 \cdot Na^{\dagger}$ in ethylamine at $-78^{\circ}C$ produced no precipitate when occasionally stirred over a 48-hour period.

Five attempts were made to synthesize Na⁺C221·Na⁻.

Two of these resulted in decomposition of the alkalide solution before any crystals could be precipitated. Of the three attempts that resulted in precipitation, in only one case could the crystals be isolated free of solvent and decomposition. A portion of these crystals was analyzed (Chapter 4). The remainder of the crystals were contained in an ampoule which was too large to transfer to the hydrogen

evolution apparatus (Chapter 4) for analysis. These crystals were transferred into a smaller ampoule in the glove box. The sample was kept cold during this transfer by using the cold wells which had been added to the glove box (see Chapter 2 for a detailed description). The crystals transferred in this manner were also analyzed; the results appear in Chapter 4. The following is a description of the synthesis that produced the crystals for analysis.

Cryptand [2,2,1], which is a liquid, was weighed (~ 0.5 mmol) into a short length of 5 mm tubing sealed at one end. This tubing was then sealed onto the apparatus as shown in Figure 16. An ampoule of sodium (∿1.0 mmol) was sealed into the sidearm by using heat shrinkable tubing. The apparatus was evacuated to 1 x 10^{-5} torr, the ampoule was broken and the metal distilled in under dynamic vacuum. After complete distillation, the sidearm was sealed off and removed. Ethylamine (6.5 ml) was distilled in and the cryptand was dissolved. This solution was cooled to -40°C and poured onto the sodium. The solution was warmed and kept between -5 and -15°C and stirred occasionally for a total of 19 hours. At this time it appeared that the dissolution of sodium had ceased and the solution was cooled slowly until frozen (-81°C). No precipitation was ob-The frozen solution was dark blue to transmitted light and gold to reflected light. The frozen solution was warmed to -78°C and melted. In an attempt to force

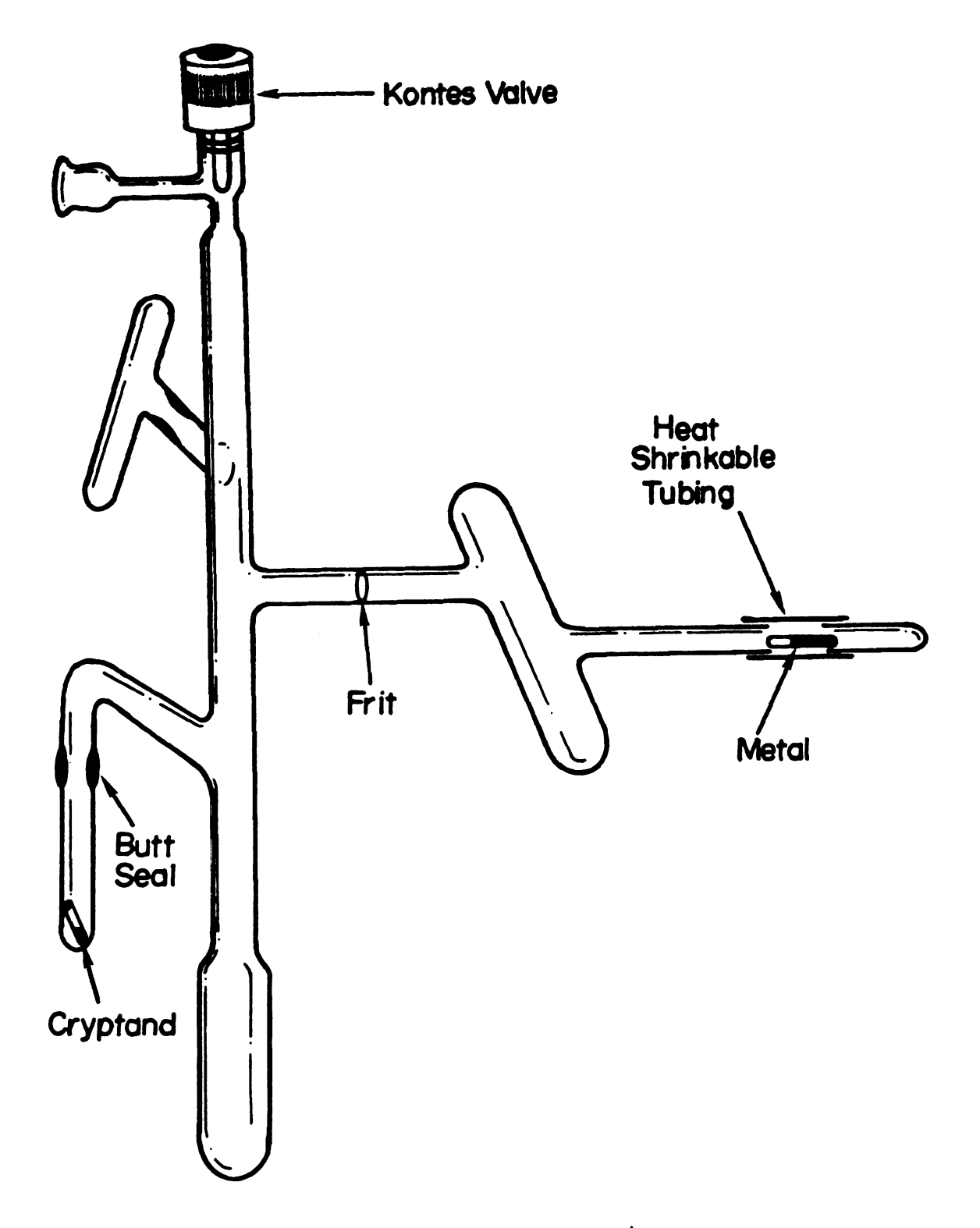


Figure 16. Synthesis Apparatus for Na⁺C221·Na⁻ and Cs⁺C322·Na.

precipitation, 2.5 ml of diethylether was added and the resulting solution was stored overnight at -78°C. precipitate was observed and an additional 4.5 ml of diethylether was added. A gold interface formed between the unmixed diethylether and the ethylamine/diethylether layers. When the two layers were mixed by shaking, the gold interface disappeared and one blue homogenous liquid phase resulted with no precipitate formation. The system now contained 6.5 ml ethylamine and 7.0 ml diethylether. Five ml of this solvent was then removed by distillation and the resulting solution was cooled to -95° C by using a $l-N_{2}$ / acetone bath. A few red/bronze crystals precipitated but dissolved completely when the system was warmed to -78°C. More solvent was removed from the apparatus until only 4 ml of the ethylamine/diethylether mixture remained. At -78°C only a very few red/bronze crystals precipitated. The alkalide salt concentration in this mixed solvent system was ~0.13 M at this stage. In order to force precipitation, ~0.2 ml of pentane was distilled in. Very slowly, over a 1-hour period, a very substantial crop of red/bronze crystals precipitated. Because the precipitation was obviously slow, the apparatus was stored at -78°C overnight before the solvent was poured away and the crystals were rinsed in several ml of pentane. Approximately half of the crystalline sample was isolated by a flame seal-off in the sidearm and stored at -78°C until analyzed. The other half was

transferred into an ampoule suitable for use in the hydrogen evolution apparatus (with the aid of the glove box).

Two other syntheses also produced crystals of Na⁺C221· Na⁻ and, although these crystals could not be isolated for analysis, several observations made during these syntheses are worthy of mention.

During a similar synthesis of Na⁺C221·Na⁻, the addition of pentane produced a substantial quantity of crystals at -78°C. However, when this system was warmed to -40°C, the crystals appeared to melt, losing their sharp crystalline edges and the crystals changed from a metallic green to a copper/bronze color. This (apparently liquid) phase looked very similar to the concentrated phase seen in metal-ammonia solutions. When it was recooled to -78° C, the "liquid phase" disappeared and the green/gold crystals slowly reformed. When the ethylamine/diethylether/pentane solvent system was replaced by pure isopropylamine, the crystals that formed appeared gold at -78°C but turned to a similar liquid phase at -40°C. When most of the solvent was poured away from the gold crystals at -78° C and they were allowed to warm, the crystals once again appeared to melt and changed from gold to blue, green, copper, and mixtures of these colors.

The crystals of Na⁺C221·Na⁻ appear to be very soluble in both ether and amine solvents. The observed very slow crystallization rates make solubility estimates unreliable

due to the very real possibility of supersaturation. It is likely that the observed "melting" of crystals of Na⁺C221·Na⁻ is the formation of a concentrated phase. The solvent-free crystals used for analysis were warmed to -20°C and above without any sign of melting. However, the crystals did show a reversible color change from copper/bronze at -78°C to a metallic green at -20°C.

III.C.5. $Cs^{\dagger}C322 \cdot Cs^{-}$

The same type of apparatus used for the synthesis of $\mathrm{Na}^+\mathrm{C221}\cdot\mathrm{Na}^-$ was used for the synthesis of $\mathrm{Cs}^+\mathrm{C322}\cdot\mathrm{Cs}^-$. The synthesis of $\mathrm{Cs}^+\mathrm{C322}\cdot\mathrm{Cs}^-$ was attempted only once and produced dark bronze crystals that decomposed violently in an evacuated vessel at $-20^{\circ}\mathrm{C}$. No crystals survived this decomposition and therefore no analytical data are available for this compound.

Cryptand [3,2,2], 0.13 mmol, and a slight excess of cesium metal were sealed into the apparatus and the system was evacuated. After distillation of the metal and dissolution of the cryptand and the cesium in ethylamine at -30°C the solution was cooled slowly to -90°C. No precipitate was observed, but upon freezing, the dark blue solution became a dark gold/bronze. The solution was warmed to -78°C and stored overnight. No precipitate was observed and ethylamine was removed from the apparatus by distillation until the solution concentration reached

0.09 M. This solution was cooled slowly to -90°C. No precipitate was observed and as the solution froze, it formed a dull metallic green solid. The solid was warmed to -78°C and 3 ml of diethylether were added. The resultant single phase dark blue liquid was stored at -78°C for 12 hours without precipitation. Pentane (2 ml) was then distilled into the apparatus. A clear upper layer of pentane and a blue lower layer were observed with a bronze-colored interface. When shaken, a single homogeneous blue liquid phase resulted; however, with time a blue/bronze film formed which coated the wall. This film was blue by transmitted light and bronze by reflected light. After one hour at -78°C. bronze crystals began to precipitate. When warmed to -40°C. the crystals appeared to melt, similarly to the crystals of Na⁺C221·Na⁻. When the system was recooled to -78°C the "liquid" phase appeared to freeze but no crystalline edges were observed. Storage at -78°C overnight produced dark bronze crystals and the disappearance of the "frozen liquid phase". The solvent, still at -78°C, was poured away from the crystals. The dry crystals were warmed slowly from -78°C to -20°C. No melting of the crystals occurred at -40°C. The crystals retained their deep reddish-bronze color until at -20°C the crystals decomposed violently and completely, forming a light yellow, completely non-metallic colored residue. This residue splattered all over the walls of the synthesis apparatus.

While it is not known why this decomposition reaction was so violent, it is likely that the ceside ion reacted with the cryptand to form $\rm H_2$ gas, and the escaping gas may have caused the splattering that was observed.

III.c.6. $\underline{\text{Ba}^{2+}\text{C222}\cdot(\text{Na}^{-})}_{2}$

Although thermochemical calculations (Chapter 6) indicate that Ba²⁺C222·(Na⁻)₂ may be stable, the work of two previous investigators and 18 additional attempts made by this researcher all ended without success. Solution decomposition and solubility problems were the two major factors preventing the synthesis of Ba²⁺C222·(Na⁻)₂ (assuming, of course, that this compound is thermodynamically stable at the temperatures used here).

ethylamine and it dissolves very slowly at the temperatures required for solution stability, even in the presence of cryptand [2,2,2]. For these reasons, ammonia was used as the initial dissolution solvent. However, alkali metal anions do not appear to survive in liquid ammonia but dissociate into M⁺ and 2e⁻_(SOLV). In order to synthesize an alkalide salt, the ammonia must be replaced by another solvent which will support alkali metal anions once the barium, cryptand, and sodium are dissolved. Two similar methods were used to effect this solvent replacement. The apparatus used for both methods is shown in Figure 17.

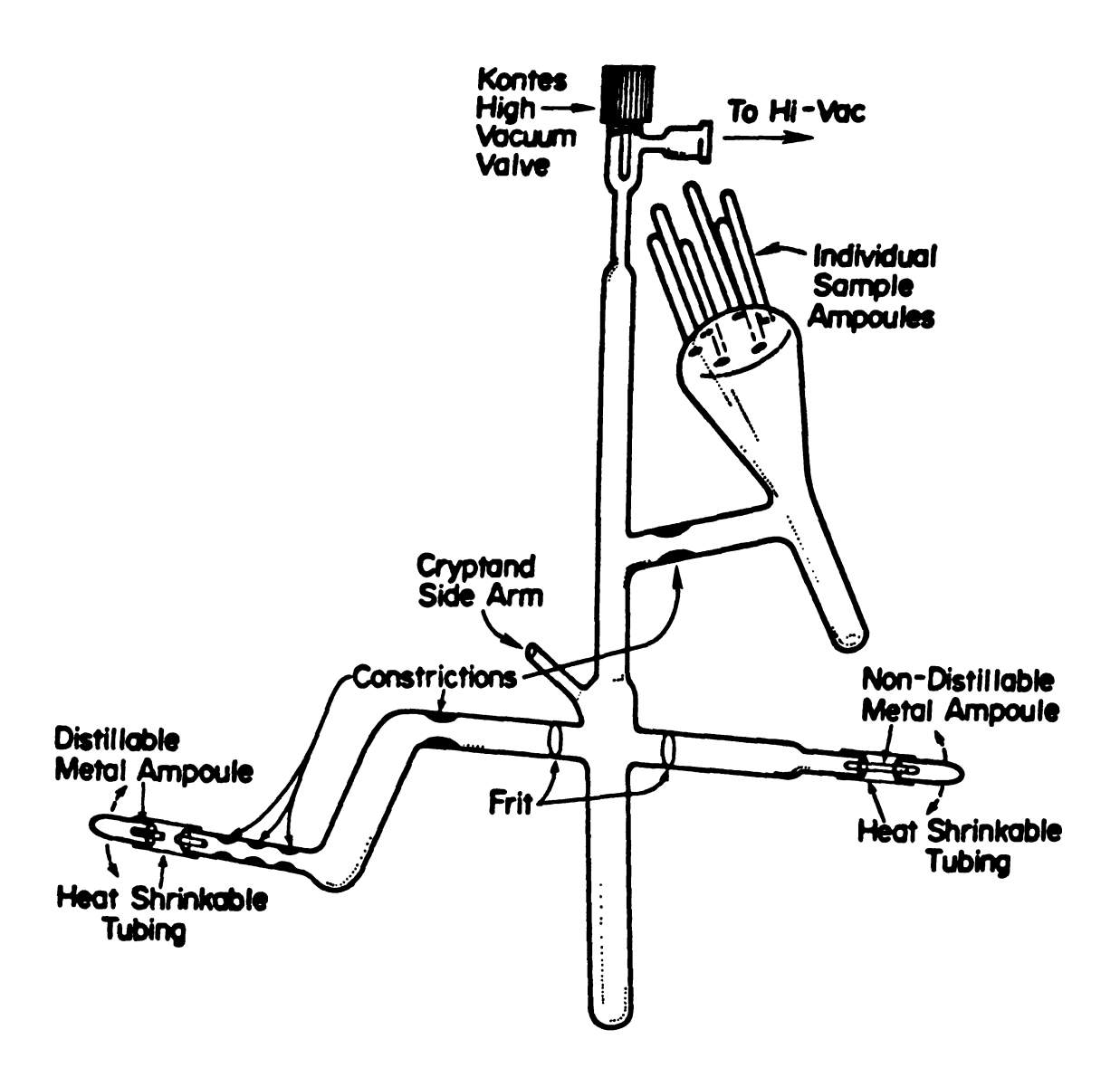


Figure 17. Ba²⁺C222·(Na⁻)₂ Synthesis Apparatus.

In the first method, the cryptand and the barium were dissolved in liquid ammonia followed by the dissolution of sodium. The ammonia was then completely removed by distillation and a new solvent such as methylamine or ethylamine was added. In the second method, the cryptand, barium, and sodium were dissolved as before in ammonia and then a cosolvent such as methylamine or ethylamine was added. Ammonia was then removed by partial distillation of the solvent mixture. Since ammonia has a much higher vapor pressure, it is preferentially removed.

The complete removal of ammonia by the first method resulted (in all but one case) in extensive decomposition even when the solution was kept at -65°C. At this temperature the vapor pressure of ammonia over the saturated solution is low and several hours were required for its removal. These attempts resulted in the formation of white decomposition products. In all cases the addition of either methylamine or ethylamine to the mixture of blue sludge and decomposition products resulted in only partial dissolution of blue/gold sludge. When these solutions were cooled to cause precipitation, the gold crystals that did precipitate were contaminated extensively with white decomposition products.

Samples prepared by using the second method where the ammonia was removed after the addition of ethylamine or methylamine were also extensively contaminated with white

decomposition products. Two samples were collected for analysis. These samples, although visibly contaminated, were thought to be pure enough to provide at least some information concerning the stoichiometry of the precipitate. The results of these analyses (Chapter 4) were inconsistent and did not point to the formation of any reasonable alkalide salt. However, one large crystal (~0.2 mm) was isolated and examined by X-ray crystallography. Preliminary measurements showed the crystal to be Na⁺C222·Na⁻. The crystal structure of Na⁺C222·Na⁻ is known (80) and the unknown crystal had the same cell dimensions and was of the same symmetry class.

The ease with which "Ba²⁺C222·(Na⁻)₂" solutions decompose and the observed formation of Na⁺C222·Na⁻ suggest that not all of the barium had been encryptated when the sodium metal was dissolved. It is possible that the 3 to 12 hours typically allowed for Ba²⁺C222 complex formation was not sufficient. Kinetics data are not available for this reaction in liquid ammonia. It seems likely that the solutions contained a mixture of Ba²⁺C222 and Na⁺C222 even though the formation constant for the barium complex is much greater than that for the sodium complex (when measured in water and/or methanol). When higher temperatures and longer reaction times were used, the solutions showed an even greater tendency to decompose. It is possible that the Ba²⁺ ion with its very high charge density is responsible for the ease with which these solutions decompose.

If a small amount of Ba²⁺C222 were present in solution when the solvent replacement was attempted, the anionic species (either Na or e_(SOLV)) would be forced into closer proximity to the Ba²⁺C222 ion. As the solvating power of the solvent was lowered, the chemical potential of the anionic species would be raised and would increase the possibility of attack of a high charge density species such as Ba²⁺C222. This mode of attack with the anionic species reducing the cryptand has been postulated for other systems where the cation is univalent.

III.C.7. Cs + C322 · Na -

Five separate attempts were made to synthesize Cs⁺C322·Na⁻. This compound proved to be very stable when isolated free of solvent. The analytical results for this compound agree extremely well with the predicted stoichiometry.

Previously obtained optical spectra (84) of a solution of cesium, sodium, and cryptand [3,2,2] showed a prominent Na band with no e or Cs bands. This evidence and the observation that sodides are more stable than cesides, leave little doubt that the predominant species in such a solution are Cs + C322 and Na.

Cs⁺C322·Na⁻ was prepared by dissolving equimolar amounts of Cs, Na, and C322 (2.4 mmol) in 8 ml of ethylamine in the apparatus shown in Figure 16. Ethylamine was then removed by distillation until only 0.5 ml

remained. This solution, now ≥ 0.5 M appeared dark blue by transmitted light and metallic-red by reflected light. It was stored for 72 hours at -78°C with no evidence of precipitation. Still at -78°C, 8 ml of diethylether was distilled into the apparatus. The resultant solution produced a very small quantity of metallic red-bronze crystals after two hours at -78°C. The amount of precipitate increased slowly throughout a 10-hour period. The solution was stored overnight at -78°C. The solvent was poured away, the crystals were rinsed in pentane and sealed into an ampoule for analysis.

IV. ANALYSIS

Introduction

The air, water, light, and heat sensitivity of alkalides make commercial analyses unreliable because of decomposition during shipping and handling. Therefore, an inhouse analytical scheme was designed and the necessary apparatus was constructed. This scheme (Figure 8) was based on the reaction of these highly reducing compounds with water to form H2 and OH. The amount of H2 produced gives the total reducing power of the sample. After reaction with water any volatiles produced, excluding ${\rm H}_2$, are collected in a 1-N $_{
m 2}$ trap and can be analyzed for the presence of solvent of crystallization. Titration of the nonvolatile residue gives the amount of OH present and, in the case of cryptands, the amount of cryptand present since cryptands have two titratable amine groups. The metal content was determined by using flame emission spectroscopy. Proton NMR was used to check for possible cryptand decomposition. Integration of the NMR signal of the complexing agent was an additional technique used to determine the amount of complexing agent present.

IV.A. Analysis Methods

IV.A.1. Hydrogen Evolution

The hydrogen evolution apparatus (Figure 9) used in this study was patterned after a similar device used by Dewald, Dye, and Lok (90,100) and it is described in detail in Chapter 2. Cold alkalide samples were placed in the apparatus and evacuated before reaction with water. Care was taken to keep the samples cold until the reaction with water was complete. This avoids thermal decomposition of the complexing agent during reaction with water. A calibrated pipet was used to measure the volume and a mercury leveling bulb was used to measure the pressure of the H_O gas.

A $1-N_2$ trap was used to collect any solvent of crystallization released during the reaction with water as well as any excess water initially introduced. The contents of the trap were dissolved in water and the pH of this solution together with the base hydrolysis constant for the amine solvent used permitted calculation of the amount of amine present.

IV.A.2. Titration

The nonvolatile residue after hydrogen evolution was dissolved in distilled water and titrated with standard HCl. The titration was carried out under N_2 to avoid CO_2 pickup.

For those samples which contained cryptand the titration curve showed two equivalence points, one for the hydroxide and the other for the two amine groups present in the cryptand. The equivalence points and, therefore, the number of moles of hydroxide and cryptand present were obtained graphically from the titration curve.

IV.A.3. Flame Emission

The nonvolatile residue was also analyzed for metal content by using flame emission spectroscopy. Samples were dissolved in distilled water and adjusted to pH 2-3. A plot of the relative emission versus concentration for standard metal solutions yielded a curve from which the unknown metal concentrations were determined. Interferences from cryptand and/or other alkali metals were found to be negligible.

IV.A.4. Proton NMR

The residue after $\rm H_2$ evolution was also analyzed for complexing agent by using quantitative $^{1}\rm H$ NMR integration. An aliquot of solution from the pH titration was evaporated to dryness and dissolved in $\rm D_2O$ which contained a known concentration of t-butyl alcohol. The relative $^{1}\rm H$ NMR integration of the t-butyl alcohol and the complexing agent were then used to calculate the amount of complexing agent

present. Problems with the gradual evaporation of t-butyl alcohol prompted a switch to potassium hydrogen phthalate (KHP) as an internal ¹H NMR integration standard.

IV.B. Results

Table 5 lists the results of the analyses in approximate increasing order of the deviations from the predicted stoichiometry. Only samples which were obviously crystalline and free of apparent decomposition were analyzed. masses could not be obtained for most systems because of the need to keep the samples cold. Therefore, for the cryptate salts the analytical results are referred to the total base present as determined by the pH titration. total amount of base can be more accurately determined than the other quantities and it is insensitive to decomposition of the cryptand. Its determination should be the most reliable measure of the total amount of sample. For the salts Cs[†]18C6·Na⁻ and K[†]18C6·Na⁻ the amount of hydrogen evolved was used rather than the total base present. The crown ether was very resistant to decomposition during the hydrogen evolution step so that this method of analysis is more reliable than that with cryptands. In addition, the titration of hydroxide ion when 18C6 is present is plagued by instability of the pH meter, especially in the vicinity of the endpoint. This was verified by titration of a mixture of alkali metal hydroxide and 1806.

Table 5. Analysis of Crystalline Alkalides.

H	H ₂ Cryptand olved By Titration 0 0 0 0 +3 -7 -3 +1	M by Flame on Emission 0	N by Flame	
1.05 0.715 0.983 1.33 1.29 	Н	0 0 -	HOISSIND	or Crown By 1H NMR
0.983 1.33 1.29 0.887 2.00 	Ţ	-10	+3	+1
	-3 +1 -51 -2		+5	-16 -8
		+1 +14		- 11 +10
1 1	-3 -6 -6	†++ ++	+2	6++ 6++
	(-5)	0	+3	\
0.053 -1 0.518 -81	+3 -1 -81 -6	-1 +16 +3		+23 -11 -30
L1 ⁺ C211·Na ⁻ 0.159 +16 2.67 -8	+16 -5 -8 +1	+ + +	+ + 8	+ 17
K [†] 18C6·Na ⁻ 0.856	(-4)	+3	+13	6+
K*c222.K* 0.597 -3 0.338 -54	-3 -14 -54 -23	+17+13		-19 -33
Cs*C222.Cs* 0.137 +5 0.077 +20	H5	+29		+23 +29
Cs ⁷ C222·Na ⁷ 0.365 -10 0.188 -12	-10	+30	-31 -18	-2 +15

The predicted stoichiometry is based on Reaction (8) where M and N are alkali metals and

$$M^{+}C \cdot N^{-} + 2H_{2}O + H_{2} + M^{+} + N^{+} + C + 2OH^{-}$$
 (8)

C is a cryptand or crown ether. The sample size was calculated as total base/4 for cryptands and as $\rm H_2$ evolved for crown ether compounds. The lack of a definite first break in the titration curve for Cs⁺C222·Cs⁻ and Cs⁺C222·Na⁻ prevented the determination of cryptand by titration.

IV.C. Estimation of Errors

The intrinsic errors of analysis depend strongly on sample size. Typical samples were in the 0.01 to 0.1 mmol range. Within this range the largest errors in the hydrogen evolution analysis arise from the pressure measurement. The estimated error is ±1 torr. At room temperature 0.01 and 0.1 mmol of hydrogen in 10 cm³ produce 18.6 and 186 torr which corresponds to approximately 5% and approximately 1% error, respectively. However, the analysis of compounds which produce products other than hydrogen (the reduction of cryptand rather than water) are subject to larger errors, particularly for this step but also for the determination of the complexant by NMR.

The analysis for total base by titration with standard

acid is subject to the smallest measurement error. Typically acid concentration, buret, and graphical errors lead to total base measurement errors of 1%. Very small samples (.01 mmol) can give errors as high as 2%. The second equivalence point, the one for total base is very sharp. The first equivalence point, required to calculate the amount of cryptand present, exhibits a much more gradual pH change at the equivalence point. The resultant titration curve has a less distinct equivalence point and the range of estimated error is increased to 5 to 2% for the 0.01 to 0.1 mmol range.

Proton NMR integration of complexant has the largest estimated error; 5% for crown ethers and 10% for cryptands. The cryptands are susceptible to larger errors due to baseline distortions caused by residual \$^1\$H_2O in the sample. The water and cryptand resonances are much closer together than are the water and crown ether resonances. In order to minimize systematic errors in NMR analyses several precautions were taken when obtaining spectra. A short pulse (1-3 microseconds) was used to assure a uniform power distribution across the entire spectrum. The largest data block available and the smallest sweep width were used in order to provide a long acquisition time. This procedure assures the complete decay of the free induction decay (FID) and avoids baseline distortion due to truncation of the FID. The delay between the pulse and the data acquisition was

for the determination of rubidium in one sample, and for hydrogen in another sample which showed extensive decomposition of the cryptand during the hydrogen evolution step. The samples of K⁺18C6·Na⁻ were reasonably stable but gave only marginally acceptable analysis. One of them was apparently contaminated with excess sodium and the other contained appreciable amounts of solvent (see Table 4).

The last three entries in Table 5 are for samples which were nominally K⁺C222·K⁻, Cs⁺C222·Cs⁻ and Cs⁺C222·Na⁻ based upon the solutions from which they were crystallized. All were difficult to prepare and handle and all were subject to thermal decomposition and decomposition of the cryptand upon addition of water during hydrogen evolution. Evidently, excess metal was present in the potasside and ceside samples. Flame photometric analysis of Cs⁺C222·Na⁻ indicated an excess of cesium and a deficiency of sodium. The sample consisted of a mixture of two types of crystals, which suggests the presence of both ceside and sodide.

The analysis of five compounds given in Table 4 also included the determination of the pH of the water which was distilled from the sample after hydrogen evolution. In three of the five cases the pH was within experimental error of the pH of the water used. In a sample of Na⁺C221·Na⁻ the pH was slightly high and indicated that up to 0.9 mol percent of amine could have been present in the initial sample. One sample of K⁺18C6·Na⁻ contained approximately

16 mol percent of amine. Since the sample had been evacuated to approximately 1×10^{-5} torr for one hour before sealoff of the sample compartment in the synthesis apparatus, it is likely that solvent had been incorporated in the crystals.

An analysis problem which was particularly troublesome with the more reactive alkalides, especially with salts of K, Rb, and Cs occurred during the hydrogen evolution step. Reaction with water, which was condensed from the vapor onto the alkalide salt, caused some decomposition of the cryptand without hydrogen evolution. When this decomposition occurred, the residue was straw colored and subsequent 1H NMR analysis showed that (unidentified) decomposition products of the cryptand were formed. believed to be the cause of low analyses for Ho in many cases. For example, a sample of $Rb^+C222 \cdot Rb^-$ (5 x 10^{-5} mol) which contained only shiny bronze crystals before reaction with water, formed a dark residue upon reaction with water at about -20°C. Only 19% of the expected ${\rm H}_2$ was formed, and while the pH titration and flame analyses were satisfactory, the $^{1}\mathrm{H}$ NMR spectra showed substantial amounts of cryptand decomposition products. These products were not identified but the complex ¹H NMR spectra showed that the cryptand had been altered. Attempts have been made to lower the alkalide temperature as low as -78°C during the condensation of water onto the sample; however, no reaction occurs

at this temperature and the samples must be warmed to -10 to -30°C for the desired reaction to occur. It is possible that an alcohol would be a more appropriate liquid to use for these analyses, the reaction between an alcohol and the alkalide may be slower and result in less decomposition of the cryptand.

V. MISCELLANEOUS EXPERIMENTS

V.A. Solution ²³Na NMR of Na⁺C221·Na⁻

V.A.1. Introduction

Alkali metal NMR is a widely used technique for the study of alkali metals in solution (101). Both chemical shifts and linewidths are useful for the identification of solution species. In fact, the most convincing evidence for the existence of alkali metal anions in solution is from alkali metal NMR (66,102). In this work Dye et al. report the chemical shifts and linewidths for Na⁺C222·Na⁻ in methylamine, ethylamine, and tetrahydrofuran. Two resonances were observed. The first, assigned to Na⁺C222 occurs at the same position as ordinary Na⁺C222 salts in these same solvents (66). The chemical shift of the cryptated sodium cation is nearly solvent independent unlike the bare cation which displays a very strong solvent dependence (103). second resonance, Na, is also solvent independent and occurs at very nearly the same chemical shift as that calculated for gaseous Na (104). This extremely narrow line (<3 Hz in THF) indicates highly symmetric species consistent with its assignment as a spherical sodide ion with two electrons in its outer 3s orbital.

The use of ²³Na NMR was a valuable technique for the identification of solution species during attempts to synthesize Na⁺C222·Na⁻. Similarly, during early attempts to synthesize crystals of Na⁺C221·Na⁻ (for this dissertation) ²³Na NMR was also used to examine solutions containing C221 and dissolved sodium metal. These solutions were prepared in the same manner as those from which crystals of Na⁺C221·Na⁻ were eventually precipitated. The spectra obtained here show two resonances similar to those obtained for Na⁺C222·Na⁻. These results are summarized in Table 6.

V.A.2. Results and Discussion

The solution used for NMR examination was prepared in the same way as those solutions used to crystallize Na⁺C221·Na⁻ (see Chapter 3). However, instead of forcing crystallization, the solution was poured into a 10 mm NMR tube and sealed away from the apparatus (Figure 18). The solution used contained 0.28 M C221 and 0.56 M dissolved sodium metal in ethylamine. The spectra were obtained with a greatly modified Varian DA-60 spectrometer (see Chapter 2). All chemical shifts reported are referenced to infinitely dilute aqueous Na⁺. The external reference used was 3 M aqueous NaCl (+0.45 ppm relative to infinitely dilute aqueous Na⁺). Positive shifts are in the downfield direction (paramagnetic). The spectra were obtained over the temperature range -67 to -6°C. The chemical shifts are not

Table 6. 23 Na Chemical Shifts for Na + C221 · Na in Ethylamine.

	Na	Na ⁺ C221		Na -	
Temp.	PPM	Δν _{1/2}	PPM	Δν _{1/2}	
- 6.4°	- 3.5	91 Hz	-61.6	9 Hz	
-14.0	- 3.6	103	- 61.8	9	
-38.4	- 5.2	201	- 62.2	13	
-47.8	-3.7	318	- 62.2	20	
- 59.8	-3. 7	494	- 62.2	25	
-67.4	-3.8	631	-62.2	25	

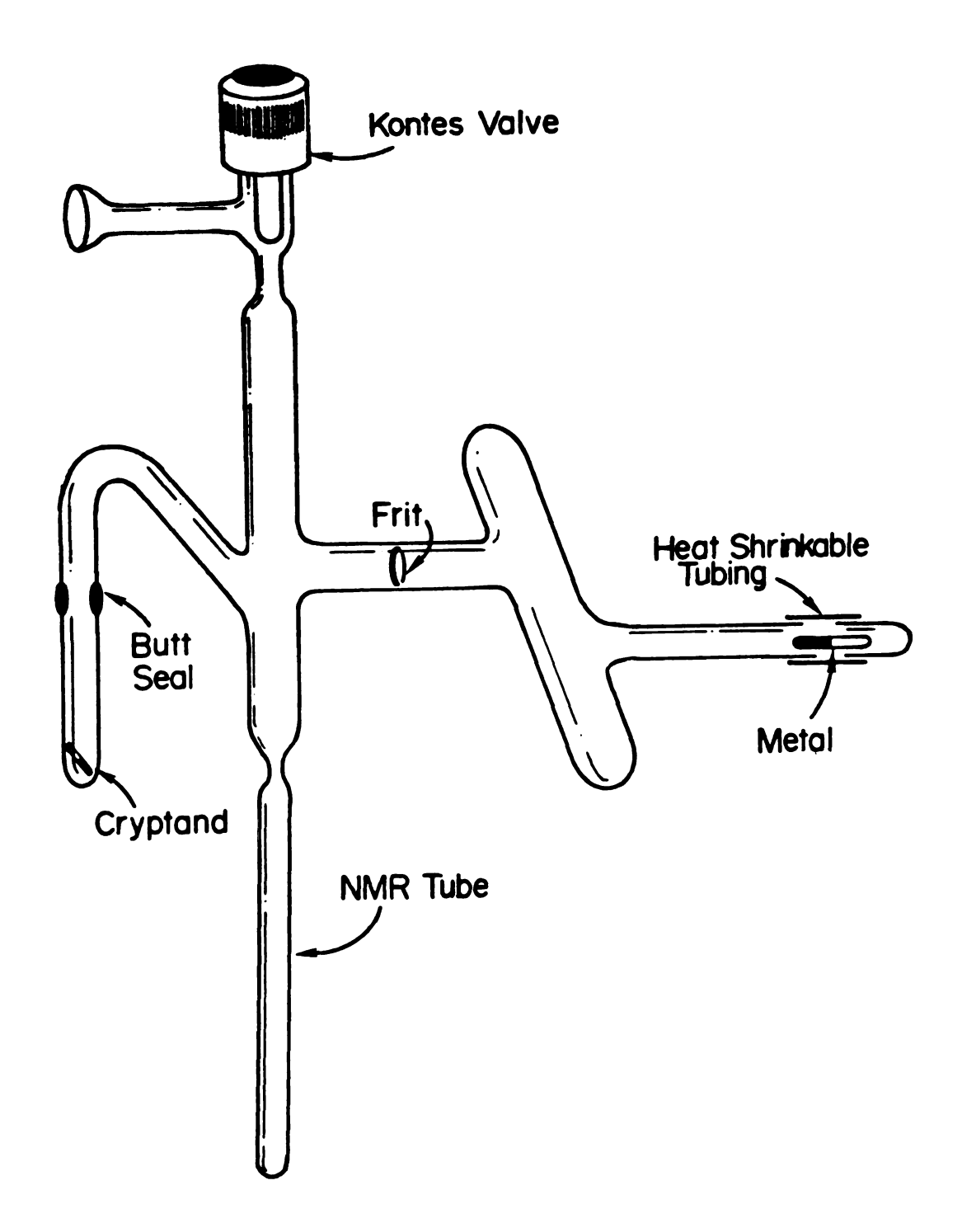


Figure 18. NMR Sample Preparation Apparatus.

corrected for bulk susceptibility.

The spectra obtained for Na⁺C221·Na⁻ are, not surprisingly, very similar to those obtained for Na⁺C222·Na⁻. The chemical shift of Na⁻ for Na⁺C221·Na⁻ differs by only 0.1 ppm from that found for Na⁺C222·Na⁻ by Dye et al. (66,102). The linewidth for Na⁻ reported by Dye of 6-9 Hz at -17 to +1°C compares well with that found here of 10 Hz at -14 to -6°C.

The chemical shift for $Na^{+}C221$ (-4.0 ppm) differs from that for $Na^{+}C222$ but agrees well with that found for $Na^{+}C221 \cdot C1^{-}$ in methanol/water (-4.25) found by Kintzinger and Lehn (105).

The presence of these two lines in the 23 Na NMR spectra at the temperatures used indicate that the exchange rate is slow on the NMR time scale. This rate is also similar to that observed for Na $^{+}$ C222·Na $^{-}$ and agrees with exchange studies of Na $^{+}$ C222·Br $^{-}$ as followed by 23 Na NMR by Ceraso et al. (106) which showed that in ethylenediamine exchange of the sodium cation into and out of the cryptand is slow below approximately $^{+}$ 20°C.

This study leaves little doubt that, at least in ethylamine, the solutions from which crystals were precipitated contained Na⁺C221 and Na⁻.

V.B. Solid State ²³Na NMR of Na⁺C222·Na⁻

V.B.1. Introduction

The Na ion is believed to be very large. The crystal structure of Na C222·Na (80) shows that the Na Na Na distance is 7.06 Å and that the minimum Na Na Na distance is 8.83 Å. In addition, Matalon, Golden, and Ottolenghi (78) have calculated the radius of Na to be approximately 2.25 Å which is slightly larger than that of I (2.16 Å). It was hoped that the unusually large size of Na would make it possible to observe a relatively narrow Na NMR signal for powdered crystalline samples of Na C222·Na.

The two major sources of NMR line broadening in solid samples are the dipolar and quadrupolar interactions. A variety of instrumental methods have been devised to reduce these effects such as magic angle spinning and high power decoupling (107). The magnitude of these interactions and, therefore, the linewidths depend on several factors including a radial dependence which varies as $1/r^3$, where r is the distance between the nucleus of interest and other nearby nuclei with I \neq 0. The $1/r^3$ dependence of this interaction implies that even without special instrumental techniques, a large ion such as Na $^-$ (approximately 2.25 Å radius) might have a significantly reduced linewidth when compared to the linewidths of salts containing Na $^+$ (approximately 0.95 Å radius).

The equipment used for solid state NMR, although commercially available, was not currently at hand and, therefore, a probe was designed and constructed by Wayne Burkhart. This probe was used in conjunction with a Bruker WH-180 spectrometer and magnet to obtain spectra for powdered crystalline samples of Na⁺C222·Na⁻, Na⁺C222·I⁻, and NaCl.

V.B.2. Results and Discussion

The probe consisted of an impedance matched parallel tuned resonance circuit (Figure 11) that was tuned with a variable capacitor to resonate at 47.62 MHz. This is the resonance frequency for ²³Na at 4.228 tesla (the field strength of the superconducting magnet used). The pulse/receiver coil was designed to accept 5 mm NMR tubes and was oriented at a right angle to the magnetic field. Samples were inserted through a hole in the probe housing directly into the coil. The probe was then inserted into the bore of the superconducting solenoid. No provisions were made to lock the magnetic field and all spectra were taken at room temperature.

Signals were obtained with a quadrature detection system and stored in 16K of memory in an Aspec 2000 computer. The duration of the excitation pulse which produced the maximum signal was found to be 3-4 microseconds. The delay between the pulse and the beginning of data acquisition

was set at 85 microseconds in order to minimize baseline distortion due to pulse feed through. Spectra windows of 50 KHz and acquisition times of approximately 0.16 s were used.

Samples were sealed in 5 mm NMR tubes. The Na⁺C222·Na⁻ sample was prepared as described in Chapter 3. The Na⁺C222·I⁻ sample was prepared as described by Moras and Weiss (108). Powdered reagent grade NaCl was used and saturated aqueous NaCl served as the reference (+0.75 ppm versus infinitely dilute aqueous Na⁺). Positive shifts are in the downfield direction (paramagnetic).

The signal-to-noise ratio (S/N) obtained for saturated aqueous NaCl in one scan was approximately 200:1. Other S/N values appear in Table 7. The linewidth ($\Delta v_{1/2}$, full width at half-height) for the reference NaCl solution varied from 18.7 Hz to 69 Hz for various trials. The natural linewidth for saturated aqueous NaCl is approximately 8 Hz (102). These data imply an inhomogeneous line broadening of 10-60 Hz, which is very small when compared to all other 23 Na linewidths observed here. See Table 7 for a complete listing of observed linewidths.

The chemical shift observed for crystalline Na⁺C222.

Na⁻, -64.1 ppm, agrees well with that obtained for Na⁻,

-62.1 ppm, in ethylamine (102). The chemical shift of

crystalline Na⁺C222·I⁻, -12.7 ppm, is also in good agree
ment with that obtained for Na⁺C222 in ethylamine -9.7

ppm. It is believed the resonance due to Na⁺C222 is

 $^{23}\mathrm{Na}$ Solid State NMR Chemical Shifts and Linewidths. Table 7.

Compound (Condition)	Chemical Shift (ppm)	Linewidth (hz)	Signal:Noise (#scans)
Na+C222.Na (Crystalline)	1.49-	2400-2800	4:1 (700)
Na + C222.T (Crystalline)	-12.7	4700	25:1 (17,000)
Na offer ()	+12.2	3200	35:1 (7500)
Nacl (crystairs)	+ 0.75	18–69	200:1 (1)
NaCl (Saturateu, aque	-62.1	6-9	!
Na (.15 M, etnytamine)	7.6 -	120-170	
Na + C222 (.15 M, eun tament			

obscured by the Na resonance and is not well resolved because the linewidths of Na C222 and Na are about the same as their chemical shift difference. Figure 19 shows the spectra obtained for Na C222·Na and Na C222·I. It is likely that the resonance due to Na C222 in the upper spectrum is partially buried to the left of the resonance assigned to Na. The arrow labeled 1 is the shift position of powdered NaCl, and the arrows labeled 2 and 3 are the shifts for Na C222 and Na respectively in ethylamine (102).

It was presumed that the signals observed for Na⁺C222 and Na⁻ could be narrowed and, thereby resolved using magic angle spinning and/or proton decoupling techniques. Indeed, these techniques were recently used to obtain solid state NMR spectra of a number of solids (109) and have proven to be useful tools for the identification of alkalide salts.

V.C. Low Temperature X-Ray Powder Patterns

V.C.1. Introduction

Attempts to prepare <u>crystalline</u> electrides in which the anion is a trapped electron had not been successful at the completion of this research. When solutions which contain metal and complexing agent in a 1:1 ratio are evaporated the solutions either decompose or form blue-black residues. Inspection under a microscope occasionally indicated that crystals might be present; however, all attempts to isolate

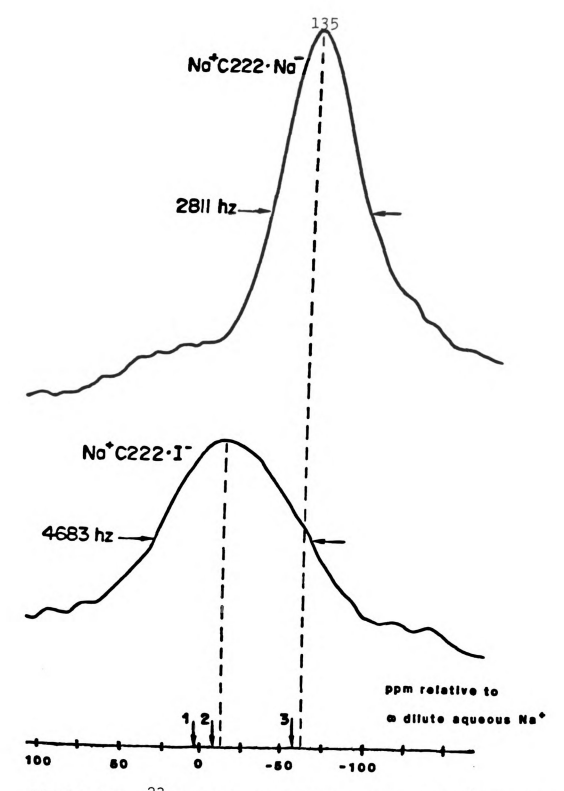


Figure 19. ²³Na Solid State NMR Spectra of Na⁺C222·Na⁻ and Na⁺C222·I⁻.

these apparently crystalline products were unsuccessful.

In order to determine whether these blue-black residues were crystalline or amorphous, low temperature X-ray powder patterns were obtained. The results of these were inconclusive but they showed the presence of diffraction lines for Cs⁺18C6·e⁻ which could not be attributed to either cesium metal or 18C6 alone.

Commercial cold X-ray powder systems were not available for this research so a camera was modified to allow for temperature control. This camera (Figure 12) permitted the passage of cold nitrogen gas over the sample during X-ray bombardment.

Several attempts were made to prepare the electride samples in a synthesis vessel which had a capillary tube sidearm. It was hoped that the electride powder, once free of solvent, could be poured into the capillary tube sidearm and sealed away from the apparatus. Every attempt failed due to either solution decomposition or to breakage of the capillary tube from manipulations in the cold bath.

Because of these failures, samples which had been previously prepared by slow solvent evaporation were used. These samples had been prepared in 3 mm (0.D.) quartz tubes and had been stored in $1-N_2$ continuously before use here. It was thought the large sample size and the thickness of the quartz tubing walls would absorb a significant percentage of the X-rays and make it difficult to observe

diffraction lines. To test this powder patterns were obtained using Na⁺C222·I⁻ in 3 mm quartz tubing. Although the diffraction lines produced were somewhat weak and broad, they were clearly discernable.

Samples of stoichiometry $\operatorname{Li}_2(\operatorname{C2l1})$ and $\operatorname{Cs}(18\operatorname{C6})$ were examined. The $\operatorname{Li}_2(\operatorname{C2l1})$ sample showed no diffraction lines. The $\operatorname{Cs}(18\operatorname{C6})$ sample produced diffraction lines. To ensure that the lines were not due to unreacted starting materials a powder pattern was obtained for 18C6 and a powder pattern for Cs was calculated by using a computer program by Larson et al. (110).

V.C.2. Results and Discussion

A Philips XRG-3000 generator with both Cu K_{α} (λ = 1.542 Å) and Mo K_{α} (λ = 0.709 Å) radiation was used at 35 kV/20 mA and 48 kV/30 mA, respectively. A Debye-Scherer powder camera (No. 170 102 00) was modified by using copper tubing as shown in Figure 12. Sample temperatures were measured using a copper-constantan thermocouple and a Doric (DS-350) digital readout.

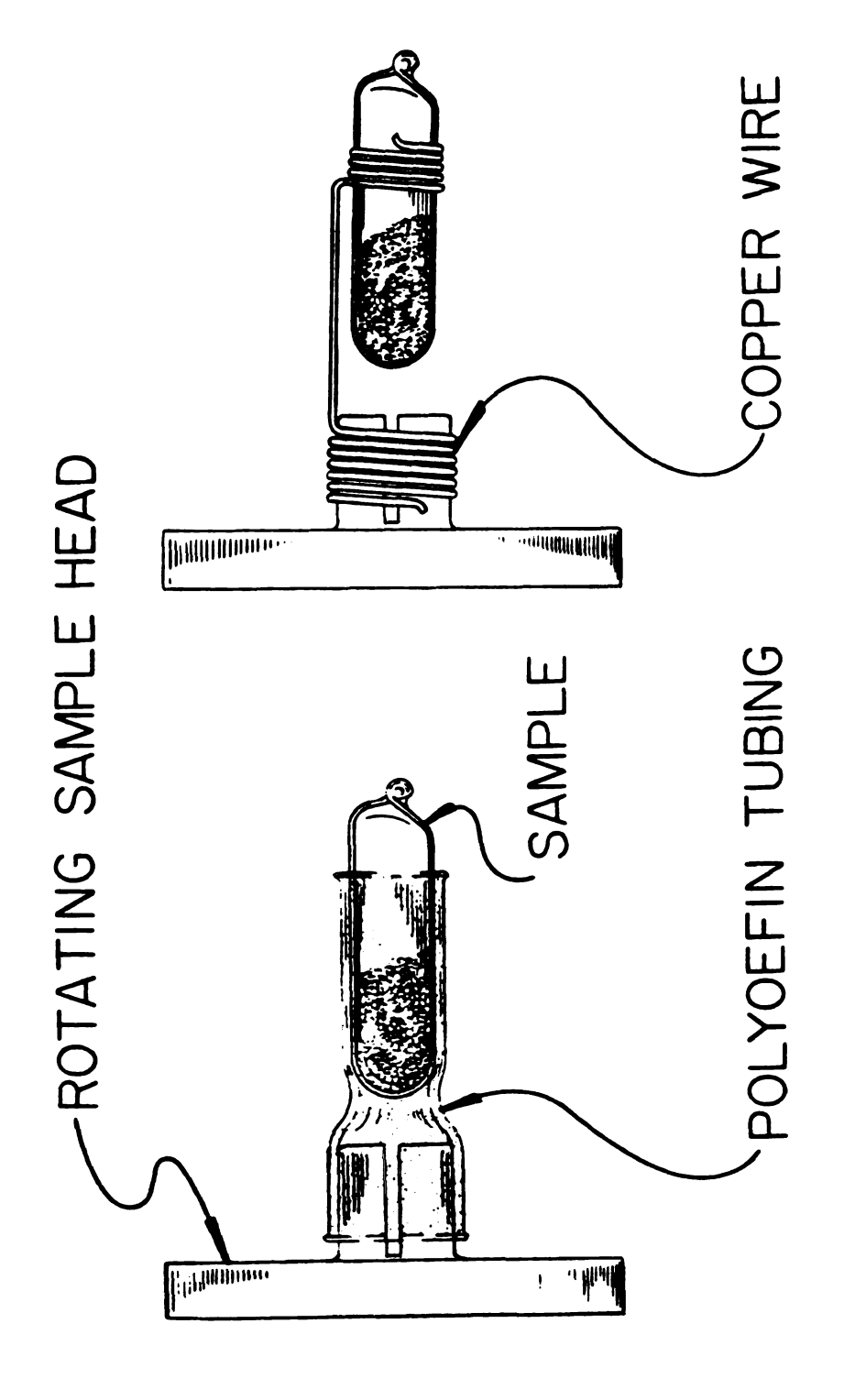
Clay is typically used to hold capillary tube samples in Debye-Scherer type cameras. The work described here required that the camera be chilled before introduction of the sample to avoid sample decomposition. Because clay is too stiff to use at these temperatures two alternative sample holders were used. The first was a length of

polyolefin heat-shrinkable tubing which was pre-shrunk to the size of the sample tube at one end and shrunk directly onto the cameras rotating sample head at the other end. The second holder was a short length of pure copper wire coiled to accept the sample tube and attached to the cameras rotating sample head (Figure 20).

Powder patterns were obtained for both holders using an empty 3 mm quartz tube. The polyolefin holder produced no diffraction lines but did cause a moderate darkening of the film from 20=8-35°. The copper holder produced the pattern expected for copper metal (110), however, the pattern was doubled due to the non-centered position of the copper in the X-ray beam (Figure 20). These lines were quite strong and easily identified as being due to the copper metal. Because copper produces a few diffraction lines it was a simple matter to account for them.

Because the low temperatures used could produce frost if any moist room air leaked into the system several samples were run from 0°C to -130°C and examined for frost immediately after X-ray bombardment. No frost was observed.

At these low temperatures it was anticipated that film shrinkage would be a problem. To test this, diffraction patterns were obtained of KBr at room temperature and at -80°C. The 420 diffraction (20 approximately 63°) at 25°C and -80°C differed by 0.25° or approximately 0.4%. Because



Cold X-ray Powder Pattern Sample Holders. Figure 20.

of the qualitative nature of this work this error was small and, therefore, ignored.

Powder patterns of 18C6 were obtained in order to assure that lines observed for Cs⁺18C6·e⁻ were not due to unreacted 18C6. Patterns were obtained using Cu K_{α} radiation with the sample in a 0.5 mm capillary tube. Patterns were also obtained from samples in 3 mm quartz tubing using Mo K_{α} radiation. Both produced diffraction patterns, however, the Mo/3 mm quartz patterns were less intense with broader lines (Table 8).

A cesium powder pattern was calculated (110) for comparison with the Cs⁺18C6·e⁻ pattern to assure that the electride pattern was not due to unreacted cesium metal. The pattern calculated for both Mo and Cu radiation are tabulated in Table 9.

Three powder patterns were obtained of $Cs^{+}18C6 \cdot e^{-}$. The first pattern was obtained using the polyolefin holder with Mo radiation. The sample was run at $-130^{\circ}C$ for 10.8 h. This low temperature apparently caused the sample to stop rotating early in the exposure because only spots and not lines were observed on the developed X-ray film. The film was completely exposed (black) for $2\theta=0^{\circ}$ to 12° and no lines could be seen. For 2θ approximately 12° to 35° diffraction spots were clearly visable. Direct measurement of the 2θ values for these spots is inaccurate because the center ($2\theta^{\circ}=0$) position could not be accurately located. Inspection of this film showed many more spots than could

Table 8. X-ray Powder Diffraction Lines for 1806.

0.5 mm) Radiation Capillary, Holder	Mo (K_{α}) 3 mm Tube, Po	Radiation lyolefin Holder
20	Intensity	2θ (Observed)	(Calc. 20 From Cu Kα Data)
15.5	S	7.2	7.1
17.2	S	8.0	7.9
19.9	S	9.0	9.1
20.8	S		9.5
21.9	М		10.0
22.8	M		10.4
24.2	VS		11.1
25.4	VS		11.6
26.5	M		12.1
30.5	W	13.8	13.9
32.9	W	15.0	15.0
38.8	M	17.8	17.6
39.5	M	18.9	
47.0	М	21.0	21.2
49.7	M	23.0	22.3

Table 9. Powder Diffraction Lines for Cesium and Copper Metals.

CESIUM					
Cu ($ extsf{K}_{oldsymbol{lpha}}$ Radiation)		Mo (Kα Radiation)			
2θ	Intensity	20	<u>~</u>	D-Spacing	HKL
20.71	100	9.49	100	4.290	011
29.45	16.6	13.44	17.3	3.034	002
36.27	35.9	16.48	38.6	2.477	112
42.13	11.2	19.05	12.5	2.145	022
47.39	15.2	21.33	17.4	1.919	013
52.24	3.6	23.39	4.3	1.751	222
56.78	16.1	25.29	19.6	1.622	123
61.10	1.5	27.07	1.9	1.517	004
COPPER					
Cu (Κ _α :	Radiation)		Mo (K $_{lpha}$ H	Radiation)	
2θ	Intensity		2θ I	O-Spacing	HKL
43.36	100	19	9.59	2.087	111
50.50	47.2	22	2.65	1.808	002
74.20	29.1	32	2.25	1.2781	022
90.04	35.4	38	3.02	1.090	113
95.26	10.6	39	.78	1.044	222
117.10	7.0	46	.26	0.904	004
136.76	34.7	50	.69	0.829	133
145.03	41.3	52	.10	0.808	024

be accounted for by cesium metal. A direct comparison between this film and the 1806 film also indicated spots that could not be accounted for by the 1806 diffraction lines.

A second pattern of Cs⁺18C6·e⁻ was obtained by using Mo radiation and the polyolefin holder. This sample was exposed at approximately -50°C and at this temperature the sample continued to rotate throughout the exposure. This exposure resulted in seven clearly discernable lines. These lines were fairly broad and light and no lines were observed for 20 approximately 7° to 13° where the film was black, due to the polyolefin holder. Although the data from this pattern are limited there are diffraction lines present which cannot be accounted for by either 18C6 or cesium metal. The seven observed lines were 20 = 15.8, 18.8, 20.2, 21.0, 23.3, 28.3, and 32.3.

An additional exposure was made using Cu radiation and the copper wire holder. The sample was exposed ll.l h at -50° C. The pattern produced was very weak, even the lines due to the copper wire. Two very weak lines were observed at $2\theta = 33.2^{\circ}$ and 58.7° that would correspond to 15.1° and 26.0° for Mo radiation. These lines do not correspond to those observed in the Mo pattern of $Cs^{+}18C6^{\circ}e^{-}$ and re- main a puzzle.

Even though these results are not conclusive it does seem likely based on this evidence that a new crystalline compound is present. It is also apparent that a smaller sample size would be an improvement to not only allow more

completely exposed and narrower lines but also allow the use of Cu ${\rm K}_{\alpha}$ radiation.

NOTE: Recently, after the conclusion of this research, other researchers have isolated single crystals of Cs⁺18C6·e⁻. One such crystal whose morphology clearly indicates crystallinity has been mounted for X-ray structure determination. This crystal produced distinct but weak diffraction spots during preliminary work.

Recent powder X-ray studies (111) have shown several sodide salts including Cs(18C6)₂·Na⁻ to be crystalline.

This work has also shown that a similar compound Cs⁺- (18C6)₂·e⁻ is crystalline.

VI. THERMODYNAMICS OF FORMATION OF ALKALIDES AND ELECTRIDES

VI.A. Introduction

The thermodynamic results and arguments presented here were used as a guide in the synthesis of alkalide and electride salts. These calculations indicate it should be possible to synthesize many thermodynamically stable alkalide and electride salts. The existence of alkali metal anions in ammonia was proposed in 1965 by Golden et al. (76,77). The thermodynamic arguments presented are similar to those used by Golden when he proposed their existence several years before the first alkalide salt was isolated (79,80). In order to address the thermodynamic stability of these compounds, a number of experimental determinations and theoretical calculations were undertaken.

The first of these determined whether $Na^{+}C222 \cdot Na^{-}(S)$ is truly thermodynamically stable or only kinetically stable at 273 K (85). The second experiment obtained an estimate of ΔH_F^o for reaction (9) by measuring the heat of decomposition of

$$2Na_{(s)} + C222_{(s)} + Na^{+}C222 \cdot Na^{-}_{(s)}$$
 (9)

 $Na^+c222\cdot Na^-_{(s)}$ with water. The third experiment determined ΔH° , ΔG° , and ΔS° for reaction (9) by measuring the temperature dependent emf of saturated $Na^+c222\cdot Na^-/c222$ solutions with $Na^+\beta$ -alumina and platinum electrodes (112). The fourth experiment determined the solubility of C222 in cyclohexane. These data when coupled with the distribution coefficient for C222 in water/cyclohexane allowed the determination of the free energy of solution for C222.

In addition to these experiments, thermodynamic calculations were also made. Portions of these calculations have been published (83,113) but the entire series in its present form has remained unpublished until now. These calculations include the heat of formation, the free energy of formation and the entropy of formation for both alkalides and electrides. Strictly speaking, the heat or free energy of formation of a compound is referenced from its elements. Because the free energy and enthalpy of formation of cryptand from its elements is unimportant for the determination of the relative stabilities of alkalide and electride salts the calculations presented here are for the following reactions:

$$M_{(s)} + N_{(s)} + C_{(s)} \rightarrow M^{+}C \cdot N^{-}_{(s)}$$
 (10)

$$M_{(s)} + 2N_{(s)} + C_{(s)} + M^{+2}C \cdot (N^{-})_{2(s)}$$
 (11)

$$M(s) + C(s) + M^{+}C \cdot e^{-}(s)$$
 (12)

$$M_{(s)} + C_{(s)} \rightarrow M^{2+}C \cdot (e^{-})_{2(s)}$$
 (13)

where M is an alkali or alkaline earth metal, N is an alkali metal, and C is a cryptand.

These calculations are based on a modified Born-Haber cycle (Figure 21). The calculated values are compared with experimental values obtained for both $Na^+C222 \cdot Na^-$ and also Na^+C222 and K^+C222 halides. Additionally, calculations are included for compounds which contain anions of Au, Ag, and Cu.

VI.B. <u>Experimental Determinations</u>

VI.B.1. Thermodynamic Versus Kinetic Stability of Na⁺C222·Na⁻

Approximately one year after one of the early successful syntheses of Na⁺C222·Na⁻ it was observed that samples of this compound had decomposed forming grey lumps; presumably sodium metal. These products could be dissolved to give blue solutions. Based on this evidence it seemed likely that this decomposition occurred according to (9). This salt is typically prepared at reduced temperatures to avoid solution decomposition and because it is also stored at reduced temperatures it seemed possible that this salt

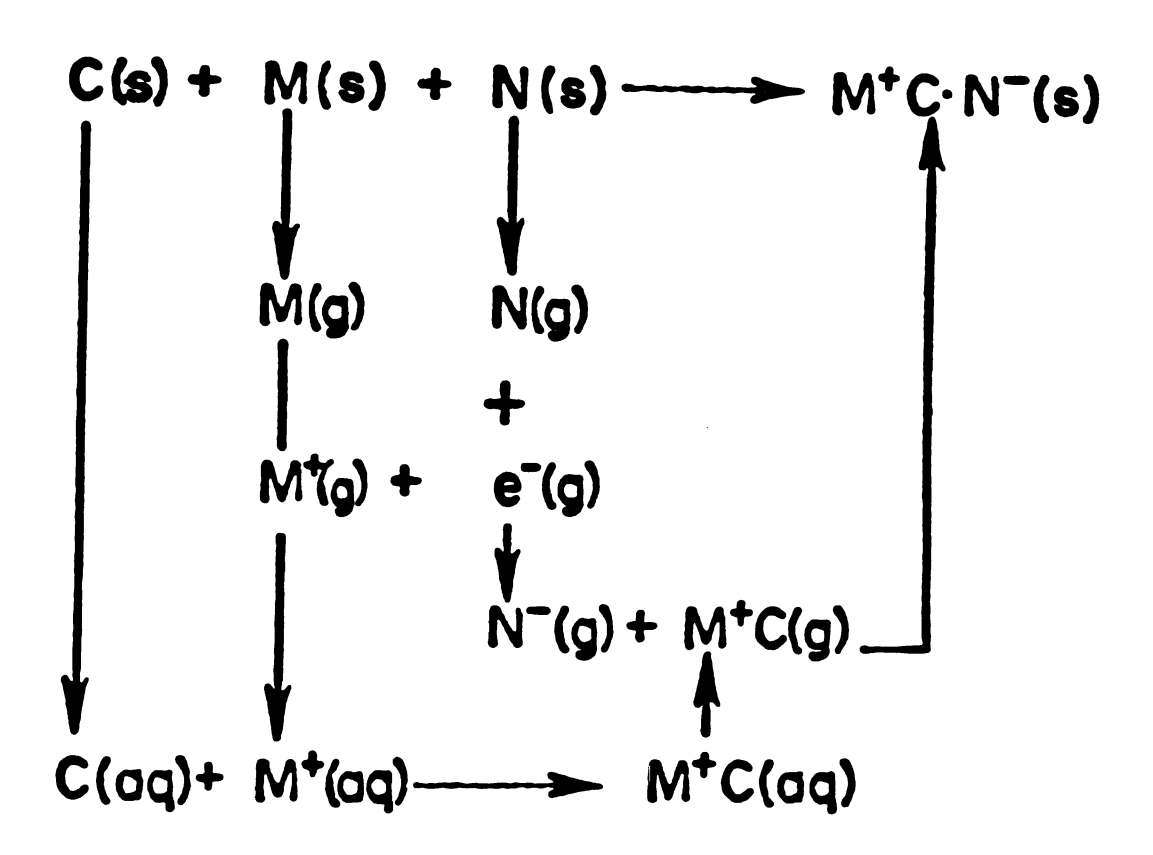


Figure 21. Thermodynamic Cycle Used to Estimate the Stability of Alkalide Salts.

was kinetically stable but not thermodynamically stable. Thermodynamic stability results only if the free energy change

$$2Na_{(s)} + C222_{(s)} \rightarrow Na^{+}C222 \cdot Na_{(s)}^{-}$$
 (9)

for (9) is negative.

DaGue (85) showed that the free energy change for (9) at 273 K is negative. He did so by allowing a 0.04 M solution of C222 in ethylamine to react with sodium metal isothermally at 273 K. He observed the formation of crystals of Na⁺C222·Na⁻ before all the sodium metal had dissolved. This experiment proves that Na⁺C222·Na⁻(s) is thermodynamically stable with respect to Na_(s) and C222_(SOLV). However, because the chemical potential of C222_(SOLV) is less than or equal to that of C222_(s) it follows directly that Na⁺C222·Na⁻(s) is thermodynamically stable with respect to Na_(s) and C222_(s).

VI.B.2. Calorimetric Determination of ΔH° for Na⁺C222·Na⁻

In order to determine experimentally the heat of formation of Na⁺C222·Na⁻(s) samples were prepared and sent to Stevenson and coworkers at Illinois State University.

Stevenson used a modified Parr solution calorimeter (114) into which break bulbs containing crystalline Na⁺C222·Na⁻ samples were placed. A push rod was used to break the bulb,

thereby allowing the salt to react directly with a known volume of water. The change in temperature was measured by using a thermocouple. Four samples were prepared as described in Chapter 3 and weighed into spherical break bulbs approximately 1" in diameter. The bulbs were evacuated and sealed prior to shipping in a $1-N_2$ cooled container.

The presumed reaction of $Na^+C222 \cdot Na^-$ (s) with water is given by (14). The heat of reaction (14) was determined

$$Na^{+}C222_{(aq)}^{+}Na^{+}_{(aq)}^{+}2OH^{-}_{(aq)}^{+}H_{2(g)}^{+}Na^{+}C222\cdot Na^{-}_{(s)}$$

$$+ 2H_{2}O_{(1)}$$
(14)

to be 102.0 ± 2 Kcal/mol (115). The enthalpies for reactions (15), (16), and (17) have been previously measured (116, 117).

$$C222_{(s)} \rightarrow C222_{(aq)}; \Delta H^{\circ} = -5.9 \text{ Kcal/mol}$$
 (15)

$$Na^{+}(aq)^{+C222}(aq)^{+}Na^{+}C222(aq); \Delta H^{\circ}=-7.6 \text{ Kcal/mol}$$
 (16)

$$^{2\text{H}}_{2}^{\text{O}}(1)^{+2\text{Na}}(s)^{+\text{H}}_{2}(g)^{+2\text{Na}}(aq)^{+2\text{OH}}(aq); \Delta \text{H}^{\circ}=-87.9 \text{ Kcal/mol}$$
(17)

$$2Na_{(s)} + C222_{(s)} + Na^{\dagger}C222 \cdot Na_{(s)}; \Delta H_f^{\circ} = +0.6 \text{ Kcal/mol}$$
(9)

The sum of (14), (15), (16), and (17) yields Reaction (9) where $\Delta H_f^o = +0.6$ Kcal/mol. This result is somewhat puzzling. If ΔH_f^o is near zero and ΔG_f (273K) is negative this implies that ΔS_f^o is either near zero or positive. This would be unusual because most 1:1 salts have ΔS_f^o of -10 to -40 cal/Kmol. It is true that Na⁺C222·Na⁻ is not a simple 1:1 salt and may not behave exactly like an alkali halide, for example. However, other experimental and theoretical determinations (vide infra) estimate ΔH_f^o for Na⁺C222·Na⁻ to be -8.1 and -9.0 Kcal/mol, respectively. If ΔG_f (273) is again negative and ΔH_f^o is -8 to -9 Kcal/mol, ΔS_f^o values could range from approximately 0 to -30 cal/Kmol much more reasonable values.

It is possible that the reaction of Na⁺C222·Na⁻ with water produced products other than those shown in reaction (14), and in retrospect a careful analysis of the organic products would have been useful. Additionally, experience with similar alkalide/water reactions in the hydrogen evolution steps of the analysis section of this work shows that frequently cryptand decomposition products are formed. If these products were formed during the calorimetric work there would undoubtedly be an error in the enthalpy obtained.

VI.B.3. Electrochemical Determination of $\Delta H_{\hat{\Gamma}}^{\circ}$, $\Delta G_{\hat{\Gamma}}^{\circ}$, and $\Delta S_{\hat{\Gamma}}^{\circ}$ for Na⁺C222·Na⁻

Schindewolf, Le, and Dye (112) have measured the emf of the cell Pt|Na_(s)|Na⁺β-alumina|Na⁺C222·Na⁻(SAT)|Na⁺C222·Na⁻(SAT)|Na⁺C222·Na⁻(SAT)|Pt as a function of temperature in several solvents. From these measurements they calculated $\Delta H_f^o = -8.1 \pm 0.5$ Kcal/mol, $\Delta G_f^o = -1.7 \pm 0.1$ Kcal/mol, and $\Delta S_f^o = -21.5 \pm 1.9$ cal/Kmol.

The electrode designed for this work was based on a high precision sodium electrode (118-120) which selectively transports sodium ions through β -alumina (121-123). Schindewold, Le, and Dye argue that the electrochemical cell given in (18) has an emf given by (19),

Pt
$$|Na_{(s)}| Na^{+} \beta$$
-alumina $|Na_{(SOLV)}^{+} \cdots e_{(SOLV)}^{-}| Pt$ (18)

$$\varepsilon = \varepsilon_{20}^{\circ} - \frac{RT}{F} \ln[(Na^{+})(e^{-})]$$
 (19)

$$Na_{(s)} \neq Na_{(SOLV)}^{\dagger} + e_{(SOLV)}^{\dagger}$$
 (20)

where $\varepsilon_{20}^{\circ} = -F\Delta G_{20}^{\circ}$. In amine solutions Na is the major species and the cell can be rewritten to give

$$\varepsilon = \varepsilon_{22}^{\circ} - \frac{RT}{2F} \ln[(Na^{+})(Na^{-})]$$
 (21)

$$2Na_{(s)} \neq Na_{(SOLV)}^{\dagger} + Na_{(SOLV)}^{\dagger}$$
 (22)

where $\varepsilon_{22}^{\circ} = -2F\Delta G_{22}^{\circ}$. ε_{20}° and ε_{22}° are related to ΔG_{24}° for reaction (23) by $\Delta G_{23}^{\circ} = 2\Delta G_{20}^{\circ} - \Delta G_{22}^{\circ}$.

$$Na^{-}(SOLV) \stackrel{?}{\leftarrow} Na^{+}(SOLV) + 2e^{-}(SOLV)$$
 (23)

If both Na⁺C222·Na⁻ and C222 are maintained at saturation then equilibria (24) and (25) are maintained and the net cell reaction is given by reaction (9).

$$Na^{+}C222 \cdot Na^{-}(s) \stackrel{?}{=} Na^{+}C222_{(SOLV)} + Na^{-}(SOLV)$$
 (24)

$$C222_{(s)} \neq C222_{(SOLV)}$$
 (25)

$$2Na_{(s)} + C222_{(s)} \neq Na^{+}C222 \cdot Na_{(s)}$$
 (9)

Therefore, the desired thermodynamic quantities are given in (26) and the emf of the cell (27) is solvent independent.

$$\Delta G_9^{\circ} = -2F; \Delta S_9^{\circ} = 2F(d\varepsilon/dT)$$
 (26)

Pt|Na(s)|Na
$$^{\dagger}\beta$$
-alumina|Na † C222·Na $^{-}$ (SAT)C222(SAT)|Pt (27)

These results, $\Delta H_{f}^{\circ} = -8.1 \pm 0.5$ Kcal/mol, $\Delta G_{f}^{\circ} = -1.7 \pm 0.1$ Kcal/mol, and $\Delta S_{f}^{\circ} = -21.5 \pm 1.9$ cal/Kmol, indicate that this salt should be stable up to approximately 90-120°C.

The decomposition temperature is 83°C (80). These results will be compared to those obtained from the theoretical calculations in the discussion section of this chapter.

VI.B.4. Free Energy of Solution for C222

The distribution coefficient for C222 in cyclohexane/ water is known, 0.0249 (116). In order to obtain the free energy of solution of C222, the saturation concentration of C222 in cyclohexane is required. This was obtained by adding excess C222 to cyclohexane at 25°C and after equilibrium was established a known volume of the saturated solution was weighed, the solvent was evaporated, and the C222 was weighed. The concentration was 0.280 M, therefore, the saturation activity in water would be 11.2 M, and ΔG°=-RTlnK or -1.43 Kcal/mol. Because the activity coefficient of C222 in cyclohexane is unknown an estimate of the error is difficult. If, however, γ is as low as 0.5, the error would be no larger than 0.4 Kcal/mol.

VI.C. Theoretical Calculations

VI.C.1. Modified Born-Haber Cycle

As shown in Figure 21, the calculations involve a modified Born-Haber cycle including the following reactions.

$$^{M}(s) \rightarrow ^{M}(g) \tag{28}$$

$$M(g) \rightarrow M^{+}(g) + e^{-}(g) \text{ or } M(g) \rightarrow M^{2+}(g) + 2 e^{-}(g)$$
 (29)

$$M^{+}(g) \rightarrow M^{+}(aq) \text{ or } M^{2+}(g) \rightarrow M^{2+}(aq)$$
 (30)

$$^{C}(s) \rightarrow ^{C}(aq) \tag{31}$$

$$^{N}(s) \rightarrow ^{N}(g) \tag{32}$$

$$e^{-}(g) + N_{(g)} + N^{-}(g)$$
 (33)

$$M^{+}(aq) + C(aq) \rightarrow M^{+}C(aq)$$
 or $M^{2+}(aq) + C(aq) \rightarrow M^{2+}C(aq)$ (34)

$$M^{+}C_{(aq)} \rightarrow M^{+}C_{(g)} \quad \text{or} \quad M^{+2}C_{(aq)} \rightarrow M^{2+}C_{(g)}$$
 (35)

$$M^{+C}(g) + N^{-}(g) \rightarrow M^{+C} \cdot N^{-}(s) \text{ or } M^{+2}C(g) + 2N^{-}(g) \rightarrow M^{+2}C \cdot (N^{-})_{2(s)}$$
 (36)

VI.C.1.a. Atomization
$$(M(s) \rightarrow M(g))$$

The atomization enthalpies and free energies for both metals M and N are tabulated in Table 10. These data were taken from Langes Handbook of Chemistry (117).

Table 10. Atomization Enthalpy and Free Energy.

Metal	ΔH° (Kcal/mol)	ΔG° (Kcal/mol)
Li	38.4	30.6
Na	25.75	18.48
K	21.3	14.5
Rb	20.51	13.35
Cs	18.3	11.9
Ba	42.8	35.1
Cu	80.86	71.37
Au	87.5	78.0
Ag	68.01	58.72
Sr	39.2	31.2
Ca	42.85	34.78

VI.C.1.b. Ionization
$$(M_{(g)} \to M^{+}_{(g)} + e^{-}_{(g)})$$
 or $M_{(g)} \to M^{2+}_{(g)} + 2e^{-}_{(g)}$

The ionization enthalpy is the sum of the ionization potential and $\Delta(PV)$. At standard conditions $\Delta(PV)$ becomes $P\Delta V$ or ΔnRT where $\Delta n = n_{M^+} + n_{e^-} - n_{M}$ and Δn is 1; for $M_{(g)} + M^{2+}$ (g) M^{2+} (g) where $\Delta n = n_{M^+} + 2n_{e^-} - n_{M}$ and $\Delta n = 2$. Expressing the ionization potential in eV, the expression becomes

$$\Delta H^{\circ} = 23.06 \text{ (I.P.[eV])} + \Delta n \text{ (0.5924)}$$
 (37)

The ionization free energy is calculated using (38), (39)

$$\Delta G^{\circ} = \Delta H^{\circ} - T \Delta S^{\circ}$$
 (38)

$$\Delta S^{\circ} = S^{\circ}_{M} + (g) + S^{\circ}_{e} - (g)^{-S^{\circ}_{M}(g)} \text{ or } S^{\circ} = S^{\circ}_{M} + (g) + 2S^{\circ}_{e} - (g)$$

$$+ S_{M(g)}^{\circ}$$
 (39)

and the Sackur-Tetrode equation for So (124).

S° = R
$$(\ln V + \frac{3}{2} \ln T + \frac{3}{2} \ln M) - 11.074 + R \ln g$$
 (40)

where R = gas constant, 1.987 cal $mol^{-1} deg^{-1}$. V = standard state volume, 24460 cm³ mol⁻¹. T = temperature, 298.15 K.

M = molecular weight of the atom or ion in grams mol^{-1} .

g = degeneracy of the ground state (2 for alkali metal atoms and gaseous electrons and 1 for alkali and alkaline earth cations and alkaline earth atoms).

The results of these calculations are summarized in Table

11. The ionization potentials were taken from The Handbook

of Chemistry and Physics (125).

VI.C.1.c. Aquation
$$(M^+(g) \rightarrow M^+(aq))$$
 or $M^{2+}(g) \rightarrow M^{2+}(aq)$

The enthalpy and free energy data used here were derived from experimentally obtained cation and anion aquation energy sums. These sums are simply the sum of the hydration energies for an anion-cation pair. For example, the enthalpy change of $M^+(g) + X^-(g)$ reacting to form $M^+(aq) + X^-(aq)$ is obtained by subtracting the enthalpy of atomization and ionization of M and X from the sum of the heat of formation and the heat of solution of $MX_{(s)}$. In order to obtain single ion hydration values these sums must be partitioned between the anion and cation. If only one single ion hydration value were accurately measured or calculated, all the others could be obtained directly. The data used here was obtained using the absolute energy of hydration

Table 11. Ionization Enthalpy and Free Energy.

Metal	ΔH° Kcal/mol	ΔG° Kcal/mol	IP (eV)	Δn	S _M cal/Kmol	S _M + cal/Kmol	S _e - cal/Kmol	
Li	124.89	123.81	5.39	1	33.14	31.76	4.99	
Na	119.07	117.99	5.138	Н	36.71	35.33	4.99	
Ж	100.65	99.57	4.339	Н	38.29	36.91	4.99	
Rb	96.89	95.81	4.176	~	40.62	39.24	4.99	
Cs	90.36	89.28	3.893		41.94	40.56	4.99	
Ça	415.78	412.80	6.111/11.868	2	36.99	36.99	4.99	
Sr	386.72	383.74	5.692/11.027	2	39.32	39.32	4.99	
Ba	351.95	348.97	5.21/10.001	5	40.66	40.66	4.99	

of $K^+_{(g)}$ ($\Delta G^{\circ}_{t} = -80.6 \text{ Kcal/mol}$, $\Delta H^{\circ}_{t} = -85.8 \text{ Kcal/mol}$) obtained by Randles (126). The free energy of hydration of $K^+_{(\sigma)}$ was measured potentiometrically where no assumptions or approximations of the ionic radius were required. This value for K^{+} is consistent with the following proton transfer values: ΔG_{t}^{o} (H⁺) = -260.5 Kcal/mol, ΔH_{t}^{o} (H⁺)= -269.8 Kcal/mol (127). Nearly all other methods of partitioning the sum of anion and cation hydration energies require an estimate of the ionic radii. The Born method as well as its various refinements all require the ionic radius of the ions. The experimental values used here to calculate the enthalpy and free energy of formation of the alkalides and electrides were taken from Goldman and Bates (128) where these experimental values are compared to calculated values. Goldman and Bates used an off-centered dipole model to characterize the permanent electrostatic properties of water for primary solvation and a Born continuum model for secondary solvation. Even though only the experimental values are used here for the energy of formation calculations it is interesting to note that the values calculated by Goldman and Bates differ by less than 5% from the experimental values. The values are listed in Table 12.

Table 12. Aquation Enthalpy and Free Energy.

Metal	-ΔH° (Kcal/mol)	-ΔG° (Kcal/mol)
Li	132.1	122.1
Na	106.0	98.2
K	85.8	80.6
Rb	79.8	75.5
Cs	72.0	67.8
Ca	398.8	380.8
Sr	363.5	345.9
Ba	329.5	315.1
Cl	81.3	75.8
Br	77.9	72.5
I	64.1	61.4

VI.C.1.d. Cryptand Aquation
$$(C(s) \rightarrow C(aq))$$

No thermodynamic quantities are currently available for this process except for those for C222 discussed in Part B of this Chapter. The values obtained for C222 were, $\Delta H^{\circ} = -5.91$ Kcal/mol and $\Delta G^{\circ} = -1.43$ Kcal/mol. Until other thermodynamic quantities become available, these values will be used as approximations for all cryptands including C322, C221, and C211. The estimated error for this assumption is less than one Kcal.

VI.C.l.e. Atomization
$$(N(s) \rightarrow N(g))$$

This process is obviously the same as $M_{(s)} \rightarrow M_{(g)}$. The enthalpies and free energies for this process are also given in Table 10.

VI.C.1.f. Electron Attachment
$$(N_{(g)} + e^{-}_{(g)} \rightarrow N^{-}_{(g)})$$

The enthalpy of electron attachment is the sum of the electron affinity and $\Delta(PV)$. The $\Delta(PV)$ term is the same as that used for the ionization calculation. For this process $\Delta n = -1$ and at standard conditions $\Delta(PV)$ becomes ΔnRT or -0.59 Kcal/mol. The alkali metal electron affinities as well as those for Au, Ag, and Cu were taken from Kasdan and Lineberger (129). The electron affinities for the halogens were taken from "The Handbook of Chemistry and Physics" (125).

$$\Delta H^{\circ} = -23.06$$
 (Electron Affinity, ev) - 0.59 (41)

The free energy is calculated from $\Delta G^{\circ} = \Delta H^{\circ} - T\Delta S^{\circ}$ (where $\Delta S^{\circ} = S_{N^{-}} - S_{N^{-}} - S_{e^{-}}$) and Equation (40).

$$S^{\circ} = R(\ln V + \frac{3}{2} \ln T + \frac{3}{2} \ln M) - 11.074 + R \ln g$$
 (40)

For this process g = 2 for N, g = 2 for e, and g = 1 for N^- . For all metals used here $\Delta S^\circ = -6.37$ cal/Kmol and $T\Delta S^\circ = -1.90$ Kcal/mol. The enthalpy, free energy, and individual entropies are shown in Table 13.

VI.C.1.g. Complexation
$$(M^+(aq) + C_{(aq)} \rightarrow M^+C_{(aq)})$$
 or $M^{2+}_{(aq)} + C_{(aq)} \rightarrow M^{2+}C_{(aq)}$

The enthalpy and free energy of cryptation of alkali and alkaline earth metals have been obtained from stability constants and calorimetric measurements. These are given in Table 14. Those for Na $^+$, K $^+$, Rb $^+$, and Cs $^+$ with C222 are from Abraham <u>et al.</u> (116), the others were taken from Kauffmann et al. (99).

VI.C.1.h. Cryptate Solvation
$$(M^{\dagger}C_{(aq)} \rightarrow M^{\dagger}C_{(g)})$$
 or $M^{2\dagger}C_{(aq)} \rightarrow M^{2\dagger}C_{(g)}$

The Born equation is used here to calculate the enthalpy and free energy for the transfer of aqueous cryptated cations to the gas phase. The Born equation assumes that

Electron Attachment Enthalpy and Free Energy. Table 13.

Atom	-∆H° kcal/mol	-AG° kcal/mol	E.A. cal/Kmol	S _N -cal/Kmol	S _N cal/Kmol	Se- cal/Kmol
Li	14.89	12.99	0.620	31.76	33.14	4.99
Na	13.23	11.33	0.548	35.33	36.71	
X	12.14	10.25	0.501	36.91	38.29	
Rb	11.80	06.6	0.486	39.24	40.62	
S S	11.43	9.53	0.470	40.56	41.94	
Au	53.86	51.96	2.31	41.73	43.11	
Ag	30.57	28.67	1.30	39.94	41.31	
Cu	28.95	27.06	1.23	38.36	39.74	
Cl	83.91	82.01	3.613	36.62	38.00	
Br	78.14	76.25	3.363	39.04	40.42	
н	71.22	69.33	3.063	40.42	41.80	

Table 14. Complexation Enthalpy and Free Energy.

Metal	Cryptand	-ΔH° (kcal/mol)	-ΔG° (kcal/mol)
Li	C211	5.1	7.5
Na	C221	5.35	7.2
Na	C222	7.62	5.42
K	C222	11.56	7.45
Rb	C222	11.77	5.78
Cs	C222	5.19	1.97
Cs	C322	5.4	2.45
Ca	C221	2.9	9.5
Ca	C222	0.2	6
Sr	C221	6.1	10.0
Sr	C222	10.3	10.9
Ba	C222	14.1	12.9

solvent is a uniform medium of unvarying dielectric constant, D. It also assumes the ion is a sphere of radius r and charge e. The energy for the transfer of charged particles from one medium to another is the difference between the work done in reversibly charging a mole, N of particles in the two media.

$$H^{\circ} = \frac{Ne^2}{2Dr} (1-LT); \quad G^{\circ} = \frac{-Ne^2L}{2Dr}$$
 (42)

$$L = -\left(\frac{d\ln D}{dT}\right)_p$$
; $L_{H_2O} = 4.63 \times 10^{-3}$, $L_{VAC} = 0$ (43)

$$\Delta H^{\circ} = H^{\circ}_{VACUUM} - H^{\circ}_{AQUEOUS} = \frac{Ne^{2}}{2r} \left(1 - \frac{1-LT}{D}\right)$$
 (44)

$$\Delta G^{\circ} = G^{\circ}_{VACUUM} - G^{\circ}_{AQUEOUS} = \frac{Ne^{2}L}{2Dr}$$
 (45)

$$\Delta H^{\circ} = \frac{166.8}{r(\text{\AA})} \text{ Kcal/mol}$$
 (46)

$$\Delta G^{\circ} = \frac{163.9}{r(A)} - 1.89 \text{ kcal/mol}$$
 (47)

The 1.89 kcal/mol in (47) is due to the volume change in going from 1 mole/liter to 1 atmosphere pressure at

298 K. For this process TAS = TR ln $\frac{V2}{V1}$ = -1.89 kcal/mol.

The radii used here for the cryptated cations were obtained by using the ligand thickness calculations taken from a paper by J.-M. Lehn (130). Lehn assumes the radius of the cation and the thickness of the cryptand, where

$$r_{M^+C} = (r_{M^+}^3 + \frac{3V_L}{4\pi})^{1/3}; \quad V_L = \sum_{i} V_i$$
 (48)

and ΣV_i is equal to the sum of 11.5 Å³ for each oxygen, 14.0 Å³ for each nitrogen, and 33.5 Å³ for each CH₂ group in the cryptand. These data appear in Table 15. The alkali cation radii were taken from Pauling (131).

Even though the large size of these cryptated cations makes them well suited to the Born equation these calculations are weak for several reasons. Effects due to changes in water structure are ignored, secondary solvation is ignored, and other deficiencies in the Born equation itself are ignored. However, because the cryptand provides the primary solvation for the cation, errors from the primary solvation, which are frequently a problem when using the Born equation, should be small. Even though absolute solvation energy calculations may contain some error, the differences or relative calculations should be much more reliable.

Table 15. Cryptate Solvation Enthalpy and Free Energy.

M ⁺ C	ΔH (kcal/mol)	ΔG (kcal/mol)	Z	r _M +c	r _M + (A)	3V _L /4π (Å)
Li ⁺ C211	32.96	30.50	1	5.06	0.60	129.6
Na ⁺ C221	31.47	29.03	1	5.30	0.95	148.4
Na ⁺ C222	30.22	27.80	1	5.52	0.95	167.1
K ⁺ C222	30.16	27.75	1	5.53	1.33	167.1
Rb ⁺ C222	30.11	27.69	1	5.54	1.48	167.1
Cs ⁺ C222	30.00	27.59	1	5.56	1.69	167.1
Cs ⁺ C322	28.96	26.56	1	5.76	1.69	185.9
Ca ²⁺ C221	125.65	121.58	2	5.31	1.00	148.4
Ca ²⁺ C222	120.87	116.88	2	5.52	1.00	167.1
Sr ²⁺ C221	125.65	121.58	2	5.31	1.16	148.4
Sr ²⁺ C222	120.65	116.66	2	5.53	1.16	167.1
Ba ²⁺ C222	120.43	116.45	2	5.54	1.36	167.1

VI.C.1.i. Lattice Energy
$$(M^{\dagger}C_{(g)} + N^{-}_{(g)} \rightarrow M^{\dagger}C \cdot N^{-}_{(s)})$$

or $MC_{(g)}^{2+} \rightarrow M^{2+}C \cdot (N^{-})_{(s)})$

This calculation was used to determine the lattice enthalpy and free energy. If the crystal type for each of the alkalide and electride salts were known, the appropriate Madelung constant and ion sizes and charges could be used to calculate the lattice energy. However, the general empirical equation of Kapustinskii (132) can be used to calculate the lattice enthalpy when the structures are unknown.

$$\Delta H^{\circ} = \frac{-287.2 \text{ VZ}_{+}Z_{-}}{r_{+} + r_{-}} \left(1 - \frac{0.345}{r_{+} + r_{-}}\right) \tag{49}$$

Where V = number of ions (2 for M⁺C·N and 3 for M²⁺C· $(N^-)_2$), Z_+ and Z_- are the charges on the cation and anion, and r_+ and r_- are the cation and anion radii. The use of this empirical formula requires the estimation of interionic distance $(r_+ + r_-)$ in alkalide and electride salts. The cation radii have been previously estimated by using the ligand thickness calculations. The anion radii can be estimated by subtracting metal cation radii from interatomic distances in the individual metals (78). In the case of Na⁺C222·Na⁻ these calculations give 5.52 Å and 2.72 Å for the ionic radii of Na⁺C222 and Na⁻, respectively. This gives a value of 8.24 Å for $r_+ + r_-$; however, in the

crystal $r_+ + r_-$ is 7.06 Å, a 14% reduction. The error in $r_+ + r_-$ is likely due to errors in both M⁺C and N⁻, but a similar comparison with Na⁺C222·I⁻ (81) gives a value for $r_+ + r_-$ which is only 4% lower than calculated. The lack of sphericity of the cation and the compression of these likely "soft" alkali metal anions may be the cause of the error observed. Until other crystal structures are available the 14% reduction will be used for all alkalide salts for the calculation of lattice enthalpy.

The lattice enthalpy for electride salts also requires the calculation of $r_+ + r_-$ where r_- refers to the radius of an electron in the lattice. No crystal structure data are available to aid in this estimate. However, because the cation size is large we can assume that the electron occupies the octahedral holes of a closest-packed lattice of cryptated cations. This packing leads to a radius of 0.414 times the cation radius. The lattice energy then is calculated as if the salt consisted of a closest-packed array of cryptated cations with hard spherical anions which fit into octahedral holes. This assumption does not take into account possible cation compression or electron delocalization which would lead to further stabilization and more negative lattice enthalpies.

The lattice free energy could be calculated if the entropy change for lattice formation were known. To obtain an estimate for this, ΔS° vs. $\frac{1}{r_{+}+r_{-}}$ was plotted for

alkali halides and also for alkaline earth halides. This results in Equation (50)

$$\Delta S^{\circ} = -48.70 - 27.57 \left(\frac{1}{r_{+} + r_{-}}\right) \text{ cal/Kmol}$$
 (50)

for alkali halides and Equation (51)

$$\Delta S^{\circ} = -71.32 - 56.60 \left(\frac{1}{r_{+} + r_{-}}\right) \text{ cal/Kmol}$$
 (51)

for alkaline earth halides. The entropies for M⁺ and M²⁺ were obtained from the ionization calculation. The entropy of crystalline alkali and alkaline earth halides were taken from Lange's Handbook (117) and the Handbook of Chemistry and Physics (125). When the calculated entropies are compared to those obtained experimentally the average error for the alkali halides is 0.68 cal/Kmol or 0.2 kcal/mol for TAS and for the alkaline earth halides the error is 0.83 cal/Kmol or 0.3 kcal/mol. These entropy data are given in Tables 16 and 17. The lattice energies are given in Tables 18 through 25.

VI.C.1.j. Final Results

The final values for $\Delta H_{\text{formation}}^{\circ}$ and $\Delta G_{\text{formation}}^{\circ}$ are obtained by addition of the values tabulated above. For $M^{+}C\cdot N^{-}$ the sum of reactions 28, 29, 30, 31, 32, 33, 34, 35

Table 16. Alkali Halide Entropies (cal/Kmol).

			1/(r++r_)					
Comp.	r_+(A)	r_(A)	(1/A)	So+ M+	S°-X-	SwX	-ASEXP	-ASCALC
LiF	09.0	1.36	0.5102	33.14	37.92	8.52	62.54	62.77
Lici	09.0	1.81	0.4149	33.14		14.17	58.43	41.09
LiBr	09.0	1.95	0.3922	33.14	41.81	16.0	8.9	59.51
Lil	09.0	2.16	0.3623	33.14	43.18	17.5	58.82	58.69
NaF	0.95	1.36	0.4329	36.72	37.92	14.0	49.09	49.09
NaCl	0.95	1.81	0.3623	36.72	39.46	17.30	58.88	58.70
NaBr	0.95	6	0.3448	36.72	41.81	20.75	57.78	58.21
NaI	0.95	2.16	0.3215	36.72	43.18	23.5	26.40	57.56
KF	1.33	1.36	0.3717	38.30	37.92	15.91	60.31	58.95
KCl	1.33	1.81	0.3185	38.30	39.46	19.76	58.00	57.48
KBr	1.33	1.95	0.3049	38.30	41.81	23.05	7.0	7 .
KI	1.33	2.16	0.2865	38.30	43.18	24.94	56.54	9
RbF	1.48	1.36	0.3521	40.63	37.92	18.0	0.5	•
RbCl	1.48	1.81	0.3040	40.63	39.46	25.6	64.75	7.0
RbBr	1.48	1.95	0.2915	40.63	41.81	25.88	56.56	6.7
RbI	1.48	2.16	4	40.63	43.18	28.21	9•	6.2
CsF	1.69	1.36	0.3279	41.94	37.92	21.1	58.76	7.7
CsCl	1.69	1.81	.285	41.94	39.46	24.18	57.22	6.5
CsBr	1.69	1.95	0.2747	41.94	41.81	27.1	56.65	.2
CsI	1.69	•1	0.2597	•	43.18	31	54.12	55.86

Table 17. Alkaline Earth Halide Entropies (cal/Kmol).

Comp.	r,(A)	r_(Å)	1/(r++r_) (1/A)	°S +W	°×	SwX	-ASEXP	-ASCALC
MgF	0.72	1.36	0.4808	35.50	37.92	13.68	99.76	98.53
$MgCI_2$	0.72	1.81	0.3953	35.50	39.46	21.42	93.00	93.69
$MgBr_{2}$	0.72	1.95	0.3745	35.50	41.81	28	91.12	92.51
MgI_{2}	0.72	2.16	0.3472	35.50	43.18	31.0	90.86	76.06
caF_2	1.00	1.36	0.4237	36.99	37.92	16.46	96.37	95.30
$cacl_2$	1.00	1.81	0.3559	36.99	39.46	25.0	90.91	91.46
$caBr_{2}$	1.00	1.95	0.3390	36.99	41.81	31.0	89.61	90.50
Calz	1.00	2.16	0.3165	36.99	43.18	34.72	88.63	89.23
SrF_2	1.16	1.36	0.3968	39.33	37.92	19.63	95.54	93.77
Src_2	1.16	1.81	0.3367	39.33	39.46	27.45	90.80	90.37
$SrBr_2$	1.16	1.95	0.3215	39.33	41.81	34.28	88.67	89.51
SrI_2	1.16	2.16	0.3012	39.33	43.18	38.03	87.66	88.30
BaF_2	1.36	1.36	0.3676	40.70	37.92	23.04	93.50	92.12
Bacl	1.36	1.81	0.3155	40.70	39.46	29.56	90.06	89.17
$BaBr_2$	1.36	1.95	0.3021	40.70	41.81	35	89.32	7. 8
BaI ₂	1.36	2.16	0.2841	40.70	43.18	39.47	87.59	87.39

Table 18. ΔH_{LAT}^{o} and ΔG_{LAT}^{o} for Lithide Salts.

Salt	-∆H° kcal/mol	-AG° kcal/mol	-AS° cal/Kmol	>	+2	2	r ₊ (Å)	r_(Å)	.86 (r ₊ +r ₋)Å
Li*c211.Li*	85.29	69.48	53.03	2			5.06	2.35	6.37
Na ⁺ C221.L1 ⁻	82.72	66.95	52.89	2	٦	٦	5.30		6.58
Na+C222.Li-	80.52	64.79	52.77	7	٦	ч	5.52		6.77
K+C222.Li-	80.41	64.68	52.77	2	Н	Н	5.53		6.78
Rb + C222 · L1 -	80.30	64.57	52.76	2	٦	٦	5.54		6.79
cs ⁺ c222·Li ⁻	80.18	64.45	52.75	2	П	Н	5.56		6.80
Cs ⁺ C322·Li ⁻	78.33	62.63	52.66	2	Т	Н	5.76		26.9
ca ²⁺ c221 · (L1 ⁻) ₂	247.80	223.97	79.91	Ω	2	н	5.31		6.59
Ca ²⁺ C222·(L1 ⁻) ₂	241.56	217.80	79.68	Υ	0	٦	5.52		6.77
Sr ²⁺ C221·(L1 ⁻) ₂	247.80	223.97	79.91	Υ	7	ч	5.31		6.59
Sr ²⁺ C222·(L1 ⁻) ₂	241.23	217.48	19.67	~	7	П	5.53		6.78
Ba ²⁺ C222·(L1 ⁻) ₂	240.89	217.14	99.62	3	7	٦	5.54		6.19

Table 19. ΔH_{LAT}° and ΔG_{LAT}° for Sodide Salts.

Salt	-AH° kcal/mol	-AG° kcal/mol	-AS° cal/Kmol	>	+2	2	r+(A)	r_(A)	.86 (r ₊ +r ₋)8
L1 ⁺ C211.Na ⁻	81.43	65.68	52.82	5			5.06	2.72	69.9
Na + C221 · Na -	79.08	63.37	52.70	2	٦	Ч	5.30		06.9
Na + C222 · Na -	77.07	61.39	52.59	7	П	Ч	5.52	-	7.09
K+C222•Na-	76.97	61.29	52.58	2	ч	Н	5.53		7.10
Rb + C222 • Na -	76.97	61.29	52.58	7	1	П	5.54		7.10
Cs + C222 • Na -	76.77	61.10	52.57	5	Н	1	5.56		7.12
Cs + C322 • Na -	75.06	59.41	52.48	7	٦	ч	5.76		7.79
ca ²⁺ c221 • (Na ⁻) ₂	236.93	213.22	79.51	Υ	2	1	5.31		6.91
ca ²⁺ c222•(Na ⁻) ₂	231.22	207.58	79.30	3	2	1	5.52		7.09
Sr ²⁺ C221•(Na ⁻) ₂	236.93	213.22	79.51	\sim	7	П	5.31		6.91
Sr ²⁺ C222•(Na ⁻) ₂	230.91	207.27	79.29	\sim	2	Н	5.53		7.10
Ba ²⁺ C222•(Na ⁻) ₂	230.91	207.27	79.29	3	7	٦	5.54		7.10

Table 20. ΔH_{LAT}° and ΔG_{LAT}° for Potasside Salts.

Li + C211.K 76.36 Na + C221.K 74.29 Na + C222.K 72.51		cal/Kmol	>	+ _Z	2	r ₊ (Å)	r_(Å)	.86 (r ₊ +r_)Å
	69.09	52.55	7	7	7	5.06	3.27	7.16
	58.66	52.44	5	Н		5.30		7.37
	26.90	52.35	5	Н	П	5.52		7.56
K ⁺ C222•K ⁻ 72.42	56.81	52.34	2	Н	ч	5.53		7.57
Rb ⁺ C222•K ⁻ 72.33	56.72	52.34	7	\vdash	Н	5.54		7.58
Cs+C222.K- 72.24	56.64	52.33	5	Н	Н	5.56		7.59
Cs+C322.K- 70.64	55.06	52.25	2	Н	ч	5.76		7.77
ca ²⁺ c221•(K ⁻) ₂ 222.58	199.03	78.99	\sim	2	Н	5.31		7.38
217.53	194.03	78.81	\sim	7	Н	5.52		7.56
222.58	199.03	78.99	3	7	Н	5.31		7.38
217.26	193.77	78.80	3	2	Т	5.53		7.57
216.99	193.50	78.79	m	2	۲-	5.54		7.58

Table 21. ΔH_{LAT}° , ΔG_{LAT}° for Rubidide Salts.

Salt	-AH° kcal/mol	-∆G° kcal/mol	-AS° cal/Kmol		+2	2	r+(A)	r_(Å)	.86 (r,+r_)Å
L1+C211.Rb-	75.26	59.61	52.49	2	7	7	5.06	3.39	7.27
Na + C211 • Rb -	73.34	57.72	52.39	2	٦	ч	5.30		7.47
Na + C222 • Rb -	71.61	56.02	52.30	2	1	٦	5.52		7.66
K+C222.Rb-	71.52	55.93	52.29	2	Т	ч	5.53		7.67
Rb + C222 • Rb -	71.43	55.84	52.29	2	٦	ч	5.54		7.68
Cs + C222 • Rb -	71.26	55.67	52.28	2	7	٦	5.56		7.70
Cs + C322 • Rb -	62.69	54.23	52.20	7	П	Н	5.76		7.87
Ca ²⁺ C221•(Rb ⁻) ₂	219.75	196.23	78.89	\sim	7	٦	5.31		7.48
Ca ²⁺ C222•(Rb ⁻) ₂	214.83	191.36	78.71	~	2	٦	5.52		99.7
Sr ²⁺ C221•(Rb ⁻) ₂	219.75	196.23	78.89	\sim	2	Н	5.31		7.48
Sr ²⁺ C222•(Rb ⁻) ₂	214.56	191.10	78.70	\sim	2	٦	5.53		79.7
Ba ²⁺ C222•(Rb ⁻) ₂	214.30	190.84	78.69	m	2	Н	5.54		7.68

Table 22. $\Delta H_{
m LAT}^{
m o}$ and $\Delta G_{
m LAT}^{
m o}$ for Ceside Salts.

Salt	-AH° kcal/mol	-AG° kcal/mol	-AS° cal/Kmol	>	+ ₂	2	r ₊ (Å)	r_(A)	.86 (r++r)A
Li +C211.Cs-	74.00	58.37	52.43	2	Н	7	5.06	3.55	7.40
Na + C221 • Cs -	72.06	94.95	52.32	~	Т	Н	5.30		7.61
Na + C222 • Cs -	70.38	54.81	52.23	2	П	Н	5.52		7.80
K ⁺ C222·Cs ⁻	70.30	54.73	52.23	~	П	Н	5.53		7.81
Rb + C222 • Cs -	70.21	54.64	52.23	2	Т	Н	5.54		7.82
cs+c222.cs-	70.13	54.56	52.22	2	1	П	5.56		7.83
cs + c322 • cs -	68.62	53.07	52.14	7	П	Н	5.76		8.01
ca ²⁺ c221•(cs ⁻) ₂	215.90	192.42	78.75	\sim	2	Н	5.31		7.62
ca ²⁺ c222•(cs ⁻) ₂	211.15	187.72	78.58	\sim	8	Ч	5.52		7.80
Sr ²⁺ c221•(cs ⁻) ₂	215.90	192.42	78.75	3	2	Н	5.31		7.62
sr ²⁺ c222•(cs ⁻) ₂	210.89	187.46	78.57	3	2	Ч	5.53		7.81
Ba ²⁺ C222•(Cs ⁻) ₂	210.64	187.22	78.56	3	8	٦	5.54		7.82

Table 23. ΔH_{LAT}^{o} and ΔG_{LAT}^{o} for Cupride Salts.

L1+C211.Cu 90.09 74.20 Na+C221.Cu 87.23 71.39 Na+C222.Cu 84.79 68.99 K+C222.Cu 84.66 68.86 Cs+C222.Cu 84.41 68.61 Cs+C222.Cu 84.41 68.61 Cs+C222.Cu 84.41 68.61 Cs+C222.Cu 84.41 68.61	53. 53.	29 2 13 2 00 2 99 2	п п п п		5.06	1.93	6.01 6.22 6.41
87.23 84.79 84.66 84.41 82.36			н н н н		5.30		6.22
84.79 84.66 84.66 84.41 82.36	ת ת ת		т т т	н н н	5.52		6.41
84.66 84.66 84.41 82.36	ת ת		г г	н н	5.53		
84.66 84.41 82.36 261.28	īΟ		٦	Н	i l		6.45
84.41					5.54		6.42
82.36	52.	98 2	П	Т	5.56		44.9
261.28	.60 52.87	7 2	٦	7	5.76		6.61
	.31 80.41	ب 3	2	Н	5.31		6.23
ca ²⁺ c222•(cu ⁻) ₂ 254.36 230.46	.46 80.15	5 3	2	٦	5.52		6.41
Sr ²⁺ c221•(cu ⁻) ₂ 261.28 237.31	.31 80.41	3	2	٦	5.31		6.23
Sr ²⁺ c222.(cu ⁻) ₂ 253.99 230.10	1.10 80.14	.4	2	٦	5.53		6.42
Ba ²⁺ c222•(cu ⁻) ₂ 253.99 230.10	80.14	.4	2	Н	5.54		6.42

Table 24. ΔH_{LAT}^{o} and ΔG_{LAT}^{o} for Argentide and Auride Salts.

Salt Ag or Au	-AH° kcal/mol	-AG° kcal/mol	-∆S° cal/Kmol	Δ	+ 2	2	r+(A)	r_(A)	.86 (r ₊ +r ₋)Å
L1+C211.A-	89.25	73.38	53.24	5	7		5.06	2.00	6.07
Na + C221 • A -	14.98	70.61	53.09	~	٦	Н	5.30		6.28
Na+C222.A-	84.05	68.26	52.96	2	Ч	Н	5.52		6.47
K+C222.A-	83.92	68.13	52.95	2	Н	٦	5.53		84.9
Rb+C222.A-	83.92	68.13	52.95	7	٦	Н	5.54		84.9
cs+c222.A-	83.68	67.90	52.94	7	Н	Т	5.56		6.50
cs+c322.A-	81.66	65.91	52.83	7	٦	٦	5.76		29.9
ca ²⁺ c221•(A ⁻) ₂	258.93	234.98	80.32	3	5	Н	5.31		6.29
Ca ²⁺ C222•(A ⁻) ₂	252.14	228.27	80.07	3	7	Н	5.55		6.47
Sr ²⁺ C221•(A ⁻) ₂	258.93	234.98	80.32	3	5	٦	5.31		6.29
Sr ²⁺ C222•(A ⁻) ₂	251.77	227.90	80.05	3	7	Т	5.53		84.9
Ba ²⁺ C222•(A ⁻) ₂	251.77	227.90	80.05	\sim	2	Н	5.54		84.9

Table 25. $\Delta H_{\rm LAT}^{\circ}$ and $\Delta G_{\rm LAT}^{\circ}$ for Electrides.

Salt	-AH° kcal/mol	-AG° kcal/mol	-AS° cal/Kmol	>	+2	2	r+(Å)	r_(A)	1 (r ₊ +r ₋)
L1 ⁺ C211.e ⁻	76.46	62.09	52.56	2	-	7	5.06	2.09	7.15
Na + C221.e-	73.16	57.54	52.38	7	٦	٦	5.30	2.19	7.49
Na C222.e-	70.30	54.73	52.23	2	ч	٦	5.52	2.29	7.81
K. C222.e	70.21	74.64	52.23	2	Н	Т	5.53	2.29	7.82
rb C222.e-	70.13	54.56	52.22	2	IJ	٦	5.54	2.29	7.83
Cs C222.e.	69.87	54.30	52.21	7	Н	Н	5.56	2.30	7.86
Ca 2+c2.	67.57	52.04	52.00	7	Н	Н	5.76	2.38	8.14
Ca ²⁺ C222 (=) ₂	218.91	195.40	78.86	m	2	Ч	5.31	2.20	7.51
Sr ² +(22) (6-)	210.89	187.46	78.57	ĸ	7	Н	5.52	2.29	7.81
Sr ²⁺ G222•(6-)	218.91	195.40	78.86	m	2	Н	5.31	2.20	7.51
Ba ²⁺ C222•(a-)	210.64	187.22	78.56	ĸ	2	٦	5.53	2.29	7.82
, , , ,	210.38	186.96	78.55	Μ	2	Н	5.54	2.29	7.83

and 36 yields the desired result. For $M^{2+}C \cdot (N^{-})_2$ the sum of 28, 29, 30, 31, 34, 35, 36 plus two times the sum of 32 and 33 produces the proper thermodynamic quantities. The electrides, $M^{+}C \cdot e^{-}$ and $M^{2+}C \cdot (e^{-})_2$ require the sum of 28, 29, 30, 31, 34, 35 and 36. These totals for the enthalpy and free energy of formation are given in Tables 26 through 34.

VI.C.2. Theoretical and Experimental Enthalpies for Alkali Cryptate Halides

The enthalpies of solution for $Na^{\dagger}c222 \cdot X^{-}(s)$ and $K^{\dagger}c222 \cdot X^{-}(s)$ where $X = Cl^{-}$, Br^{-} , and I^{-} have been measured by Abraham <u>et al</u>. (116). These thermodynamic quantities allow the calculation of $\Delta H^{o}_{formation}$ of these six compounds using only experimentally obtained values. These experimentally obtained enthalpies can be compared to corresponding enthalpies obtained using the modified Born-Haber cycle. Summing reactions (52) through (55) yields (62) for the experimental enthalpy of formation and summing reactions (56) through (61) also yields (62) for the theoretical enthalpy of formation. The results of these calculations appear in Table 35. The enthalpy for reaction (55) was taken from Lange's Handbook of Chemistry.

$$M^{+}C_{(aq)} + X^{-}_{(aq)} \rightarrow M^{+}C \cdot X^{-}_{(s)}$$
 (52)

Table 26. $\Delta H_{\text{formation}}^{\text{o}}$ and $\Delta G_{\text{formation}}^{\text{o}}$ for Lithide Salts.

Salt	ΔH° kcal/mol	ΔG° kcal/mol	ΔS° cal/Kmol
Li ⁺ C2ll·Li ⁻	- 8.6	+ 2.0	-35.7
Na ⁺ C221 • L1 ⁻	- 0.2	+ 9.3	-31.9
Na ⁺ C222•Li ⁻	- 1.5	+12.0	-45.4
K ⁺ C222•Li ⁻	- 8.1	+ 5.3	-44.7
Rb ⁺ C222•Li ⁻	- 6.8	+ 7.2	-46.8
Cs ⁺ C222•Li ⁻	- 1.1	+10.7	-39.7
Cs ⁺ C322•Li ⁻	- 0.5	+11.0	-38.7
Ca ²⁺ C221 • (Li ⁻) ₂	-24.1	-11.3	-42.9
Ca ²⁺ C222•(Li ⁻) ₂	-20.0	- 6.4	-45.6
Sr ²⁺ C221 • (Li ⁻) ₂	-24.7	- 9.6	- 50.9
Sr ²⁺ C222•(Li ⁻) ₂	-27.4	- 8.9	-61.9
Ba ²⁺ C222•(Li ⁻) ₂	-28.2	-10.8	-58.3

Table 27. $\Delta H_{\text{formation}}^{\text{o}}$ and $\Delta G_{\text{formation}}^{\text{o}}$ for Sodide Salts.

Salt	ΔH° kcal/mol	ΔG° kcal/mol	ΔS° cal/Kmol
Li ⁺ C2ll·Na ⁻	-15.8	- 4.7	-37.3
Na ⁺ C221•Na ⁻	- 7.5	+ 2.5	- 33.5
Na ⁺ C222•Na ⁻	- 9.0	+ 5.0	-47.0
K ⁺ C222•Na ⁻	-15.6	- 1.8	-46.3
Rb ⁺ C222•Na ⁻	-14.4	0.0	-48.4
Cs [†] C222•Na ⁻	- 8.7	+ 3.6	-41.3
Cs ⁺ C322•Na ⁻	- 8.2	+ 3.8	-40.4
Ca ²⁺ C221 • (Na ⁻) ₂	-35.2	-21.5	-46.1
Ca ²⁺ C222•(Na ⁻) ₂	- 31.6	-17.1	-48.8
Sr ²⁺ C221 • (Na ⁻) ₂	- 35.8	-19.7	-54.0
Sr ²⁺ C222•(Na ⁻) ₂	-39.0	-19.6	-65.1
Ba ²⁺ C222·(Na ⁻) ₂	-40.2	- 21.9	-61.5

Table 28. ΔH° and ΔG° formation for Potasside Salts.

Salt	ΔH° kcal/mol	ΔG° kcal/mol	ΔS° cal/Kmol
Li ⁺ C2ll·K ⁻	-14.1	- 2.6	-38.6
Na ⁺ C221·K ⁻	- 6.1	+ 4.3	-34.8
Na ⁺ C222·K ⁻	- 7.8	+ 6.6	-48.3
K ⁺ C222·K ⁻	-14.4	- 0.2	-47.6
Rb ⁺ C222·K ⁻	-13.1	+ 1.7	-49.7
Cs ⁺ C222·K ⁻	- 7.5	+ 5.2	-42.6
Cs ⁺ C322·K ⁻	- 7.2	+ 5.3	-41.7
Ca ²⁺ C221·(K ⁻) ₂	-27.6	-13.1	-48.6
Ca ²⁺ C222·(K ⁻) ₂	-24.6	- 9.3	-51.4
Sr ²⁺ C221·(K ⁻) ₂	-28.2	-11.3	- 56.6
Sr ²⁺ C222·(K ⁻) ₂	-32.1	-11.9	-67.7
sa ²⁺ c222·(K ⁻) ₂	-33.0	-13.9	-64.0

Table 29. $\Delta H_{\text{formation}}^{\text{o}}$ and $\Delta G_{\text{formation}}^{\text{o}}$ for Rubidide Salts.

Salt	ΔH° kcal/mol	ΔG° kcal/mol	ΔS° cal/Kmo]
Li ⁺ C2ll•Rb ⁻	-13.4	- 2.3	-37.3
Na ⁺ C221•Rb ⁻	- 5.6	+ 4.4	-33.5
Na ⁺ C222•Rb ⁻	- 7.4	+ 6.7	-47.1
K ⁺ C222•Rb ⁻	-14.0	- 0.1	-46.4
Rb ⁺ C222•Rb ⁻	-12.7	+ 1.8	-48.4
Cs ⁺ C222•Rb ⁻	- 7.0	+ 5.4	-41.4
Cs ⁺ C322•Rb ⁻	- 6.8	+ 5.3	-40.4
Ca ²⁺ C221 • (Rb ⁻) ₂	- 25 . 7	-11.9	-46.2
Ca ²⁺ C222·(Rb ⁻) ₂	- 22.8	- 8.2	-48.9
Sr ²⁺ C221•(Rb ⁻) ₂	-26.3	-10.1	-54.1
Sr ²⁺ C222•(Rb ⁻) ₂	-30.3	-10.8	-65.2
Ba ²⁺ C222•(Rb ⁻) ₂	-31.2	- 12.9	-61.6

Table 30. $\Delta H^o_{formation}$ and $\Delta G^o_{formation}$ for Ceside Salts.

Salt	ΔH° kcal/mol	ΔG° kcal/mol	ΔS° cal/Kmol
Li ⁺ C211•Cs ⁻	-14.0	- 2.1	-39.8
Na ⁺ C221•Cs ⁻	- 6.2	+ 4.6	- 36.0
Na ⁺ C222•Cs ⁻	- 8.0	+ 6.8	-49.6
K ⁺ C222•Cs ⁻	-14.6	0.0	-48.9
Rb ⁺ C222•Cs ⁻	-13.3	+ 1.9	- 50 . 9
Cs ⁺ C222•Cs ⁻	- 7.7	+ 5.4	-43.9
Cs ⁺ C322•Cs ⁻	- 7.4	+ 5.4	- 42.9
Ca ²⁺ C221•(Cs ⁻) ₂	- 25 . 5	-10.3	-51.1
Ca ²⁺ C222•(Cs ⁻) ₂	- 22.8	- 6.8	- 53.9
Sr ²⁺ C221•(Cs ⁻) ₂	-26.1	- 8.5	- 59 . 1
Sr ²⁺ C222•(Cs ⁻) ₂	-30.3	- 9.4	- 70.2
Ba ²⁺ C222•(Cs ⁻) ₂	-31.2	-11.4	-66.5

Table 31. $\Delta H_{\text{formation}}^{\text{o}}$ and $\Delta G_{\text{formation}}^{\text{o}}$ for Cupride Salts.

Salt	ΔH° kcal/mol	ΔG° kcal/mol	ΔS° cal/Kmol
Li ⁺ C211•Cu ⁻	+15.0	+24.0	-30.3
Na ⁺ C221•Cu ⁻	+23.7	+31.6	-26.4
Na ⁺ C222•Cu ⁻	+21.6	+34.5	-43.3
K ⁺ C222•Cu ⁻	+16.1	+27.8	-39.2
Rb ⁺ C222•Cu ⁻	+17.3	+29.6	-41.3
Cs ⁺ C222•Cu ⁻	+22.3	+33.3	-36.7
Cs ⁺ C322•Cu ⁻	+23.9	+33.8	-33.2
Ca ²⁺ C221•(Cu ⁻) ₂	+19.2	+28.7	-32.0
Ca ²⁺ C222•(Cu ⁻) ₂	+24.1	+34.4	-34.7
Sr ²⁺ C221•(Cu ⁻) ₂	+18.6	+30.5	- 39.9
Sr ²⁺ C222•(Cu ⁻) ₂	+16.7	+31.9	- 51.0
Ba ²⁺ C222•(Cu ⁻) ₂	+15.5	+29.6	-47.3

Table 32. $\Delta H^{\circ}_{\text{formation}}$ and $\Delta G^{\circ}_{\text{formation}}$ for Argentide Salts.

Salt	ΔH° kcal/mol	ΔG° kcal/mol	ΔS° cal/Kmol
Li ⁺ C211•Ag ⁻	+ 1.3	+10.6	-30.9
Na ⁺ C221•Ag ⁻	+10.0	+18.1	-27.1
Na ⁺ C222•Ag ⁻	+ 8.9	+21.0	-40.6
K ⁺ C222•Ag ⁻	+ 2.4	+14.3	-39.9
Rb ⁺ C222•Ag ⁻	+ 3.6	+16.1	-42.0
Cs ⁺ C222•Ag ⁻	+ 9.3	+19.7	-34.9
Cs ⁺ C322•Ag ⁻	+10.1	+20.2	- 33.9
Ca ²⁺ C221•(Ag ⁻) ₂	- 7.4	+ 2.6	-33.3
Ca ²⁺ C222•(Ag ⁻) ₂	- 2.7	+ 8.1	-36.0
Sr ²⁺ C221•(Ag ⁻) ₂	- 8.0	+ 4.3	-41.3
Sr ²⁺ c222·(Ag ⁻) ₂	-10.0	+ 5.6	-52.3
a ²⁺ C222•(Ag ⁻) ₂	-11.2	+ 3.3	-48.7

Table 33. $\Delta \text{H}^{\circ}_{\text{formation}}$ and $\Delta \text{G}^{\circ}_{\text{formation}}$ for Auride Salts.

Salt	ΔH° kcal/mol	ΔG° kcal/mol	ΔS° cal/Kmol
Li ⁺ C211•Au ⁻	- 2.5	+ 6.5	-30.2
Na ⁺ C221•Au ⁻	+ 6.2	+14.1	-26.4
Na ⁺ C222•Au ⁻	+ 5.1	+17.0	- 39 . 9
K ⁺ C222•Au ⁻	- 1.4	+10.3	- 39.2
Rb ⁺ C222•Au ⁻	- 0.3	+12.1	-41.3
Cs ⁺ C222•Au ⁻	+ 5.5	+15.7	-34.2
Cs ⁺ C322•Au ⁻	+ 6.3	+16.2	-33.2
Ca ²⁺ C221•(Au ⁻) ₂	-15.0	- 5.5	-31.9
Ca ²⁺ C222•(Au ⁻) ₂	-10.3	0.0	-34.6
Sr ²⁺ C221 • (Au ⁻) ₂	-15.6	- 3.7	-39.9
Sr ²⁺ C222•(Au ⁻) ₂	-17.6	- 2.5	- 50.9
Ba ²⁺ C222•(Au ⁻) ₂	-18.8	- 4.7	-47.3

Table 34. $\Delta H^{\circ}_{\text{formation}}$ and $\Delta G^{\circ}_{\text{formation}}$ for Electride Salts.

Salt	ΔH° formation kcal/mol	$_{ m kcal/mol}^{ m \Delta G}$	ΔS° formation cal/Kmol
Li ⁺ C211•e ⁻	-23.3	- 6.9	- 55.0
Na ⁺ C221•e ⁻	-14.1	+ 1.1	- 51.2
Na + C222 • e -	-14.8	+ 4.5	-64.7
K ⁺ C222•e ⁻	-21.4	- 2.3	-64.0
Rb ⁺ C222•e ⁻	-20.1	- 0.4	-66.0
Cs ⁺ C222•e ⁻	-14.3	+ 3.3	- 59 . 0
Cs ⁺ C322•e ⁻	-13.3	+ 4.0	- 58.0
Ca ²⁺ C221·(e ⁻) ₂	-42.2	-18.0	-81.4
Ca ²⁺ C222•(e ⁻) ₂	-36.3	-11.2	-84.1
Sr ²⁺ C221•(e ⁻) ₂	-42.9	- 16.2	-89.4
Sr ²⁺ C222•(e ⁻) ₂	-43.8	-13.9	-100.4
Ba ²⁺ C222•(e ⁻) ₂	-44.7	- 15.9	- 96 . 7

Table 35. Enthalpy of Formation for Alkali Cryptate Halides.

Experimental ΔH° (kcal/mol)			
Salt	Cl	Br	I
Na ⁺ C222·X ⁻ K ⁺ C222·X ⁻	-102.0 -113.1	-96.4 -104.1	-83.8 -93.8
	Theoretical ΔH°	(kcal/mol)	
Na + C222 • X -	-74.0	-64.9	-61.3
K+C222•X-	-81.0	-72.4	-69.5
$\Delta \Delta H_f^{\circ}$ (ΔH	f (Theoretical) -	ΔH° (Experiment	cal)
Na ⁺ C222·X	+28.0	+31.4	+22.5
K ⁺ C222•X	+32.1	+31.7	+24.3

$$M^{+}(aq) + C(aq) + M^{+}C(aq)$$
 (53)

$$C(s) \rightarrow C(aq)$$
 (54)

$$M(s) + 1/2X_2 + M^+(aq) + X^-(aq)$$
 (55)

$$M^{+}C_{(g)} + X^{-}_{(g)} \rightarrow M^{+}C \cdot X^{-}_{(s)}$$
 (56)

$$M^{+}C_{(aq)} \rightarrow M^{+}C_{(g)}$$
 (57)

$$M^{+}(aq) + C(aq) \rightarrow M^{+}C(aq)$$
 (58)

$$^{C}(s) \rightarrow ^{C}(ag) \tag{59}$$

$$X^{-}(aq) \rightarrow X^{-}(g) \tag{60}$$

$$M_{(s)} + 1/2 X_2 \rightarrow M^{+}_{(aq)} + X^{-}_{(aq)}$$
 (61)

$$M_{(s)} + 1/2 X_2 + C_{(s)} \rightarrow M^{+}C \cdot X^{-}_{(s)}$$
 (62)

The theoretical calculations give values of $\Delta H_{\mathbf{f}}^{o}$ which are approximately 20-30 kcal less exothermic than the experimental values for these six salts. The two thermodynamic steps most likely to give rise to this discrepancy are the Born approximation for cryptate solvation and the Kapustinskii approximation for lattice energy. The Born solvation

enthalpy for both Na⁺C222 and K⁺C222 is +30.2 kcal/mol. If the majority of the 20-30 kcal error in the calculation were in this step the enthalpy of cryptate solvation would be approximately 0-10 kcal/mol. This small an enthalpy of solvation is unlikely and it therefore appears that the majority of the error is in the lattice energy calculation.

The estimation of $r_+ + r_-$ for $Na^+C222 \cdot I^-$ used in the lattice calculation is 7.68 Å, the experimentally observed value is 7.40 \mathring{A} (108), a difference of only about 4%. This 4% difference corresponds to about 2.7 kcal/mol. For $K^{\dagger}C222 \cdot I^{-}$ the experimentally observed value for $r_{+} + r_{-}$ is 6.95 Å (82) and the theoretical estimation is 7.69 Å, a 10% difference. This difference corresponds to a 7.2 kcal/mol difference using the Kapustinskii approximation for lattice energy. The experimental cation-anion distances for the iodides do allow closer agreement between the experimentally obtained values for $\Delta H_{\mathbf{f}}^o$ and those obtained using the Kapustinskii approximation, however, the differences are still 17-20 kcal/mol. Because the Kapustinskii equation is based on an electrostatic model it is possible these errors are due to the neglect of possible covalency between the cation and available p-orbitals on the halide ions. This argument is of little help in explaining errors in the alkalide calculations because the outer s-orbitals of the alkali anions are not likely to be involved in covalency with the cation.

VI.D. Discussion

The vaporization, ionization, electron affinity, and complexation data used in these calculations are well known and contribute only a few kcal or less to the total error in these calculations. The approximations used for the transfer of the complexed cation to the gas phase and for the lattice energy are far less certain and probably contribute significantly to the total error. Even though significant errors are probably present the availability of ΔH_f^o , ΔS_f^o and ΔG_f^o for $Na^{\dagger}C222 \cdot Na^{\dagger}$ allow these calculated values to be "adjusted" to remove some of the systematic errors present.

The potentiometric determination of ΔH_{f}° and ΔG_{f}° for Na⁺C222·Na⁻ by Schindewolf, Le and Dye (112) allows a direct comparison with the theoretical calculations for this salt. The emf data yield $\Delta H_{f}^{\circ} = -8.1\pm1.0$ kcal/mol, $\Delta G_{f}^{\circ} = -1.7\pm.3$ kcal/mol, and $\Delta S_{f}^{\circ} = -22\pm4$ cal/Kmol. As found in Table 27 the calculated values are $\Delta H_{f}^{\circ} = -9.0$ kcal/mol, $\Delta G_{f}^{\circ} = -5.0$ kcal/mol, and $\Delta S_{f}^{\circ} = -47$ cal/Kmol. The enthalpy values are in surprisingly good agreement and probably result from the cancellation of errors in the calculations. The calculated value of ΔS_{f}° is 25 cal/Kmol more negative than the experimentally observed value. This difference is believed to be due to errors in the lattice entropy and cryptate solvation entropy calculations.

The lattice entropy was calculated by extrapolating the entropy change vs. ion size for simple salts as they are brought from the gas phase to the crystalline phase. This treatment completely ignores specific effects due to cryptand entropy changes and it is possible that configurational entropy changes during packing are important. Additionally, the entropy calculation for the removal of cryptated cations from water to the gas phase was based on the Born model and any entropy changes due to water structure making and breaking are ignored. Even though these calculations contain significant errors the relative stabilities are probably much more accurate. These calculations do not preclude decomposition by reduction of the cryptand which seems to be thermodynamically favored and is found to be quite common in synthesis.

Salts containing Li have not been observed. Even though the calculated free energy of formation of Li C211. Li is 3 kcal/mol more negative than that for Na C222.Na many attempts to synthesize lithide salts have resulted in either decomposition or in the formation of the electride, Li C211.e. Absorption spectra of films containing excess lithium show only e with no evidence for the formation of Li (Chapter 1). The calculated free energy of formation of Li C211.e is nearly 9 kcal/mol more negative than that for the lithide salt and it is possible that the favored product is the electride and any lithide salt

formed would spontaneously disproportionate by reaction (63).

$$\text{Li}^{\dagger}\text{C2ll} \cdot \text{Li}^{\dagger}_{(s)} \rightarrow \text{Li}^{\dagger}\text{C2ll} \cdot \text{e}^{\dagger}_{(s)} + \text{Li}_{(s)}$$
 (63)

The sodide salts are shown by laboratory experience to be the most stable of the 1:1 alkalide salts. Sodide salts of all the alkali cryptate cations have been isolated. Dye (113) calculated that the formation of the hypothetical sodide salt, Na⁺·Na⁻, from sodium metal is endothermic by only 14 kcal/mol. This calculation required only one estimate, the lattice energy, which was obtained by scaling the interionic distance in Na⁺·I⁻ to that in sodium metal. As Dye pointed out, in favorable cases the energy of cation complexation and lattice energy could offset this 14 kcal/mol and produce thermodynamically stable sodide salts.

The interionic distance in Na⁺C222·Na⁻ (80) is 14% smaller than that calculated from size estimates of Na⁺C and Na⁻. As discussed above this is not the case for similar halide salts and it appears that the primary source of error is the size estimate for Na⁻. It appears the sodide and possibly all the alkali metal anions are "soft" ions. These calculations show that Na⁺C222·Na⁻, and probably all the alkalides owe their stability to the relatively large lattice energies produced by the "softness" of these anions.

The free energy of formation of the potasside, rubidide, and ceside salts of the same cation are usually separated by only a few tenths of a kcal/mol. When the sodides are compared to the other alkalides the sodides are more stable by ~2 kcal/mol. This trend is substantiated by experimental evidence which shows the sodides to be not only more thermally stable in the crystalline form, but also less likely to decompose during synthesis.

Also, listed in these calculations are salts which contain anions of copper, silver, and gold. These metals have been included because of their high electron affinities. The free energy of electron attachment for the alkali metals ranges from -10 to -13 kcal/mol while those for copper, silver, and gold are -27, -29, and -52 kcal/mol respectively. These large negative free energies however, are offset by large atomization free energies. The atomization free energies for the alkali metals range from 20 to 40 kcal/mol while those for copper, silver, and gold range from 60 to 80 kcal/mol. Based on these calculations the aurides should be the most stable followed by the argentides and the cuprides. In fact, in the most favorable case the free energy of formation of Li +C211.Au is estimated to be -0.2 kcal/mol. (This estimate includes the -6.7 kcal/mol "correction" from the emf determination for Na⁺C222·Na⁻). This calculated stability should not be too surprising however, since the ionic compound Cs + Au

is known (133) and more recent work by Peer and Lagowski (134) gives spectral and electrochemical evidence for the existence of Au in liquid ammonia.

Also tabulated are the enthalpies and free energies of formation of cryptated alkaline earth salts. While these calculations clearly show these compounds should be thermodynamically stable with respect to cryptand and free metal it is also equally clear from laboratory experience that these have the greatest tendency to decompose by destruction of the cryptand. The free energy of formation of $\mathrm{Ba}^{2+}\mathrm{C222}\cdot(\mathrm{Na}^{-})_{2}$ was calculated to be 26.9 kcal/mol more stable than Na⁺C222·Na⁻. These calculations indicate $Ba^{2+}C222 \cdot (Na^{-})_{2}$ is the most stable alkalide salt and therefore, it was thought to be a good choice for the first divalent salt synthesis. As discussed in Chapter 3 all synthetic attempts resulted in decomposition and crystals of Ba²⁺C222·(Na⁻), have not yet been isolated. While it is possible that these calculations are in error by 20 kcal/mol or more, it is also possible that Ba²⁺C222. (Na⁻)₂ would be stable if cryptand decomposition could be prevented. The Kapustinskii approximation gives lattice energies for 2:1 salts which are 3 times larger than those for 1:1 salts with the same interionic distance. relatively small error in the interionic distance estimate would result in a substantial error in the lattice energy calculation.

Estimates have also been made for compounds of the general formulas $M^+C \cdot e^-$ and $M^{2+}C \cdot (e^-)_2$, the electrides. Because no structural data are available to estimate the interionic distances it was assumed that the electrons occupy octahedral holes provided by a closest packing of cryptated cations. Although it is possible this method underestimates the interionic distance which leads to an artificially high lattice energy any electron delocalization is also ignored by the Kapustinskii approximation and these errors should at least partially cancel. Laboratory experience shows that the electrides are highly susceptible to decomposition by destruction of the cryptand. calculations show Li + C211.e and K + C222.e to be the two most stable 1:1 electrides. These two salts have been synthesized on numerous occasions by DaGue (85) and Landers (84) and are known to be very thermally sensitive and must be synthesized and stored well below 0°C.

Until structural or further thermodynamic data are available for both the divalent alkalides and the electrides these calculations should not be used too literally. The calculated values for $M^{2+}C \cdot (N^{-})_2$ result from the difference of a very large thermodynamic estimates and the calculated values for $M^{+}C \cdot e^{-}$ and $M^{+2}C \cdot (e^{-})_2$ result from a proposed structure which has as yet no experimental support.

VII. SUMMARY AND SUGGESTIONS FOR FUTURE WORK

VII.A. Summary

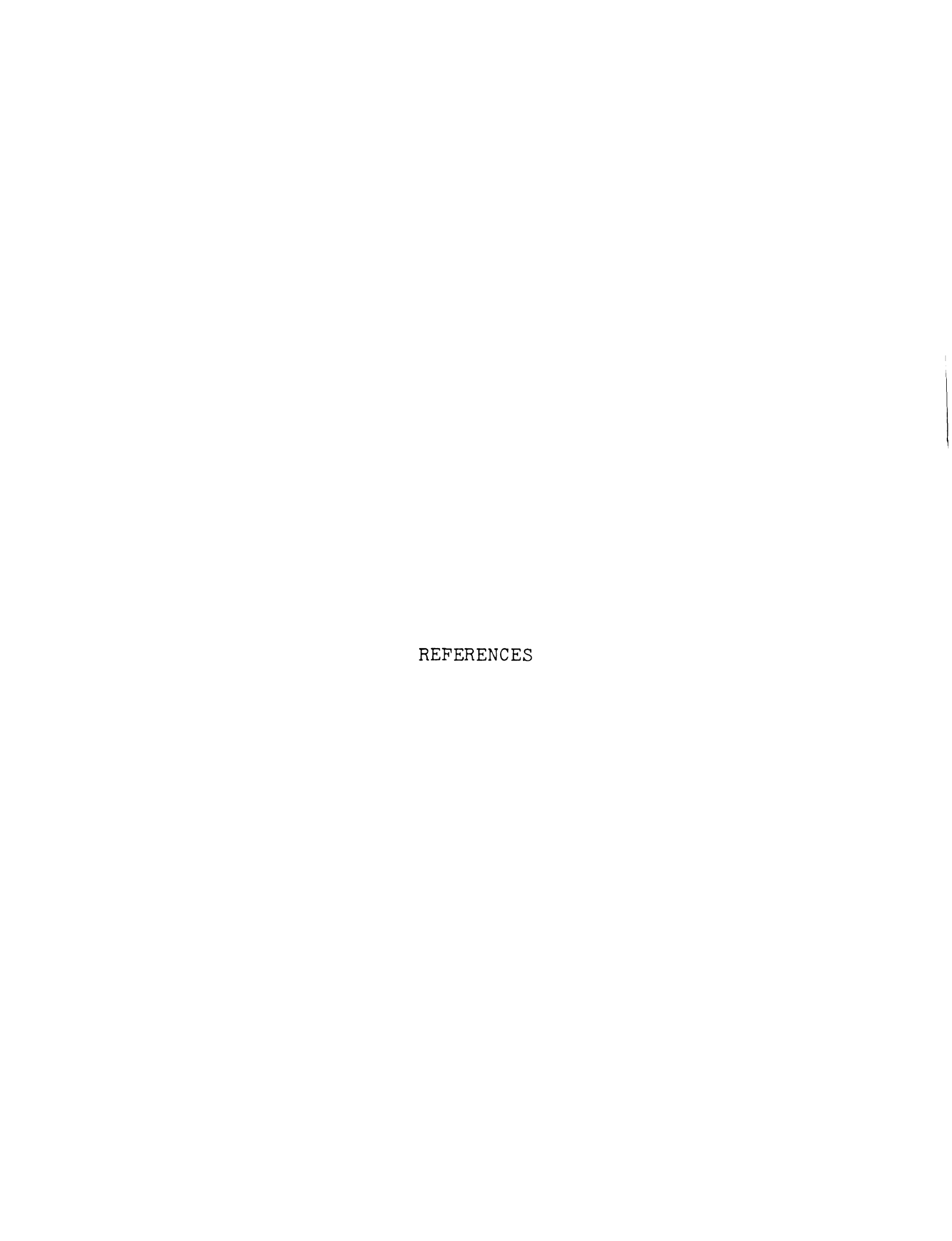
The use of high purity metals, solvents, and complexing agents in vacuo at reduced temperatures has made the synthesis of an entire series of crystalline alkalide salts possible. These salts were crystallized by precipitation from amine and/or ether solvents that contained dissolved metal and complexing agent. The analysis of these salts showed most to be in general accord with the predicted stoichiometry. The deviations from the predicted stoichiometry are primarily due to either partial prior decomposition of these reactive salts and/or decomposition of the complexing agent during analysis.

Solution NMR spectra substantiate previous work that shows that in most amine and ether solvents these salts dissolve to form M^+C and N^- . Solid state NMR spectra described herein, and a previously obtained X-ray structure determination of $Na^+C222 \cdot Na^-$, as well as subsequent solid state NMR studies all demonstrate that in the crystalline state these compounds are <u>true</u> 1:1 salts which contain complexed alkali-metal cations and alkali-metal anions.

VII.B. Suggestions For Future Work

The most serious problems associated with synthesis and analysis of alkalides has been decomposition either in solution or by reduction of the complexing agent in solvent free crystals. In order to more fully characterize these salts it is important to minimize this tendency to decompose. The use of different solvents which are less susceptible to reduction and the use of solvent-free vapor phase synthesis have both been shown to be useful and should be pursued further.

The characterization of these compounds should also be pursued. Crystal structures, single crystal electrical conductivity and photoconductivity studies would be useful to elucidate the electronic properties of these salts which are known to be semiconductors. The use of more stable complexing agents may make it possible to produce alkalide salts suitable for use as infrared sensitive detectors by making use of photoconductivity and a presumably low electron emission work function.



REFERENCES

- 1. W. Weyl, Ann. Phys., 197, 601 (1863).
- 2. P. P. Edwards, Adv. Inorg. Chem. Radiochem., <u>25</u> 135 (1982).
- 3. G. Lepoutre and M. J. Sienko (eds), "Metal-Ammonia Solutions, Colloque Weyl I", W. A. Benjamin (New York) 1964.
- 4. J. J. Lagowski and M. J. Sienko (eds.), "Metal-Ammonia Solutions", Colloque Weyl II, IUPAC, Butter-worths (London) 1970.
- 5. J. Jortner and N. R. Kestner (eds.), "Electrons in Fluids", Colloque Weyl III, Springer (Berlin) 1973.
- 6. "Colloque Weyl IV. Electrons in Fluids The Nature of Metal-Ammonia Solutions", J. Phys. Chem. 79, 26 (1975).
- 7. J. Phys. Chem., <u>84</u> 1065-1298 (1980).
- 8. C. A. Kraus, J. Chem. Educ. <u>30</u>, 83 (1953).
- 9. W. L. Jolly, Prog. Inorg. Chem., $\underline{1}$ 235 (1959).
- 10. M. C. R. Symons, Q. Rev., <u>13</u> 99 (1959).
- 11. U. Schindewolf, Angew. Chem., <u>80</u> 165 (1968); Angew. Chem., Int. Ed. Engl. <u>7</u> 190 (1<u>968</u>).
- 12. T. P. Das, Adv. Chem. Phys., 4, 303 (1962).
- 13. J. L. Dye, Sci. Am. 216 77 (February 1967).
- 14. M. H. Cohen and J. C. Thompson, Adv. Phys. <u>17</u> 857 (1968).
- 15. J. C. Thompson, "Electrons in Liquid Ammonia", Clarendon Press (Oxford) 1976.
- 16. J. L. Dye, M. G. DeBacker, and L. M. Dorfman, J. Chem. Phys., 52 6251 (1970).

- J. L. Dye, M. G. DeBacker, J. A. Eyer, and L. M. Dorfman, J. Phys. Chem., 76 839 (1972).
- 18. C. A. Hutchinson and R. C. Pastor, J. Chem. Phys., 21 1959 (1953).
- 19. H. F. Hnizda and C. A. Kraus, J. Am. Chem. Soc. <u>71</u> 1565 (1949).
- 20. R. R. Dewald and J. H. Roberts, J. Phys. Chem. <u>72</u> 4224 (1968).
- 21. R. R. Dewald, J. Phys. Chem. 23 2615 (1969).
- 22. J. V. Acrivos and K. S. Pitzer, J. Phys. Chem., <u>66</u> 1693 (1962).
- 23. J. P. Telieur, P. Damay, and G. Lepoutre, J. Phys. Chem. 69 2879 (1975).
- 24. E. Huster, Ann. Phys., 33 477 (1938).
- 25. S. Freed and N. Sugarman, J. Chem. Phys., <u>11</u> 354 (1943).
- 26. C. A. Hutchison and R. C. Pastor, Rev. Mol. Phys., 25 285 (1953).
- 27. A. Demortier and G. Lepoutre, C. R. Acad. Sci. Paris, 268 453 (1969).
- 28. A. Demortier, M. DeBacker, and G. Lepoutre, J. Chim. Phys., 69 380 (1972).
- 29. T. A. Beckman and K. S. Pitzer, J. Phys. Chem. <u>65</u> 1527 (196).
- 30. A. M. Stacy and M. J. Sienko, Inorg. Chem., <u>21</u> 2294 (1982).
- 31. P. P. Edwards, A. R. Lusis and M. J. Sienko, J. Chem. Phys., 72 3103 (1980).
- 32. J. R. Buntaine, M. J. Sienko and P. P. Edwards, J. Phys. Chem., 84 1230 (1980).
- 33. P. P. Edwards, J. R. Buntaine and M. J. Sienko, Phys. Rev. B, 19 5835 (1979).
- 34. R. B. Von Dreele, W. S. Glaunsinger, A. L. Bowman and J. L. Yarnell, J. Phys. Chem., 79 2992 (1975).

- 35. W. S. Glaunsinger, J. Phys. Chem., 84 1163 (1980).
- 36. R. Hagedorn and J.-P. Lelieur, J. Phys. Chem., <u>84</u> 3652 (1980).
- 37. Y. Nakamura, Y. Horie, and M. Shimoji, TRans. Faraday Soc. I, 70 1376 (1974).
- 38. J. W. Fletcher, W. A. Seddon, J. Jevcok and F. C. Sopchyshyn, Chem. Phys. Lett., 18 592 (1973).
- 39. J. W. Fletcher, W. A. Seddon, J. Jevcok and P. C. Sopchyshyn, Can. J. Chem. 51 2975 (1973).
- 40. F. Y. Jou and L. M. Dorfman, J. Chem. Phys. <u>58</u>, 4715 (1973).
- 41. R. Bockrath and L. M. Dorfman, J. Phys. Chem. 77 1002 (1973).
- 42. L. M. Dorfman, F. Y. Jou and R. Wageman, Ber. Bunsenges Phys. Chem., 75 681 (1971).
- 43. J. L. Dye, M. G. DeBacker and L. M. Dorfman, J. Chem. Phys., 52 6251 (1970).
- 44. N. Mammano in "Metal-Ammonia Solutions", J. J. Lagowski and M. J. Sienko (eds.), Colloque Weyl II IUPAC, Butterworths (London) 1970, page 369.
- 45. L. J. Gillings, J. G. Kloosterboer, R. P. H. Rett-schnick, and J. D. W. van Voorst, Chem. Phys. Lett. 8 457, 462 (1971).
- 46. G. Gabor and K. H. Bar-Eli, J. Phys. Chem. <u>75</u> 286 (1971).
- 47. A. Gaathon and M. Ottolenghi, Israel J. Chem. $\underline{8}$ 165 (1970).
- 48. J. W. Fletcher and W. A. Seddon, J. Phys. Chem. 79 3055 (1975).
- 49. L. R. Dalton, M. S. Thesis, Michigan State University, 1966.
- 50. W. A. Seddon, J. W. Fletcher, F. C. Sopchyshyn, and R. Catterall, Can. J. Chem. <u>55</u> 3356 (1977).
- 51. K. D. Vos and J. L. Dye, J. Chem. Phys. <u>38</u> 2033 (1963).

- 52. V. A. Nicely and J. L. Dye, J. Chem. Phys. <u>53</u> 119 (1970).
- 53. W. A. Seddon, J. W. Fletcher, and R. Catterall, Can. J. Chem. <u>55</u> 2017 (1977).
- 54. J. L. Dye, in "Metal-Ammonia Solutions", J. J. Lagowski and M. J. Sienko (eds.), Colloque Weyl II IUPAC, Butterworths (London) 1970, page 77.
- 55. J. L. Dye, M. G. DeBacker, and V. A. Nicely, J. Am. Chem. Soc. 92 5226 (1970).
- 56. J. L. Dye, M. T. Lok, F. J. Tehan, R. B. Coolen, N. Papadakis, J. M. Ceraso and M. G. DeBacker, Ber. Bunsenges Phys. Chem. 75 659 (1971).
- 57. C. J. Pedersen, J. Am. Chem. Soc. 89 2495 (1967).
- 58. C. J. Pedersen, J. Am. Chem. Soc. <u>89</u> 7017 (1967); <u>90</u> 3299 (1968).
- 59. B. Dietrich, J.-M. Lehn, and J.-P. Sauvage, Tetrahedron Lett., <u>34</u>, 2885 (1969).
- 60. G. W. Gokel and H. D. Durst, Synthesis, 168 (1976).
- 61. A. C. Knipe, J. Chem. Ed. 53 618 (1976).
- 62. J.-M. Lehn, Pure Appl. Chem. 49 857 (1977).
- 63. J.-M. Lehn, Acc. Chem. Res. <u>11</u> 49 (1978).
- 64. J. L. Dye in "Progress in Macrocyclic Chemistry", R. M. Izatt and J. J. Christensen (eds.), Wiley-Interscience (New York) 1979, Vol. I, pp 63-113.
- 65. I. M. Kolthoff, Anal. Chem. <u>51</u> 1R (1979).
- 66. J. M. Ceraso and J. L. Dye, J. Chem. Phys. <u>61</u> 1585 (1974).
- 67. J. L. Dye, C. W. Andrews, and S. E. Matthews, J. Phys. Chem. <u>79</u> 3065 (1975).
- 68. P. P. Edwards, S. C. Guy, and D. M. Holton, J. C. S Chem. Comm., 1185 (1981).
- 69. J.-M. Lehn and J. P. Sauvage, J. Am. Chem. Soc. <u>97</u> 6700 (1975).

- 70. M. T. Lok, F. J. Tehan, and J. L. Dye, J. Phys. Chem. <u>76</u> 2975 (1972).
- 71. J. L. Dye, M. R. Yemen, and M. G. DaGue, and J.-M. Lu, J. Chem. Phys. <u>68</u> 1665 (1978).
- 72. M. G. DaGue, J. S. Landers, H. L. Lewis, and J. L. Dye, Chem. Phys. Lett. 66 169 (1979).
- 73. J. L. Dye, M. G. DaGue, M. R. Yemen, J. S. Landers, and H. L. Lewis, J. Phys. Chem. <u>84</u> 1096 (1980).
- 74. V. M. Dukel'skii, E. Ya Zandberg and N. I. Ionov, Doklady. Adak. Nauk. S.S.S.R. 62 232 (1948).
- 75. T. A. Patterson, H. Hotop, A. Kasdan, D. W. Norcross, and W. C. Fineberger, Phys. Rev. Lett. 32 189 (1974).
- 76. S. Golden, C. Guttman, and T. R. Tuttle, Jr., J. Am. Chem. Soc. 87 135 (1965).
- 77. S. Golden, C. Guttman, and T. R. Tuttle, Jr., J. Chem. Phys. 44 3791 (1966).
- 78. S. Matalon, S. Golden, and M. Ottolenghi, J. Phys. Chem. 73 3098 (1969).
- 79. J. L. Dye, J. M. Ceraso, M. T. Lok, B. L. Barnett, and F. J. Tehan, J. Am. Chem. Soc. 96 608 (1974).
- 80. F. J. Tehan, B. L. Barnett, and J. L. Dye, J. Am. Chem. Soc. 96 7203 (1974).
- 81. D. Moras, B. Metz, and R. Weiss, Acta Crystallogr. Sect. B 29 388 (1973).
- 82. D. Moras, B. Metz and R. Weiss, Acta Crystallogr. Sect. B. 29 383 (1973).
- 83. J. L. Dye, Angew. Chem., Int. Ed. Engl., <u>18</u> 587 (1979).
- 84. J. S. Landers, Ph.D. Dissertation, Michigan State University, 1981.
- 85. M. G. DaGue, Ph.D. Dissertation, Michigan State University, 1979.
- 86. A. Ellaboudy, P. B. Smith, and J. L. Dye, to be published.

- 87. B. Dietrich, J.-M. Lehn, J. P. Sauvage, and J. Blanzat, Tetrahedron 29, 1629 (1973).
- 88. G. W. Gokel, D. J. Cram, C. L. Liotta, H. P. Harris and F. L. Cook, J. Org. Chem. 39 2445 (1974).
- 89. R. N. Green, Tetrahedron Lett., 1793 (1973).
- 90. M.-T. Lok, Ph.D. Dissertation, Michigan State University, 1973.
- 91. J. M. Ceraso, Ph.D. Dissertation, Michigan State University, 1975.
- 92. F. J. Tehan, Ph.D. Dissertation, Michigan State University, 1973.
- 93. P. B. Smith, Ph.D. Dissertation, Michigan State University, 1978.
- 94. D. S. Issa, Ph.D. Dissertation, Michigan State University, 1982.
- 95. L. D. Le, D. S. Issa, B. Van Eck, J. L. Dye, J. Phys. Chem., 86 7 (1982).
- 96. I. Hurley, T. R. Tuttle, Jr., and S. Golden, J. Chem. Phys. <u>48</u> 2818 (1968).
- 97. V. Gutmann and E. Wycheva, Inorg. Nucl. Chem. Lett. 2 257 (1966).
- 98. J. L. Dye, J. Phys. Chem. 84 1084 (1980).
- 99. E. Kauffmann, J.-M. Lehn, J. P. Sauvage, Helv. Chim. Acta, <u>59</u> 1099 (1976).
- 100. R.R.Dewald, J. L. Dye, J. Phys. Chem., 68 128 (1964).
- 101. P. Laszlo, Angew. Chem. Int. Ed. Engl. <u>17</u> 254-266 (1978).
- 102. J. L. Dye, C. W. Andrews, and J. M. Ceraso, J. Phys. Chem. <u>79</u> 3076 (1975).
- 103. M. S. Greenberg and A. I. Popov, Spectrochim. Acta 31A 697 (1975).
- 104. G. Mali and S. Frago, Theor. Chim. Acta, <u>5</u> 275 (1966).

- 105. J. P. Kintzinger and J.-M. Lehn, J. Am. Chem. Soc., 96 3313 (1974).
- 106. J. M. Ceraso, P. B. Smith, J. S. Landers, and J. L. Dye, J. Phys. Chem. <u>81</u> 760 (1977).
- 107. R. G. Griffin, Anal. Chem. 49 951A (1977).
- 108. D. Moras, R. Weiss, Acta Crystallogr., Sect. B, 29 396 (1973).
- 109. A. Ellaboudy, M. L. Tinkham, B. Van Eck, J. L. Dye and P. B. Smith, in press.
- 110. A. C. Larson, R. B. Roof, Jr., and D. T. Cromer, U.S. Atomic Energy Commission Rep. LA3335, Los Alamos, New Mexico (1965).
- 111. J. L. Dye unpublished results.
- 112. U. Schindewolf, L. D. Le, J. L. Dye, J. Phys. Chem. 86 2284 (1982).
- 113. J. L. Dye, J. Chem. Educ. 54 332-9 (1977).
- 114. G. R. Stevenson, E. Williams, Jr., G. Caldwell, J. Am. Chem. Soc. 101 520 (1979).
- 115. G. R. Stevenson, private communication.
- 116. M. H. Abraham, A. F. Danil de Namor, and R. A. Schultz, J. Chem. Soc., Faraday Trans. 1, 76 869 (1980).
- 117. J. A. Dean: Lange's Handbook of Chemistry, 11th Ed. McGraw-Hill, New York 1973.
- 118. U. Schindewolf and M. Warner, J. Phys. Chem. 84, 1123-7 (1980).
- 119. M. Werner and U. Schindewolf, Ber. Bunsenges. Phys. Chem. 84 547-50 (1980).
- 120. W. Gross and U. Schindewolf, Ber Bunsenges, Phys. Chem. 85 112 (1981).
- 121. K. Ichikawa and J. C. Thompson, J. Chem. Phys. <u>59</u> 1680-1692 (1973).
- 122. K. Ichikawa and J. C. Thompson, J. Chem. Phys. <u>62</u> 4958-9 (1975).

- 123. L. Hsueh and D. N. Bennion, J. Electrochem. Soc., 118 1128-30 (1971).
- 124. S. Glasstone: Textbook of Physical Chemistry 2nd Edit. Van Nostrand, New York 1946, p. 87.
- 125. Robert C. Weast (Editor): Handbook of Chemistry and Physics, 53rd Edition, Chemical Rubber Publishing Co., Cleveland, OH.
- 126. J. E. B. Randles, Trans. Faraday Soc. <u>52</u> 1573 (1956).
- 127. J. E. Desnoyers and C. Jolicoeur in "Modern Aspects of Electrochemistry", J. O. M. Bockris and B. E. Conway, Ed. Vol. 5, Plenum Press, New York, NY, 1969, Chapter 1.
- 128. S. Golden, R. G. Bates, J. Am. Chem. Soc. <u>94</u>, 1476 (1972).
- 129. A. Kasdan and W. C. Lineberger, Phys. Rev. A Vol. 19 1658 (1974).
- 130. J.-M. Lehn, Struct. Bonding 16 1 (1973).
- 131. L. Pauling: The Nature of the Chemical Bond, 3rd Ed. Cornell University Press, Ithaca, NY 1960.
- 132. A. F. Kapustinskii, Q. Rev. Chem. Soc. <u>10</u> 283 (1956).
- 133. W. E. Spicer, A. H. Sommer, J. G. White, Phys. Rev. <u>115</u> 57 (1959).
- 134. T. H. Teherani, W. J. Peer, J. J. Lagowski, Allen J. Bard, JACS, 100 7768 (1978).
- 135. B. VanEck, L. D. Le, D. Issa, and J. L. Dye, Inorg. Chem., <u>21</u> 1966 (1982).

